ACTA PROTOZOOLOGICA

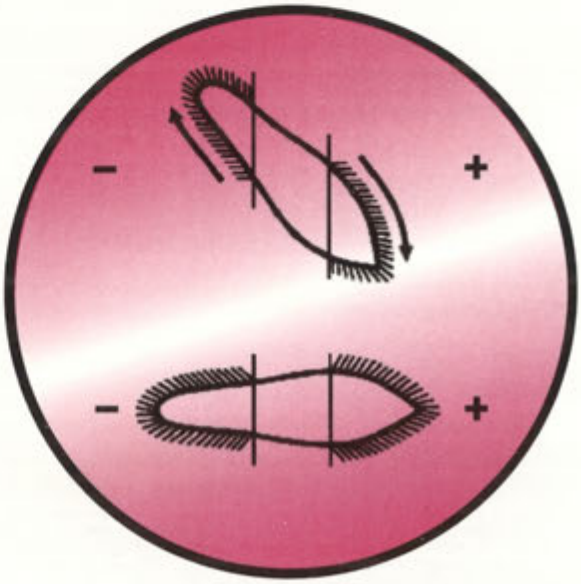

NENCKI INSTITUTE OF EXPERIMENTAL BIOLOGY
WARSAW, POLAND
1993
VOLUME 32 NUMBER 1
ISSN 0065-1583

Polish Academy of Sciences
Nencki Institute of Experimental Biology

ACTA PROTOZOOLOGICA

International Journal on Protistology

ACTA PROTOZOOLOGICA appears quarterly.

Indexed in Current Contents in CABS and in Protozoological Abstracts.

Front cover: The ciliary reversal on cathodal side of *Paramecium*. S. Dryl 1963, Acta Protozool. 1,193-199

Acta Protozoologica (1993) 32: 1 - 16

ACTA
PROTOZOOLOGICA

The Influence of Ecological Factors on the Abundance of Different Ciliated Protozoa Populations in the Danube River. I. Investigation of the Ecological Amplitude

Magdolna Cs. BERECZKY and János N. NOSEK

Hungarian Danube Research Station, Hungarian Academy of Sciences, Göd, Hungary

Summary. Based on data obtained during years of different hydrological regimes, the ecological amplitude of 30 ciliate species occurring with at least 10 percent relative frequency each, were studied. It was investigated to what extent the ecological factors chosen by us could be regarded as limiting ones as to the population-forming capacity of each species in the Danube. The quantitative changes of the individual ecological factors were analyzed along with the extent to which the indicator nature of the individual species could be determined by them.

During these studies no parameter was found which could have been considered an absolute inhibiting factor to the spread of the species. This means that the Danube is a suitable milieu for the 30 species investigated. Therefore, concerning population-forming capacity, not the individual factors, but their mutual effect seems to be decisive. The differences in indicator character were apparent in two large groups of factors. The majority of species exhibited tolerance for water discharge, water temperature, pH and dissolved oxygen content. The other part of species, on the other hand, proved to have a wide tolerance for factors suggesting anthropogenic effects, such as oxygen demand, ammonium and two different kinds of bacterial population.

Key words. Ciliate, Danube, ecological amplitude, running water, tolerance.

INTRODUCTION

The investigation of ecological amplitude aim at revealing the external factors which determine the conditions of life for a particular organism, as well as the effects of those conditions on the species. More than ten years ago, attempts were made to obtain information concerning the ecological amplitude of ciliates occurring in that period with the highest frequencies and to compare these results with those of other authors (Bereczky 1977). The previous study differed from the present one in its method of evaluation and the species investigated were also different. The statistical analysis of the frequency distributions enabled us to determine the optimal conditions for the species in running water. The literature is mainly concerned with laboratory results. The majority of field studies focus on lacustrine environments adopting an easier methodological approach. The papers by Bick (1966a, b, 1968, 1972a, b), Wilbert (1969) and those of their followers (Pätsch 1974,

Paper presented on the 2nd International Conference of Hungary on Protozoology "Current Problems in Protozoan Ecology", 26-30 August 1991, Tihany, Hungary.

Address for correspondence: M. Cs. Bereczky, Hungarian Danube Research Station, Hungarian Academy of Sciences, Göd, Jávorka S. str. 14. H-2131, Hungary.

Schmitz 1986) present the most concrete data on the ecology of Protozoa. Cairns jr. (1965, 1986) and Pratt et al. (1985, 1987a, b) report mainly on the theoretical aspects of the new results.

During our investigations conducted for two decades, substantial information has been accumulated on the protozoan fauna of the Danube. Similar to other animal populations, the protozoan populations of the Danube show seasonal changes both in species composition and individual number (Bereczky 1973). The results have been reported in several papers (Bereczky 1969, 1971, 1973).

A reservoir and an electric power-plant are under construction on the Danube at Kiliti (1842 riv. km) and at Bôs (1819 riv. km). As a result of the large-scale construction works, the biota of the Danube will change, since changes in the environment produce alterations in the animal and plant life. The ability of the individual species to accommodate to these changes differs greatly, as demonstrated by Bick (1966a, b) in connection with *Coleps hirtus, Glaucoma scintillans* and several other species. The changes will also determine the distribution of the species, since, due to a chain of barrages and the lengthening of the retention time of water along an about 220 km section of the Danube, flow velocity will be modified. Changes brought about by the engineering structures and by communal and industrial effluent in the river had also been previously registered (Bereczky 1978).

In our study we have tried to analyze the relation between some environmental factors and the occurrence and abundance of 30 Ciliata species on the basis of different approaches and methods. In this paper the results of ecological amplitude investigations are presented. In this analysis an answer was also sought to the question how much the indicator character of species is reflected by the ecological amplitude curves.

Table 1

The species investigated with their relative frequency and indicator character (ob - oligo-betameso-, b - betameso-, ba - beta-alfameso-, a - alfa-, p - polysaprobic species, – - species without indicator character)

species	relative frequency	indicator character
Carchesium polypinum (Linnaeus, 1758)	24.3	a
Codonella cratera (Leidy, 1877)	49.3	ob
Coleps hirtus (O.F.Mueller, 1786)	66.4	ba
Coleps hirtus var. *lacustris* (Faure-Fremiet, 1924)	22.9	–
Colpidium campylum (Stokes, 1886)	21.4	p
Colpidium colpoda (Losana, 1829)	16.4	p
Epistylis plicatilis (Ehrenberg, 1831)	15.7	a
Epistylis pyriformis Perty	33.6	–
Glaucoma scintillans Ehrenberg, 1830	22.9	p
Paramecium caudatum Ehrenberg, 1833	39.3	a
Paramecium putrinum Claparede & Lachmann, 1859	27.9	p
Phascolodon vorticella Stein, 1859	80.0	b
Prorodon teres Ehrenberg, 1833	23.6	a
Pseudovorticella margaritata (Fromentel, 1876)	65.7	b
Staurophrya elegans Zacharias, 1893	50.7	b
Stentor polymorphus (O.F. Mueller, 1773)	55.0	b
Stokesia vernalis Wenrich, 1929	45.0	b
Strobilidium caudatum (Fromentel, 1876)	10.9	ob
Strombidium viride Stein, 1867	21.4	b
Tintinnidium fluviatile (Stein, 1863)	75.0	ob
Trithigmostoma cucullulus (O.F.Mueller, 1786)	27.1	a
Urotricha farcta Claparede & Lachmann, 1859	32.9	a
Vorticella campanula Ehrenberg, 1831	70.0	b
Vorticella convallaria (Linnaeus, 1758)	37.1	a
Vorticella incisa Stiller	52.9	–
Vorticella microstoma Ehrenberg, 1830	37.9	p
Vorticella nebulifera O.F.Mueller, 1773	79.3	–
Vorticella similis Stokes, 1887	80.0	–
Zoothamnium minimum Stiller	30.7	–
Zoothamnium varians Stiller	44.3	–

MATERIAL AND METHODS

Samples used for the study were obtained from the main branch of the Danube at Göd (1669 riv. km). Sampling had been made for more than two decades at weekly intervals. As in running waters the water discharge is regarded to be the most important abiotic environmental factor, for detailed analysis from this long term data series four years (1981, 1985, 1986 and 1987) were selected in a way that the range of water discharge values could be the widest possible (Fig.1). The total number of samples was 140.

Protozoological data originated from 100 l water being filtered through a 10 µm mesh-size plankton net. Analysis was carried out from the filtrate, partly under living and partly under fixed conditions by protargol impregnation modified by Wilbert (1974) and by the staining method by Bereczky (1985) for counting. The successive discussion of species was made according to the system proposed by Corliss (1979) and Foissner (1988).

Those Ciliata species were involved in the study which were present in at least 10 percent of the samples collected during the four years (Table 1). The species included 12 euplanktonic and 18 tychoplanktonic or sessile ones.

Nine environmental factors were selected to reflect the natural conditions and the anthropogenic effects, too. Of the physical parameters of the water body, water discharge and water temperature, of the chemical ones, pH, total dissolved solids, dissolved oxygen content, chemical oxygen demand and ammonium ion content, and

Table 2

The environmental parameters investigated with their extreme values

parameter	minimum	mean values	maximum
ammonium content (mg l^{-1})	.00	.47	2.68
chemical oxygen demand (mg l^{-1})	5.00	7.20	17.30
dissolved oxygen content (mg l^{-1})	6.59	10.36	20.00
No. of *Coli*-form bacteria (ind l^{-1})	.00	222.40	931.00
No. of psychrophil bacteria (10^3 ind l^{-1})	1.00	6.05	21.00
pH	7.24	8.15	9.68
total dissolved solids (mg l^{-1})	230.00	322.40	466.00
water discharge (m^3 sec^{-1})	986.00	2375.00	6100.00
water temperature (°C)	.40	12.72	22.00

of those referring to the living environment, the number of psychrophile bacteria and the coli bacteria were involved in the analysis. These environmental factors, their codes and extreme values are listed in Table 2.

Dissolved oxygen content was determined by Winkler's method, the ammonium content by the Nessler method and the chemical oxygen demand by acid potassium permanganate ($KMn0_4$). Total dissolved solids means the evaporation residue of the filtered water. Bacterial counts were determined after incubation at 20 and 37 °C by counting the colonies developed.

Chemical data originate from the laboratory of our station.

The bacteriological analyses were carried out in the Institute for Public Health and Epidemiology of the City of Budapest.

The traditional form of ecological amplitude is a list containing the lower and upper values of several environmental factors regarding the occurrence of a species (e.g. Heuss and Wilbert 1973). This range, however, reveals only the presence of the species without providing information about which intervals within the range were favourable or unfavourable for the species investigated. The analysis of the frequency distribution curves involve both the extreme values, and the shape of the curve gives additional information about the subintervals preferred within the range of the occurrence.

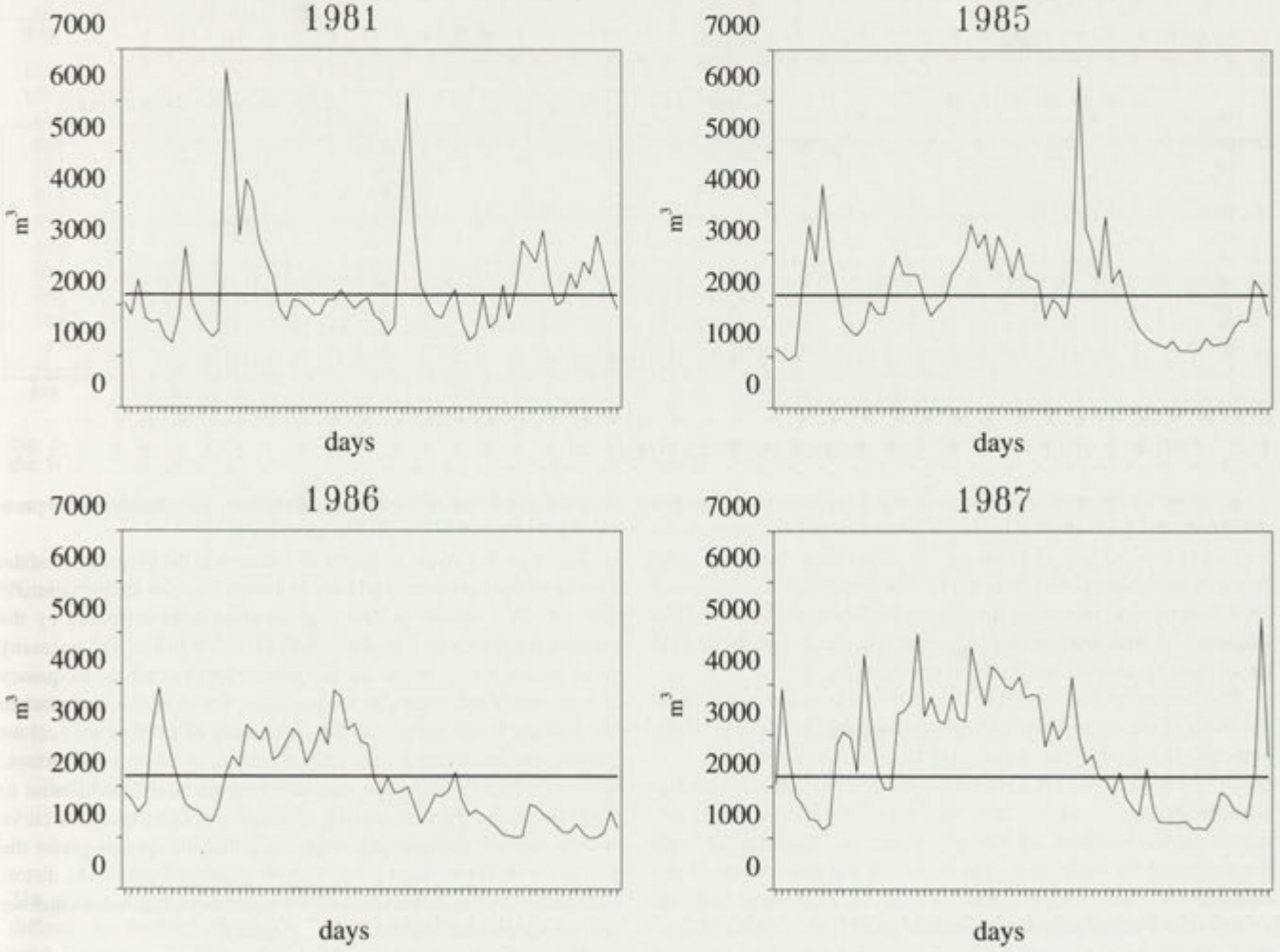

Fig. 1. Changes of water discharges in the years investigated (m^3s^{-1}). Horizontal line represents the mean discharge (2200 m^3s^{-1}) of the last decade (1981-1991)

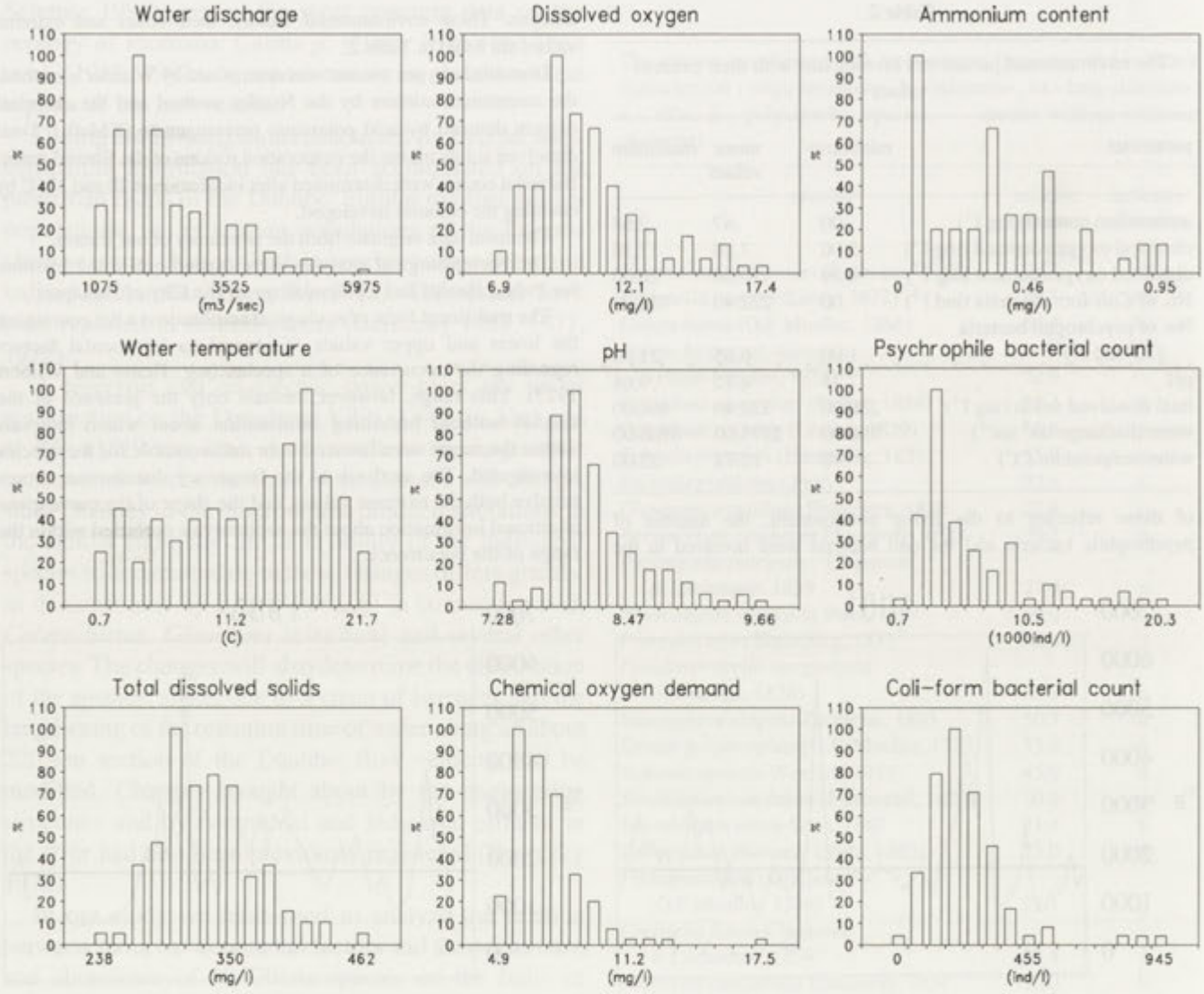

Fig. 2. Frequency distribution of the environmental parameters investigated

In our study the range of each parameter, i.e. the interval between the lowest and the highest value occurred in the pooled samples, was uniformly divided into 15 classes. (The class mean values are to be found in the headings of Tables 3-11). The frequency distribution of each species was related to the classes obtained in this way. The frequency distribution of the physical, chemical and biological parameters themselves were also determined (Fig. 2).

The frequency distribution of the species was calculated both on the basis of the occurrence and abundance data. In the case of the presence frequency distributions (PFD) only the occurrence of a given species was recorded regardless of its abundance. Regarding also the abundance values, definitely more information can be obtained on the demands of the given species. This fact is well demonstrated for example by the dissolved oxygen content or pH diagrams of *Phascolodon vorticella* (Fig. 3). Regarding only the occurrences the species is present almost in all classes. Nevertheless the optimal range is towards the higher values of dissolved oxygen or pH. That means the interval with the greatest abundance values of a species does not absolutely coincide with the interval characterized by the highest rate of occurrence. Therefore, the abundance frequency distribution (AFD) was also calculated.

To avoid distortion caused by differences in the frequencies of the classes of the environmental factors themselves, the frequencies (PF and AF) of a species within a given class were weighted by the relative frequency of that class (WPFD and WAFD). The necessity of weighting is easy to see. Let us examine for example the frequency distribution of the water discharge values. The most frequent class in the Danube is the third, with the class mean of 1775 m^3sec^{-1}. If we present the unweighed frequency distribution of an euplanktonic species, which is present in almost all sample and is indifferent to water discharge fluctuations (e.g. *Phascolodon vorticella*), the curve will be skewed towards left, suggesting that the species prefer the periods with lower water level. The weighting eliminate the distortion caused by the distribution of the water discharge values and we get the real picture (cf. Fig. 3, WD diagram).

The original presence frequency ($f_{i,j,k}$) of species i in class j of parameter k is the number of occurrence of species i in the j-th class of parameter k. The weighted presence frequency ($WPF_{i,j,k}$) is:

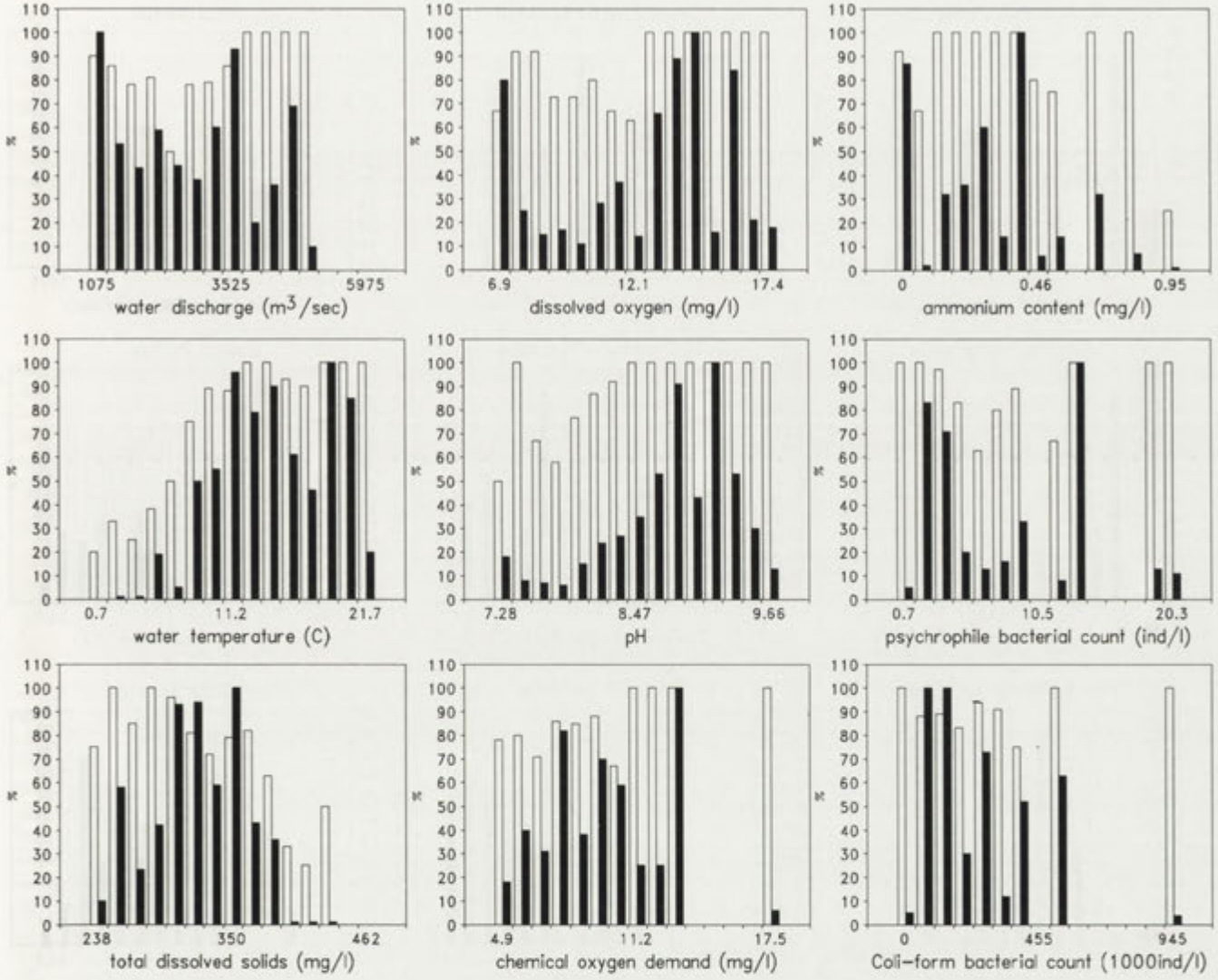

Fig. 3. Frequency distributions of *Phascolodon vorticella* Stein, 1859, related to the different environmental factors. Empty bars represent the WPF, filled bars represent the WAF values

$$WPF_{i,j,k} = f_{i,j,k}/w_{j,k} \; ; \; w_{j,k} = g_{j,k}/N \; ; \; \Sigma w_{j,k} = 1 \; ; \; \Sigma g_j = N$$

where g is the frequency of the j-th class of parameter k and N is the number of samples 140. The abundance frequency ($a_{i,j,k}$) is:

$$a_{i,j,k} = \Sigma n_{i,j,k,s} / f_{i,j,k}$$

where $n_{i,j,k,s}$ is the number of individuals of species i in the s-th occurrence within the j-th class of parameter k, that is $a_{i,j,k}$ is the average abundance per occurrence in class j.

The weighted abundance frequency ($WAF_{i,j,k}$) is:

$$WAF_{i,j,k} = a_{i,j,k} * WPF_{i,j,k} = \Sigma n_{i,j,k,s} / w_{j,k}$$

The absolute WPF and WAF values of the different species were different, so to make possible the comparison, percentile values were used. The maximal frequency value within each frequency distribution was regarded as 100% and the other values were related to this maximum.

RESULTS AND DISCUSSION

The relationship between the admittedly cosmopolitan ciliates and their biotopes manifests in a variety of their population densities. In order to understand the function of biotope as an environment or to ecologically interpret a coexistence pattern, it is important to investigate the problems of limit. Limitation can, however, be proved or made questionable only by analyzing the amplitude of the ecological factors. It appears, that during our work we could find answers to most of our questions.

In the subsequent evaluation we focused on the environmental factors, since the behaviour of the species is demonstrated well by the WAFD-s. The most explicit

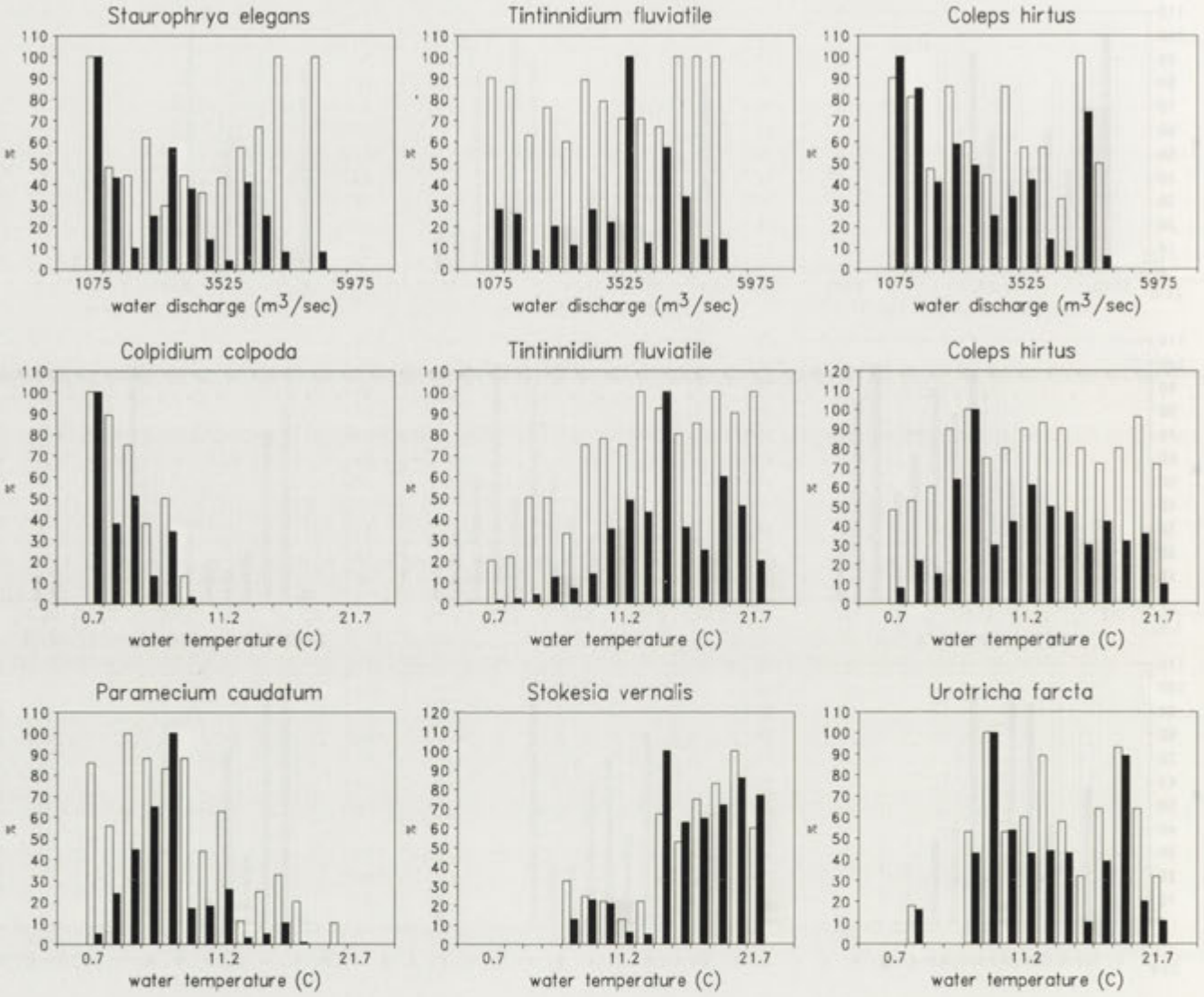

Fig. 4. Frequency distributions of some species, related to the categories of water discharge and water temperature. Empty bars represent the WPF, filled bars represent the WAF values

interpretation of a frequency distribution is the bar diagram (cf. eg. Stössel 1979). In lack of space it is impossible to present all of the bar diagrams (the total number would be 540!), so only the WAFD-s are given in tabular form (Tables 3-11). (The extreme values of the WPFD-s are identical with that of the presented WAFD-s). Only a few characteristic diagrams are presented, such as the diagrams of *Phascolodon vorticella*, which is one of the characteristic and dominant species of protozoa plankton in the Danube (Fig. 3).

Water discharge (Table 3)

Water discharge and the morphology of the riverbed jointly determine the velocity of water movement, which is considered in the monographs on streams to be the greatest selecting factor. (Flow velocities measured at Göd ranged between 0.8 and 1.5 ms^{-1}.) The streaming turbulent motion of water made it questionable for a long time, whether there were possibilities for the potamoplankton to develop in this environment. Several papers have recently been published, which besides reporting the results of the acknowledged zooplankton and phytoplankton investigations, do not inform about Protozoa, or only treat them superficially.

According to the distributions, the flow of water does not necessarily limit the spread of Protozoa. In the Danube there is an abundance of protozoan species. The best example of that is *Tintinnidium "fluviatilis"* also in

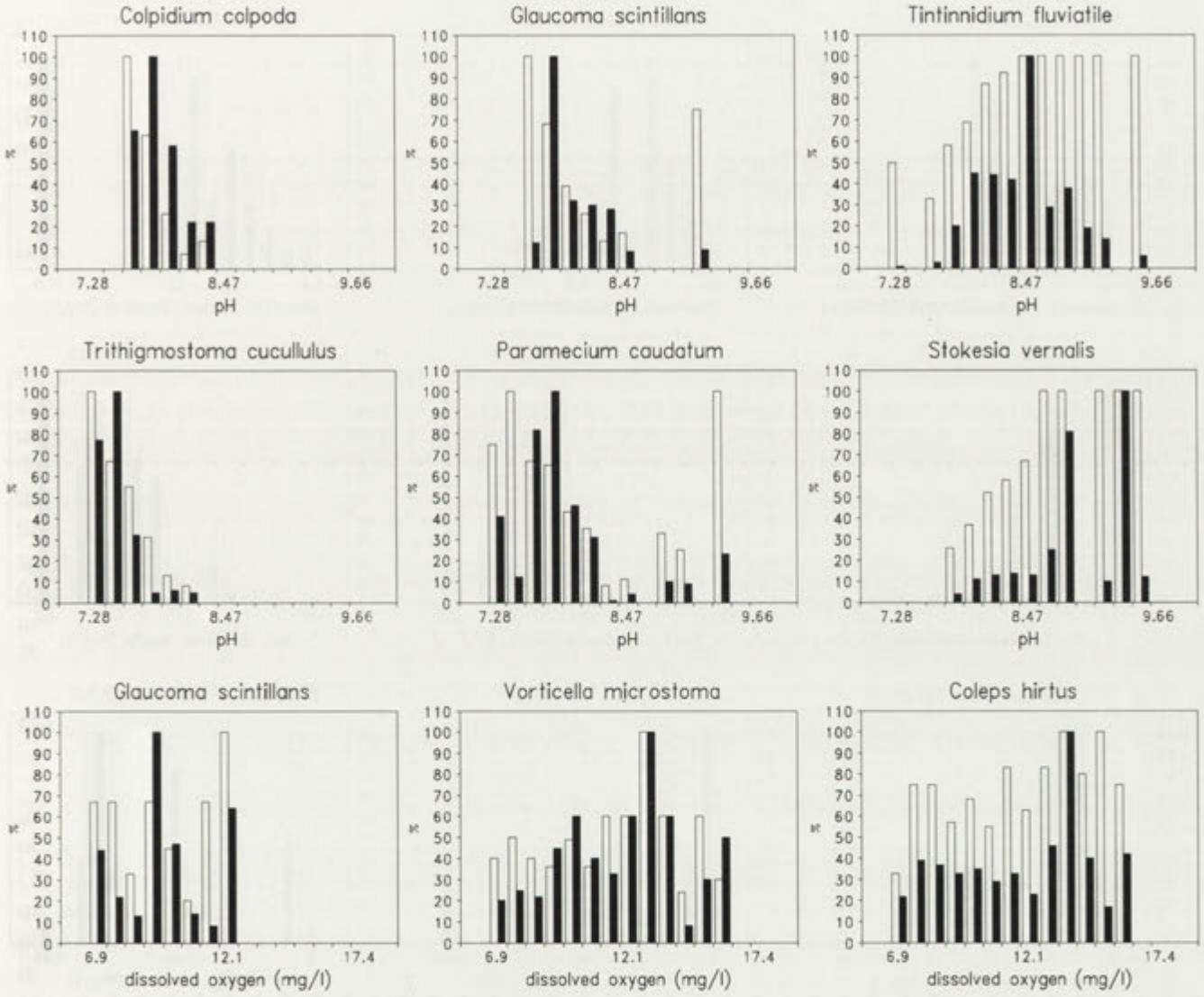

Fig. 5. Frequency distributions of some species, related to the categories of pH and dissolved oxygen content. Empty bars represent the WPF, filled bars represent the WAF values

its species name, which has been proved to be euplanktonic protozoan, inhabiting streams (Fig. 4).

It can be stated, contrary to most assumptions, that the planktonic population is not only composed of Protozoa carried into the open water from the periphyton or lenitic catchments, but also of those feeding and proliferating in the open water and exhibiting a real planktonic life. If this were not true, their diagrams would always show a rising tendency towards higher water discharges, and such true euplanktonic species, like e.g. the members of the abundant, dominant and constant genera *Phascolodon, Coleps, Tintinnidium, Staurophrya*, etc., (Fig. 4) would be missing.

Water Temperature (Table 4)

Analyzing the effects of water temperature as a limiting factor, one should proceed with great caution. The protozoan species living within the range of temperature values measurable in the Danube can be divided into two groups: the group living in the temperature range of 0-10°C and that living above that range. The frequency of the genuine alpha-mesosaprobic species is higher in the colder range of temperature, while that of the beta-mesosaprobic ones in the temperature range above 10°C. The *Paramecium* and *Colpidium* species have affinities for low temperatures (Fig. 4), in agreement with Schönborn's (1982) investigations, who

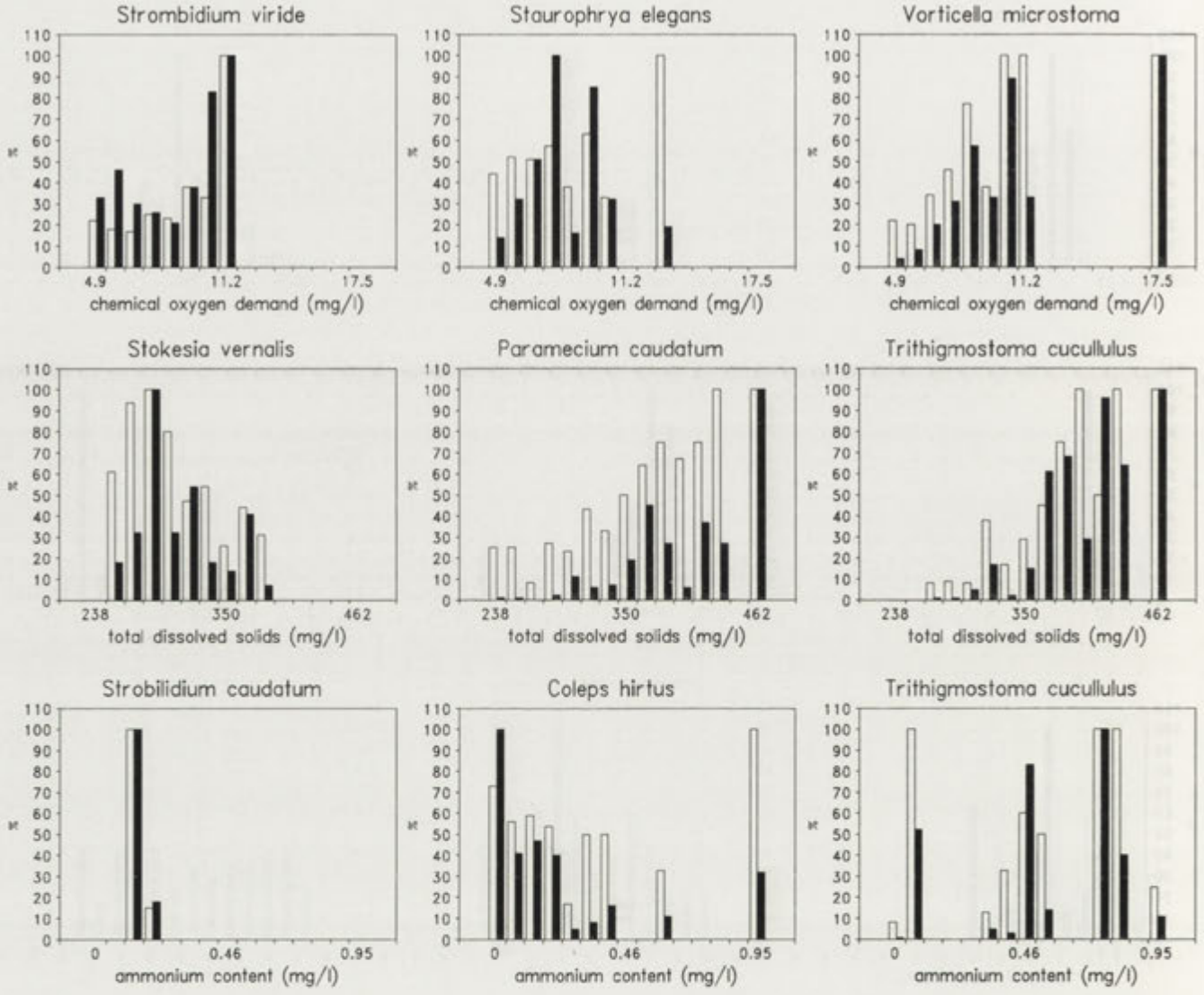

Fig. 6. Frequency distributions of some species, related to the categories of chemical oxygen demand, total dissolved solids and ammonium content. Empty bars represent the WPF, filled bars represent the WAF values

had found the same species abundant in colder periods, while the *Phascolodon, Stokesia, Tintinnidium,* and *Urotricha* species prefer higher ones (Fig. 4). In more than one species the limiting factor is, however, not temperature itself but the temperature-dependent food supply. Though there are algae and bacteria present in both temperature ranges, for many species the preferred food is not present. The food organism of *Phascolodon*, e.g. *Eudorina, Pandorina, Gonium,* etc., seldom occur at temperatures below 10°C. Besides the species, which belong to the two temperature groups, there are also ones which do not unequivocally belong to the one or the other group. Such is e.g. *Coleps hirtus* (Fig. 4). This species was found both in ice-cold water and in waters of temperatures above 20°C, though, on the basis of its distribution, the mesothermic range appears optimal for it. It is likely that this great tolerance is again related to the conditions of nutrition, since *Coleps hirtus* is predatory, necrophagous (omnivorous) and so its feeding possibilities do not depend on temperature.

pH (Table 5)

Free CO_2, one of the acknowledged limiting factors of ciliates (e.g. of *Codonella cratera*), is not present in the Danube water due to its hydrogen ion concentration. Of the species investigated, several occur within a rather narrow range of pH, like e.g. the species of the genera of *Colpidium, Glaucoma, Paramecium, Trithigmostoma* (Fig. 5). The pH-sensitive species mostly belong to the

group of alpha-mesosaprobic organisms. The majority of beta-mesosaprobic species (e.g. *Phascolodon vorticella, Stokesia vernalis, Tintinnidium fluviatile*, (Fig. 5) etc.), however, exhibit a surprisingly great tolerance for the changes of hydrogen ion concentration in the alkaline range.

Dissolved Oxygen (Table 6)

The species discussed here are aerobic ones, with the exception of two organisms (*Glaucoma scintillans, Vorticella microstoma*), which are known to be facultatively anaerobic. Since no oxygen deficiency should be reckoned with in the Danube, not even during the night, the distribution of the various species only show which of them and to which degree is affected by the oversaturation of water with oxygen. In this respect again the species of different saprobities exhibit but slight differences. It can be stated that in the Danube oxygen is not a limiting factor which affects the densities of the 30 protozoan species investigated (Fig. 5).

Chemical Oxygen Demand (Table 7)

The chemical oxygen demand data demonstrate that in the years investigated the Danube was a moderately polluted surface water at Göd. Even the highest value (18.0 mg/l) was below the limit of the worst water quality. Therefore, it is not surprising that such polysaprobic species, like *Vorticella microstoma* occur in the whole range measured (Fig 7). The majority of oligo-beta-mesosaprobic and beta-mesosaprobic species, including *Strombidium viride* or *Staurophrya elegans*, only occur at the lower values of the chemical oxygen demand range (Fig. 6). The results show that this is the situation where one factor of the chemical environment does not indicate different water quality than do the indicator species.

Total Dissolved Solid (Table 8)

The total dissolved solid values measured in the Danube do not impose any difficulty for the spread of the species investigated. Most of these species can tolerate such quantitative changes of total dissolved solids in the Danube. Compared to others, the alpha-mesosaprobic organisms also show a slightly different behaviour in this respect. They occur with higher frequencies at the higher values, which, however, cannot either be interpreted as the result of a direct effect (Fig. 6).

Ammonium (Table 9)

Comparing the diagrams of species, the conclusion can be drawn that, true to their indication nature, the alpha- and polysaprobic species are tolerant of the amount of ammonia measured in the Danube, and the majority of the beta-mesosaprobic species are really sensitive to ammonia. Some species, for example *Strobilidium caudatum* can virtually tolerate only ammonia-free environments (Fig. 6).

Psychrophile and Coli Bacteria (Tables 10 and 11)

The distributions based on psychrophile bacterial count did not give information about the feeding habit of the species. Their saprobity ranging were, however, well reflected by both kind of distributions.

Acknowledgements. The authors would like to express their thanks to Mrs. Maria Kopasz for her valuable technical assistance and to Dr. Laszlo Nemedi (Institute for Public Health and Epidemiology of the City of Budapest) for the bacteriological data.

APPENDIX

Table 3

The weighted abundance frequency distributions of species related to the classes of water discharge

class mean (m^3sec^{-1}) Species	1075	1425	1775	2125	2475	2825	3175	3525	3875	4225	4575	4925	5275	5625	5975
Carchesium polypinum	100	21	18	19	10	5	10	21	28	16	0	24	0	0	*
Codonella cratera	18	49	21	56	46	41	30	35	33	14	14	11	100	0	*
Coleps hirtus	100	85	41	59	49	25	34	42	14	8	74	6	0	0	*
Coleps hirtus var. *lacustris*	68	56	13	27	0	17	9	36	11	0	25	100	0	0	*
Colpidium campylum	100	43	85	64	29	46	71	2	0	0	0	7	0	0	*
Colpidium colpoda	87	51	100	65	9	66	61	0	0	0	0	0	0	0	*
Epistylis plicatilis	10	79	13	29	30	44	7	0	14	0	0	100	0	0	*
Epistylis pyriformis	78	100	9	10	9	12	11	76	7	21	37	0	0	0	*
Glaucoma scintillans	100	62	75	26	21	26	64	2	3	0	0	0	0	0	*
Paramecium caudatum	100	33	14	10	21	7	3	1	1	3	0	1	0	0	*
Paramecium putrinum	52	50	68	14	100	44	34	17	6	0	0	60	0	0	*
Phascolodon vorticella	100	53	43	59	44	38	60	93	20	36	69	10	0	0	*
Prorodon teres	30	39	33	57	978	8	0	0	32	100	0	38	0	0	*
Pseudovorticella margaritata	100	47	33	19	25	8	23	24	24	61	13	2	0	0	*
Staurophrya elegans	100	43	10	25	57	38	14	4	41	25	8	0	8	0	*
Stentor polymorphus	100	33	17	10	14	12	9	11	11	16	10	2	0	0	*
Stokesia vernalis	32	91	55	100	82	44	35	88	88	41	26	88	26	0	*
Strobilidium caudatum	0	8	44	33	18	58	100	0	0	0	0	0	0	0	*
Strombidium viride	18	2	9	6	18	0	16	45	7	0	100	50	0	0	*
Tintinnidium fluviatile	28	26	9	20	11	28	22	100	12	57	34	14	14	0	*
Trithigmostoma cucullulus	100	35	25	26	26	28	5	4	3	0	0	0	0	0	*
Urotricha farcta	100	36	26	12	6	9	17	16	15	41	0	10	21	0	*
Vorticella campanula	100	37	23	14	32	12	11	9	7	10	24	9	3	0	*
Vorticella convallaria	100	15	19	6	18	5	16	14	2	0	0	2	0	0	*
Vorticella incisa	54	36	100	48	45	44	77	38	28	38	0	71	0	0	*
Vorticella microstoma	23	46	100	81	65	76	57	0	24	0	0	14	0	0	*
Vorticella nebulifera	100	20	12	6	5	7	9	16	7	18	8	0	0	0	*
Vorticella similis	84	91	62	69	42	54	76	62	42	43	100	50	7	0	*
Zoothamnium minimum	100	40	19	22	26	8	8	11	27	0	0	19	0	0	*
Zoothamnium varians	100	42	31	19	76	29	27	24	0	24	12	24	0	0	*

* - this class was omitted from the evaluation since water discharge greater than 5800 m^3sec^{-1} occurred only one occasion during the four years

Table 4

The weighted abundance frequency distributions of species related to the classes of water temperature

class mean (°C) Species	0.7	2.2	3.7	5.2	6.7	8.2	9.7	11.2	12.7	14.2	15.7	17.2	18.7	20.2	21.7
Carchesium polypinum	32	47	80	100	53	23	36	33	24	4	7	11	0	11	0
Codonella cratera	0	0	4	7	5	12	14	16	18	63	60	50	43	100	58
Coleps hirtus	8	22	15	64	100	30	42	61	50	47	30	42	32	63	10
Coleps hirtus var. *lacustris*	0	12	0	0	0	30	12	20	100	22	19	40	18	69	21
Colpidium campylum	100	14	60	9	38	5	0	2	1	0	0	0	0	0	0
Colpidium colpoda	100	38	51	13	34	3	0	0	0	0	0	0	0	0	0
Epistylis plicatilis	18	0	45	23	15	17	0	6	5	15	73	9	8	100	36
Epistylis pyriformis	0	0	0	7	9	38	60	21	22	100	75	12	20	2	0
Glaucoma scintillans	100	32	41	22	32	2	6	8	0	0	0	0	0	1	0
Paramecium caudatum	5	24	45	65	100	17	18	26	3	5	10	1	0	0	0
Paramecium putrinum	100	36	66	36	40	16	6	14	0	1	1	1	0	1	3

Phascolodon vorticella	0	1	1	19	5	50	55	96	79	90	61	46	100	85	20
Prorodon teres	0	97	0	18	12	100	16	36	8	12	29	55	6	51	29
Pseudovorticella margaritata	61	40	27	100	85	36	24	49	47	49	26	48	11	31	12
Staurophrya elegans	0	19	2	61	18	100	45	77	14	32	35	41	8	48	0
Stentor polymorphus	5	33	28	94	100	16	25	36	19	27	33	12	9	16	15
Stokesia vernalis	0	0	0	0	13	23	21	6	5	100	63	65	72	86	77
Strobilidium caudatum	0	0	0	0	0	0	44	100	11	33	0	5	8	60	0
Strombidium viride	0	8	0	5	25	14	8	100	42	67	13	10	8	65	23
Tintinnidium fluviatile	1	2	4	12	7	14	35	49	43	100	36	25	60	46	20
Trithigmostoma cucullulus	69	49	91	46	100	9	3	7	0	1	0	0	0	0	0
Urotricha farcta	0	16	0	0	43	100	54	43	44	43	10	30	89	20	11
Vorticella campanula	53	76	30	100	43	36	26	38	17	12	8	16	6	23	7
Vorticella convallaria	28	63	35	78	100	11	9	11	26	1	2	4	1	6	2
Vorticella incisa	0	52	20	5	27	44	36	16	20	21	42	23	28	100	87
Vorticella microstoma	100	61	23	27	27	27	18	6	1	15	1	7	4	18	0
Vorticella nebulifera	6	7	6	21	100	7	5	8	13	5	6	4	5	4	2
Vorticella similis	0	34	1	44	13	78	82	47	100	51	41	45	47	68	18
Zoothannium minimum	0	59	13	100	36	83	77	33	18	40	28	21	4	32	11
Zoothannium varians	28	56	100	78	99	61	15	17	32	8	8	3	3	5	3

Table 5

The weighted abundance frequency distributions of species related to the classes of pH

class mean (pH) Species	7.28	7.45	7.62	7.79	7.96	8.13	8.30	8.47	8.64	8.81	8.98	9.15	9.32	9.49	9.66
Carchesium polypinum	25	0	67	87	70	30	8	11	0	17	0	0	100	0	0
Codonella cratera	0	0	7	11	20	31	35	61	100	65	11	8	0	0	0
Coleps hirtus	17	0	73	63	40	45	86	100	52	55	55	20	82	82	0
Coleps hirtus var. *lacustris*	0	0	0	5	15	28	32	100	53	8	68	23	0	0	0
Colpidium campylum	25	0	20	100	35	29	7	0	0	0	0	0	0	0	0
Colpidium colpoda	0	0	65	100	58	22	22	0	0	0	0	0	0	0	0
Epistylis plicatilis	10	0	0	5	6	1	2	4	0	7	0	100	20	0	0
Epistylis pyriformis	0	0	0	2	12	19	4	58	26	100	2	6	0	0	6
Glaucoma scintillans	0	0	12	100	32	30	28	8	0	0	0	9	0	0	0
Paramecium caudatum	41	12	82	100	46	31	1	4	0	10	9	0	23	0	0
Paramecium putrinum	31	0	73	100	26	15	10	0	5	0	0	0	0	16	0
Phascolodon vorticella	18	8	7	6	15	24	27	35	53	91	43	100	53	30	13
Prorodon teres	29	50	22	2	10	4	1	4	22	8	0	0	100	17	0
Pseudovorticella margaritata	45	88	100	94	60	57	45	43	10	65	69	0	88	75	63
Staurophrya elegans	0	0	21	9	25	24	17	8	83	100	7	0	56	24	9
Stentor polymorphus	0	100	100	83	52	57	42	28	63	96	38	13	25	0	0
Stokesia vernalis	0	0	0	4	11	13	14	13	25	81	0	10	100	12	0
Strobilidium caudatum	75	0	0	32	0	9	0	0	17	83	25	0	0	100	100
Strombidium viride	0	0	100	55	47	26	40	7	65	70	45	0	0	0	0
Tintinnidium fluviatile	1	0	3	20	45	44	42	100	29	38	19	14	0	6	0
Trithigmostoma cucullulus	77	100	32	5	6	5	0	0	0	0	0	0	0	0	0
Urotricha farcta	0	0	24	5	10	30	10	29	48	36	46	100	0	0	0
Vorticella campanula	38	25	88	55	57	31	7	14	52	57	36	1	100	78	0
Vorticella convallaria	0	0	100	45	26	12	15	3	6	10	80	0	0	0	52
Vorticella incisa	19	0	100	27	25	47	13	35	43	63	4	38	30	53	0
Vorticella microstoma	100	0	26	58	22	7	5	0	34	6	32	0	65	71	0
Vorticella nebulifera	0	5	34	100	36	20	27	16	15	33	12	14	10	15	13
Vorticella similis	31	4	53	20	26	35	37	73	97	82	100	35	37	55	49
Zoothannium minimum	100	0	89	49	45	55	33	74	33	11	17	0	0	0	0
Zoothannium varians	100	33	44	94	63	25	36	7	8	11	42	0	67	0	0

Table 6

The weighted abundance frequency distributions of species related to the classes of dissolved oxygen content

class mean (mg l^{-1}) Species	6.9	7.6	8.4	9.1	9.9	10.6	11.4	12.1	12.9	13.6	14.4	15.1	15.9	16.6	17.4
Carchesium polypinum	0	40	40	92	57	72	100	15	0	0	24	0	0	0	0
Codonella cratera	13	6	23	13	10	5	4	20	42	13	11	0	3	100	10
Coleps hirtus	22	39	37	33	35	29	33	23	46	100	40	17	42	0	0
Coleps hirtus var. *lacustris*	11	3	6	9	8	38	6	13	56	0	73	17	25	0	100
Colpidium campylum	3	28	22	43	70	16	26	100	0	0	4	0	0	0	0
Colpidium colpoda	0	9	0	48	51	7	30	100	0	0	0	0	0	0	0
Epistylis plicatilis	0	92	13	20	43	10	0	50	33	0	10	100	0	0	0
Epistylis pyriformis	6	2	1	2	1	3	8	15	2	5	5	0	1	100	2
Glaucoma scintillans	44	22	13	100	47	14	8	64	0	0	0	0	0	0	0
Paramecium caudatum	60	87	97	100	97	25	80	11	21	36	4	0	14	0	0
Paramecium putrinum	47	35	57	75	36	78	51	100	8	24	0	0	0	0	0
Phascolodon vorticella	80	25	15	17	11	28	37	14	66	89	100	16	84	21	18
Prorodon teres	0	11	6	29	15	53	83	8	67	100	13	67	0	67	0
Pseudovorticella margaritata	22	69	71	83	59	51	21	26	22	28	36	33	69	100	22
Staurophrya elegans	11	8	1	13	8	4	42	3	7	100	27	0	9	27	6
Stentor polymorphus	93	42	48	48	65	32	38	38	57	30	36	10	15	100	40
Stokesia vernalis	26	10	3	9	8	9	8	11	12	7	26	5	0	100	0
Strobilidium caudatum	0	0	3	1	4	0	27	0	27	40	0	100	20	0	0
Strombidium viride	13	10	17	24	27	46	47	0	37	100	16	40	30	0	0
Tintinnidium fluviatile	73	29	36	47	22	100	46	26	54	68	84	9	52	57	23
Trithigmostoma cucullulus	10	22	28	51	100	19	36	65	3	0	0	0	0	0	0
Urotricha farcta	100	23	16	5	5	11	20	6	20	11	22	0	36	0	22
Vorticella campanula	28	33	28	73	34	23	44	26	64	100	32	56	38	0	10
Vorticella convallaria	11	83	75	81	95	98	53	92	25	17	20	50	58	0	100
Vorticella incisa	12	58	45	34	35	30	36	13	79	18	91	100	18	0	0
Vorticella microstoma	20	25	22	45	60	40	33	60	100	60	8	30	50	0	0
Vorticella nebulifera	39	24	38	60	100	22	10	25	13	14	28	8	119	18	21
Vorticella similis	27	22	12	11	10	20	23	14	24	58	44	12	40	14	100
Zoothamnium minimum	100	19	39	12	36	32	8	8	17	0	27	0	8	0	0
Zoothamnium varians	20	27	33	30	44	47	23	23	5	0	12	0	5	0	100

Table 7

The weighted abundance frequency distributions of species related to the classes of chemical oxygen demand

class mean (mg l^{-1}) Species	4.9	5.8	6.7	7.6	8.5	9.4	10.3	11.2	12.1	13.0	13.9 ,	14.8	15.7	16.6	17.5
Carchesium polypinum	78	36	83	25	54	0	0	0	0	0	0	0	0	0	100
Codonella cratera	100	57	76	49	40	15	0	0	0	0	0	0	0	0	0
Coleps hirtus	29	40	43	55	19	40	27	20	20	100	0	0	0	0	20
Coleps hirtus var. *lacustris*	7	13	15	31	5	29	0	33	0	100	0	0	0	0	0
Colpidium campylum	5	54	100	50	13	13	48	0	0	0	0	0	0	0	0
Colpidium colpoda	0	39	100	29	34	13	0	0	0	0	0	0	0	0	0
Epistylis plicatilis	6	11	9	37	0	0	0	0	100	0	0	0	0	0	0
Epistylis pyriformis	10	37	42	38	74	16	0	0	0	100	0	0	0	0	0
Glaucoma scintillans	11	54	100	80	2	55	0	0	0	0	0	0	0	0	0
Paramecium caudatum	28	64	94	49	19	77	61	0	0	100	0	0	0	0	33
Paramecium putrinum	65	87	77	100	90	55	73	0	0	0	0	0	0	0	0
Phascolodon vorticella	18	40	31	82	38	70	59	25	25	100	0	0	0	0	6
Prorodon teres	15	3	10	20	33	25	100	0	67	33	0	0	0	0	0

Pseudovorticella margaritata	48	58	80	75	54	60	100	78	0	0	0	0	0	0	26
Staurophrya elegans	14	32	51	100	16	85	32	0	0	19	0	0	0	0	0
Stentor polymorphus	14	21	26	26	15	34	13	10	0	100	0	0	0	0	0
Stokesia vernalis	33	38	52	100	85	13	67	40	20	0	0	0	0	0	0
Strobilidium caudatum	0	2	5	1	9	0	0	100	0	0	0	0	0	0	0
Strombidium viride	33	46	30	26	21	38	83	100	0	0	0	0	0	0	0
Tintinnidium fluviatile	30	48	27	28	7	18	2	7	5	100	0	0	0	0	2
Trithigmostoma cucullulus	9	55	100	28	34	40	47	0	0	0	0	0	0	0	40
Urotricha farcta	2	9	17	28	0	41	0	0	0	100	0	0	0	0	0
Vorticella campanula	18	29	54	41	41	27	85	68	36	100	0	0	0	0	9
Vorticella convallaria	43	75	100	36	40	14	28	55	28	28	0	0	0	0	0
Vorticella incisa	7	13	20	27	20	14	64	100	0	18	0	0	0	0	0
Vorticella microstoma	4	8	20	31	57	33	89	33	0	0	0	0	0	0	100
Vorticella nebulifera	29	100	89	30	9	22	9	23	0	11	0	0	0	0	0
Vorticella similis	25	49	47	100	46	99	41	74	0	12	0	0	0	0	49
Zoothamnium minimum	11	28	37	43	23	56	100	0	0	50	0	0	0	0	0
Zoothamnium varians	17	23	19	17	13	20	13	0	0	0	0	0	0	0	100

Table 8

The weighted abundance frequency distributions of species related to the classes of total dissolved solids

class mean (mg l^{-1}) Species	230	254	270	286	302	318	334	350	366	382	398	414	430	446	462
Carchesium polypinum	0	0	7	12	34	11	2	10	51	22	89	100	0	0	0
Codonella cratera	100	56	51	72	61	24	33	25	29	9	0	4	0	0	32
Coleps hirtus	8	27	5	6	24	15	18	27	17	25	3	27	41	0	100
Coleps hirtus var. *lacustris*	26	6	18	7	33	19	23	100	16	13	0	0	0	0	0
Colpidium campylum	0	0	1	1	1	7	2	3	23	50	71	100	15	0	61
Colpidium colpoda	0	0	0	0	0	14	3	10	32	78	100	95	17	0	0
Epistylis plicatilis	32	32	49	0	25	31	100	32	35	16	0	0	0	0	0
Epistylis pyriformis	0	31	10	100	23	100	6	32	79	23	0	12	8	0	0
Glaucoma scintillans	0	0	0	1	4	5	9	20	20	65	100	54	49	0	0
Paramecium caudatum	1	1	0	2	11	6	7	19	45	27	6	37	27	0	100
Paramecium putrinum	0	0	7	7	3	10	22	24	41	84	100	47	19	0	94
Phascolodon vorticella	10	58	23	42	93	94	59	100	43	36	1	1	1	0	0
Prorodon teres	32	0	13	19	18	31	17	15	19	11	100	11	21	0	0
Pseudovorticella margaritata	37	44	17	62	54	38	19	60	100	91	0	74	88	0	59
Staurophrya elegans	0	2	14	51	100	29	30	94	64	71	0	2	20	0	26
Stentor polymorphus	9	9	4	10	17	11	10	21	45	34	5	7	4	0	100
Stokesia vernalis	0	18	37	100	32	54	18	14	41	7	0	0	0	0	0
Strobilidium caudatum	0	40	0	29	49	23	18	11	44	100	0	0	0	0	0
Strombidium viride	10	0	90	84	100	84	12	30	34	63	0	0	0	0	84
Tintinnidium fluviatile	29	100	31	16	48	86	28	31	27	28	1	2	13	0	19
Trithigmostoma cucullulus	0	0	1	1	5	17	2	15	61	68	29	96	64	0	100
Urotricha farcta	16	24	12	17	37	29	43	91	48	100	0	0	80	0	0
Vorticella campanula	6	8	15	29	45	26	17	82	70	96	81	36	29	0	100
Vorticella convallaria	0	2	1	5	16	8	12	6	44	47	31	22	3	0	100
Vorticella incisa	100	38	12	55	34	31	32	25	26	63	0	8	0	0	0
Vorticella microstoma	8	0	6	6	7	27	26	10	35	76	13	58	100	0	10
Vorticella nebulifera	7	9	5	6	18	12	8	11	100	48	17	47	8	0	39
Vorticella similis	9	40	18	18	43	25	30	63	9	42	4	10	19	0	100
Zoothamnium minimum	0	0	2	8	8	5	4	6	15	18	22	3	0	0	100
Zoothamnium varians	5	2	5	2	8	9	13	21	26	20	61	20	41	0	100

Table 9

The weighted abundance frequency distributions of species related to the classes of ammonium content

class mean (mg l^{-1}) Species	0.00	0.04	0.11	0.18	0.25	0.32	0.39	0.46	0.53	0.60	0.67	0.74	0.81	0.88	0.95
Carchesium polypinum	6	0	71	0	20	36	12	100	18	0	71	0	0	0	18
Codonella cratera	0	34	9	100	61	30	39	13	12	0	9	0	0	0	13
Coleps hirtus	100	41	47	40	5	8	16	0	0	11	0	0	0	0	32
Coleps hirtus var. *lacustris*	0	100	0	25	82	25	12	6	32	0	0	0	0	0	0
Colpidium campylum	0	1	48	0	0	0	12	100	25	0	53	0	61	30	0
Colpidium colpoda	0	3	0	0	0	0	10	40	8	0	0	100	50	0	23
Epistylis plicatilis	100	0	0	0	0	42	16	0	0	0	0	0	0	0	0
Epistylis pyriformis	0	27	4	7	33	13	100	6	11	0	15	0	0	6	0
Glaucoma scintillans	0	6	17	0	0	0	17	48	12	0	3	0	100	67	0
Paramecium caudatum	9	91	0	0	0	15	8	100	29	0	15	10	66	0	0
Paramecium putrinum	0	4	52	0	0	0	50	61	35	0	7	0	89	100	0
Phascolodon vorticella	87	2	32	36	60	14	100	6	14	0	32	0	7	0	1
Prorodon teres	0	100	100	100	50	15	0	0	0	0	100	0	0	0	75
Pseudovorticella margaritata	0	45	100	41	71	33	88	84	24	0	91	0	88	31	57
Staurophrya elegans	0	39	100	97	5	16	22	73	4	0	42	0	19	0	5
Stentor polymorphus	0	25	90	4	22	6	11	100	35	0	14	0	54	0	16
Stokesia vernalis	3	0	100	0	13	5	58	8	3	0	10	0	0	0	0
Strobilidium caudatum	0	0	100	18	0	0	0	0	0	0	0	0	0	0	0
Strombidium viride	0	12	24	0	0	19	100	24	24	0	0	0	0	0	0
Tintinnidium fluviatile	13	4	2	10	41	13	100	3	5	0	40	1	8	0	3
Trithigmostoma cucullulus	1	52	0	0	0	5	3	83	14	0	0	100	40	0	11
Urotricha farcta	100	65	97	19	33	22	35	21	5	0	10	0	0	0	0
Vorticella campanula	23	100	13	3	10	22	22	55	32	0	24	39	17	0	17
Vorticella convallaria	0	1	100	4	29	6	7	86	15	0	29	0	53	63	7
Vorticella incisa	0	30	46	100	33	15	6	13	13	0	42	0	0	3	13
Vorticella microstoma	0	7	24	0	0	0	6	3	39	0	39	0	0	100	41
Vorticella nebulifera	0	4	16	6	11	7	16	100	24	0	19	0	32	0	5
Vorticella similis	0	51	100	25	77	53	20	0	20	0	17	0	0	14	42
Zoothamnium minimum	0	29	100	0	8	0	17	49	3	0	15	0	23	0	0
Zoothamnium varians	0	6	100	0	18	10	20	82	15	0	14	0	0	7	14

Table 10

The weighted abundance frequency distributions of species related to the classes of psychrophile bacterial count

class mean (ind l^{-1}) Species	0.7	2.1	3.5	4.9	6.3	7.7	9.1	10.5	11.9	13.3	14.7	16.1	17.5	18.9	20.3
Carchesium polypinum	0	3	17	11	0	0	100	0	0	23	45	0	0	90	0
Codonella cratera	45	45	27	19	24	51	70	82	6	0	0	0	0	0	100
Coleps hirtus	0	73	60	60	100	53	51	76	59	0	25	51	13	25	13
Coleps hirtus var. *lacustris*	0	42	51	42	9	10	64	100	0	0	0	0	0	0	50
Colpidium campylum	0	0	2	7	31	0	37	0	100	2	0	29	62	0	0
Colpidium colpoda	0	0	1	6	20	0	38	0	100	0	0	40	100	0	0
Epistylis plicatilis	0	100	5	0	27	43	24	0	36	0	0	0	0	0	0
Epistylis pyriformis	0	100	24	7	4	4	4	0	0	25	13	0	0	0	0
Glaucoma scintillans	0	3	4	2	28	0	47	0	29	2	0	100	68	0	0
Paramecium caudatum	0	7	18	28	19	0	100	0	40	4	17	0	8	51	0
Paramecium putrinum	0	0	7	17	17	0	4	0	56	25	0	100	25	0	0
Phascolodon vorticella	5	83	71	20	13	16	33	0	8	100	0	0	0	13	11
Prorodon teres	0	38	23	8	38	40	22	0	33	0	100	0	50	0	0

Pseudovorticella margaritata	0	26	20	20	21	23	48	0	29	9	36	32	7	100	32
Staurophrya elegans	0	38	38	12	9	7	27	0	24	0	100	0	0	0	0
Stentor polymorphus	20	58	40	52	25	8	88	0	67	50	100	0	0	80	20
Stokesia vernalis	18	71	29	12	14	22	18	0	0	100	0	0	0	0	0
Strobilidium caudatum	0	0	0	0	0	0	0	0	0	0	0	0	0	100	0
Strombidium viride	0	100	28	23	0	65	3	0	36	0	0	0	0	0	0
Tintinnidium fluviatile	6	100	47	13	17	20	25	0	1	17	27	0	1	12	54
Trithigmostoma cucullulus	0	0	3	16	11	0	62	0	87	4	31	0	100	0	0
Urotricha farcta	0	28	44	12	19	3	13	0	25	100	0	0	0	0	30
Vorticella campanula	3	23	19	17	17	5	89	0	57	5	100	6	18	19	0
Vorticella convallaria	0	2	6	18	18	0	32	0	100	7	35	84	17	56	0
Vorticella incisa	0	6	7	6	6	3	5	4	15	5	4	0	19	4	100
Vorticella microstoma	0	0	2	15	10	4	11	0	37	0	0	100	50	0	0
Vorticella nebulifera	14	27	30	18	27	9	53	0	49	25	93	0	30	100	16
Vorticella similis	13	78	98	67	52	40	76	0	73	38	100	13	6	6	50
Zoothamnium minimum	0	15	41	88	0	20	39	0	67	50	50	0	100	100	0
Zoothamnium varians	0	15	22	40	38	7	56	0	75	13	100	0	75	25	0

Table 11

The weighted abundance frequency values of species related to the classes of *Coli*-form bacterial count

class mean (ind l^{-1}) Species	0	35	105	175	245	315	385	455	525	595	665	735	805	875	945
Carchesium polypinum	8	2	3	7	2	3	0	0	100	0	0	0	15	77	15
Codonella cratera	11	23	15	15	13	31	100	0	11	0	0	0	0	6	0
Coleps hirtus	66	23	80	40	78	100	60	27	93	0	0	0	27	53	0
Coleps hirtus var. *lacustris*	25	31	80	23	24	23	88	0	0	0	0	0	0	0	100
Colpidium campylum	6	1	0	2	0	3	23	67	0	0	0	0	0	100	0
Colpidium colpoda	14	0	1	3	0	0	29	64	0	0	0	0	0	100	36
Epistylis plicatilis	36	100	2	12	9	3	18	0	36	0	0	0	0	0	0
Epistylis pyriformis	10	100	34	31	31	67	10	0	10	0	0	0	20	0	0
Glaucoma scintillans	2	0	3	4	0	3	12	100	28	0	0	0	0	84	96
Paramecium caudatum	14	1	3	7	2	17	2	6	100	0	0	0	6	55	67
Paramecium putrinum	0	4	5	10	0	26	33	100	0	0	0	0	0	33	0
Phascolodon vorticella	5	100	100	30	73	12	52	0	63	0	0	0	0	0	4
Prorodon teres	0	10	13	27	24	15	100	0	0	0	0	0	80	0	0
Pseudovorticella margaritata	6	6	14	10	18	20	20	0	100	0	0	0	23	35	32
Staurophrya elegans	15	28	10	34	37	14	18	0	79	0	0	0	100	3	41
Stentor polymorphus	25	17	12	9	22	33	4	17	100	0	0	0	42	17	100
Stokesia vernalis	0	100	26	26	72	16	68	0	25	0	0	0	0	0	0
Strobilidium caudatum	0	0	0	100	0	0	0	0	0	0	0	0	0	0	0
Strombidium viride	0	7	100	16	38	16	0	0	0	0	0	0	0	0	0
Tintinnidium fluviatile	3	42	100	32	34	38	90	3	52	0	0	0	35	8	11
Trithigmostoma cucullulus	3	1	1	2	0	7	12	9	18	0	0	0	9	100	24
Urotricha farcta	68	22	100	32	73	35	27	0	0	0	0	0	0	0	0
Vorticella campanula	10	3	6	4	4	10	3	25	71	0	0	0	30	0	100
Vorticella convallaria	50	11	5	13	4	32	23	20	100	0	0	0	33	13	20
Vorticella incisa	12	100	27	62	37	30	17	0	0	0	0	0	23	0	0
Vorticella microstoma	7	0	9	17	6	14	29	0	0	0	0	0	0	100	0
Vorticella nebulifera	100	7	12	12	12	21	28	28	73	0	0	0	51	18	28
Vorticella similis	0	92	80	71	87	69	50	0	72	0	0	0	100	0	31
Zoothamnium minimum	100	7	24	8	13	60	21	0	57	0	0	0	29	29	0
Zoothamnium varians	100	15	13	19	9	36	30	20	60	0	0	0	80	100	100

REFERENCES

Bereczky M. Cs. (1969) Untersuchungen über die Protozoenfauna der Donau bei Alsógöd (Ungarn). Danub. Hung. LII. Opusc. Zool. Budapest 9: 87-96.

Bereczky M. Cs. (1971) Einfluss der Wassertemperatur auf die Gestaltung der Ciliatenfauna im Donauabschnitt bei Alsógöd. Danub. Hung. LVI. Ann. Univ. Sci. Budapest, Sect. Biol. 13: 291-294.

Bereczky M. Cs. (1973) Kennzeichnung der saprobiologischen Verhältnisse der Donauabschnittes bei Budapest und Unterhalb von Budapest durch bioindikative Ciliaten. 16. Arbeitstagung der IAD: 1-6.

Bereczky M. Cs. (1976-1977) Kurzfristige Untersuchungen über die Auswirkung des abnehmenden Donauwasserstandes auf die planktische Ciliatenpopulation und die Gestaltung ihrer saprobiologischen Verhältnisse. Danub.Hung. LXXII. Ann. Univ. Sci. Budapest, Sect. Biol. 18-19: 179-188.

Bereczky M. Cs. (1978) Gestaltung der Ciliata- und Testaceapopulationen der Donau unter der Einwirkung des Flussregimes und der Wasserkunstbauten zwischen Vác und Göd. Danub. Hung. LXXXIX. Ann. Univ. Sci. Budapest, Sect. Biol. 20-21: 105-227.

Bereczky M. Cs. (1985) Fixations- und Färbungsschnellverfahren bei quantitativen Ökologische Untersuchungen von Protozoen in Binnengewässern. Arch. Protistenk. 129: 187-190.

Bick H. (1966a) Ökologische Untersuchungen an Ciliaten des Saprobiensystems. I. Beitrag zur Autoökologie von *Cyclidium citrullus, Glaucoma scintillans, Litonotus lamella* und *Paramecium caudatum*. Int.Revue ges. Hydrobiol. 51: 489-520.

Bick H. (1966b) Ökologische Untersuchungen an Ciliaten des Saprobiensystems. II. Ergebnisse von Sukzessionsstudien mit besonderer Berücksichtigung der Autökologie von *Coleps hirtus*. Verh. IVL. (Warschau) 16: 845-853.

Bick H. (1968) Autökologische und saprobiologische Untersuchungen an Süsswasserciliaten. Hydrobiologia (Den Haag) 31: 17-36.

Bick H. (1972a) Ciliated Protozoa. An illustrated guide to the species used as biological indicators in freshwater biology. World Health Organization, Geneva.

Bick H. (1972b). Ciliata. Die Binnengewässer. (Stuttgart) XXVI/1: 31-83.

Cairns J. Jr. (1965) The environmental requirements of freshwater protozoa. Biol. Problems in Water Pollution. Third Seminar, 1962: 48-52.

Cairns J. Jr. (1986) Management of water quality and natural habitats to enhance both human and wildlife needs. Environmental Regeneration II.: Praeger Publisher, Philadelphia, Pennsylvania, 86-99.

Corliss J. O. (1979) The Ciliated Protozoa. 2ed. Pergamon Press Inc., New York 10523, USA.

Foissner W. (1988) Taxonomic and nomenclatural revision of Sládecek's list of ciliates (Protozoa: Ciliophora) as indicators of water quality. Hydrobiologia 166: 1-64.

Heuss K., Wilbert N. (1973). Zur Morphologie und Ökologie von *Trochilia minuta* Roux,1901 (Ciliata, Cyrtophorina). Gewässer and Abwasser, 52: 32-43.

Pratt J. R., Cairns J. Jr. (1985) Functional Groups in the Protozoa. Roles in Differing Ecosystems. J.Protozool. 32: 415-423.

Pratt J. R., Horwitz R., Cairus J. Jr. (1987a) Protozoa communities of the Flint River-Lake Blackshear ecosystem (Georgia, USA). Hydrobiologia 148: 159-174.

Pratt J. R. Niederlehner B.R., Bowers N. J., Cairns J. Jr. (1987b) Effects of zinc on freshwater microbial communities. Int. Conference Heavy Metals in the Environment. New Orleans, 2: 324-326.

Pätsch B. (1974) Die Aufwuchsciliaten des Naturlehrparks Haus Wildenrath. Dissertation aus der Math.-Naturwissenschaftlichen Fakultät der Universität Bonn Gefördert durch Sachbeihilfen des Landschaftsverbandes Rheinland, 78.

Schmitz M. M. (1986) Ökologische und systematische Untersuchungen an Ciliaten (Protozoa, Ciliophora) im oberen Niederrhein. Inaugural-Dissertation, Bonn,: 1-246.

Stössel F. (1979) Autökologische Analyse der in schweizerischen Fliessgewässern häufig vorkommenden Ciliatenarten und ihre Eignung als Bioindikatoren. Schweiz. Z. Hydrol. 41: 113-140.

Wilbert N. (1969) Ökologische Untersuchungen der Aufwuchs-und Planktonciliaten eines eutrophen Weihers. Arch. Hydrobiol. 35: 411-518.

Wilbert N. (1974) Eine verbesserte Technik der Protargol-impregnation für Ciliaten. Mikrokosmos 6: 171-178.

Received on 2nd March, 1992; accepted on 17th July, 1992

Acta Protozoologica (1993) 32: 17 - 26

ACTA
PROTOZOOLOGICA

Morphology of the Gametocysts and Oocysts of *Gregarina korogi* Hoshide (Apicomplexa, Eugregarinorida)

Kazumi HOSHIDE[*] and Kenneth S. TODD, JR.[**]

[*]Biological Institute, Faculty of Education, Yamaguchi University, Yamaguchi, Japan; [**]Department of Veterinary Pathobiology, College of Veterinary Medicine, University of Illinois, Urbana, USA

Summary. The ultrastructure of gametocysts and oocysts of *Gregarina korogi* Hoshide, 1952 are described for the first time. The ultrastructure of the gametocyst change after they are eliminated from the host. Mature gametocysts were composed of five parts, a wall, homogeneous layer, spongiform layer, centrosphere and sporoduct. The oocysts were covered with thick homogeneous walls and there were three openings in the walls. The oocysts had numerous small projections on the surface and 14 to 15 concentric folds at both ends of the longitudinal axis. Eight sporozoites were arranged longitudinally within the oocysts. The sporozoites usually had one nucleus, but in some no nucleus but elongate strands were present.

Key words. *Gregarina korogi*, gametocyst, oocyst, sporozoite, sporoduct, ultrastructure.

INTRODUCTION

The life cycle of *Gregarina korogi* consists of five stages, sporozoite, cephalin, gamont, gametocyst and oocyst. The former three stages are inside the host's intestine and latter two stages are outside the host. The life cycle is shown by a shematic figure.

There are many reports on the ultrastructure of the gamonts of gregarines (Beam et al. 1957, Desportes 1974, Hoshide 1973, Reger 1967), but there are few reports on the ultrastructure of the gametocysts or oocysts. The difficulty of infiltration of fixation solutions and embedding resin into gametocysts and oocysts hinders making ultra thin sections. In the present study, the infiltration of the embedding resin was not ideal, but the improved methods of infiltration made it possible to produce thin sections and observe the ultrastructure of gametocysts and oocysts. The terminology used in the present study was that proposed by (Levine 1971).

Address for correspondence: K. Hoshide, Biological Institute, Faculty of Education, Yamaguchi University, Yamaguchi 753, Japan.

MATERIALS AND METHODS

Crickets, *Gryllus yemma*, were collected in a field of the suburbs of Yamaguchi City, Japan, in September, 1987 and gametocysts of *Gregarina korogi*, (Hoshide 1952) were collected from their feces. The gametocysts were kept in a moist chamber for several days to allow maturation and then fixed in 5% glutaraldehyde (v/v) in cacodylate buffer pH 7.2 and postfixed with 1.5% osmium tetroxide (w/v) in the same buffer. After fixation, they were dehydrated in a graded series of ethanol and propylene oxide and embedded in araldite. At the time of transition from propylene oxide to embedding resin, the ratio of propylene oxide was gradually decreased and the ratio of araldite increased by 10% each day for 10 days. The blocks

were sectioned with a diamond knife using an LKB Ultratome. The sections were mounted on copper grids, with supporting membrane, double stained with uranyl acetate and lead citrate (Reynolds 1963), and then examined with a JEOL-1200 EX electron microscope.

RESULTS

For the clarity of presentation the following observations will be divided into four parts, gametocysts, sporoducts, oocysts and sporozoites.

Gametocysts

When examined with light microscopy, gametocysts were spherical, brown in colour, varied from 200 to 300 µm in diameter and covered with an outer gelatinous layer and an inner homogeneous layer (Figs. 1, 2).

After the gametocyst were eliminated from the host, the structure of the gametocysts changed rapidly in the moist chamber within a few days.

When first passed in the feces, ultrastructurally, gametocysts consisted of an outer wall and an inner endoplasm. The wall had a uniform thickness of 8 µm. The endoplasm of gametocysts was similar to that of gamonts (Beam et al. 1957, Reger 1967) and contained numerous vacuoles and granules (Fig. 3). One to two days after gametocyst maturation, the outer wall became thick and oocysts appeared in the centrosphere. The mature gametocysts exhibited five parts, an outer wall, a homogeneous space, a spongiform layer, a centrosphere and several sporoducts (Fig. 4). The wall, which increased in thickness during maturation, was composed of many layers of alternating high and low electron density (Fig. 5). The property of the wall was fragile and often fractured during sectioning. Just inside of the wall, lay the homogeneous space. It was not electron dense and had no special structures. The outer boundaries of the homogeneous space were smooth, but the inner limits were irregular (Figs. 4, 5).

The spongiform layer occupied the area between the homogeneous space and the centrosphere. This layer was divided into many small compartments surrounded by thin membranes. The vacuoles, which are similar to those which fill the endoplasm of immature gamonts, and gametocysts became fragments and were scattered in the spongiform layer. Numerous oocysts were formed in the centrosphere region (Fig. 4). The centrosphere was separated from the spongiform layers by thin membranes and contained few structures except the oocysts.

Sporoducts

When the gametocysts were mature, they contained several sporoducts and discharged many oocysts through them at the end of maturation. At the time of discharge the sporoducts everted and extended from the centrosphere through the spongiform layer, the homogeneous space and the gametocyst wall to the exterior. Sporoducts were widest at the base and tapered at the distal tip (Fig. 2). The structure of the sporoducts inside the gametocysts differed at the distal end. Homogeneous spaces surrounded the sporoducts within the gametocysts and they were limited by a single layer. The diameter of the inner tube was approximately the same from the base to the tip except at the entrance of the inner tube the diameters were 4 or 5 times greater than at the other parts. Many oocysts accumulated in this area. A mass of fibrous structures adhered to the inner surface of the outer boundary of the sporoducts at their base (Fig. 6). Outer and inner tubes were observed in cross sections of sporoducts exterior to the gametocysts. The wall of the outer tube was thicker than the wall of the inner tube. The inner wall consisted of 2 double membranes (Fig. 7).

Oocysts

When immature, the oocysts were ovoid or ellipsoid and 2.2 to 2.5 x 4.0 to 4.5 µm. With maturation, they became larger, more elongate and at the time of sporozoites formation were 2.4 to 2.6 x 6.2 to 6.5 µm. They were covered by thick homogeneous walls which were 120 to 140 nm thick (Figs. 8-10). Each oocyst was surrounded by a thin double membrane (Fig. 10). The surfaces were smooth initially, but later numerous small wart-like projections appeared at regular intervals on their surface (Figs. 11-15). There were several openings in the wall along the longitudinal axis.

Oocysts had a series of circular folds on the surface at both ends which consisted of 14 or 15 concentric structures arranged at regular intervals (Figs. 9, 11, 12, 13). The diameters of the circular folds were 1.7 to 2.4 µm and the thicknes of them were 0.3 to 0.8 µm (Figs. 9, 12, 13).

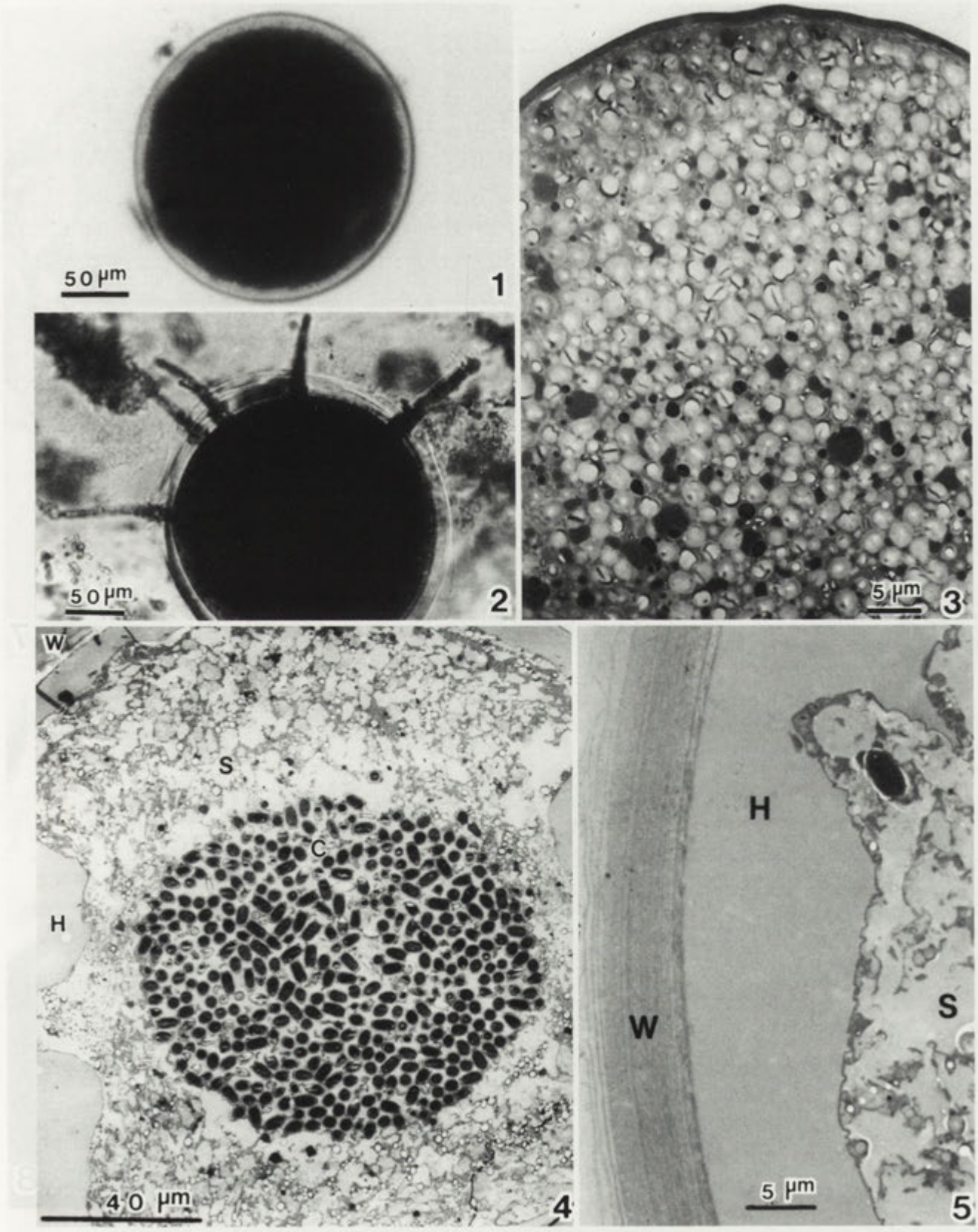

Figs. 1-5. *Gregarina korogi* gametocysts. 1-2 – light microscopy; 1 – immature gametocyst, 2 – matured gametocyst with extruded sporoducts. 3-5 – crosssection of gametocyst ; 3 – immature gametocyst contained numerous vacuoles and gametocyst, 4 – mature gametocyst with many oocysts, 5 – wall. C- centrosphere, H- homogeneous layer, S- spongiform layer, W- wall

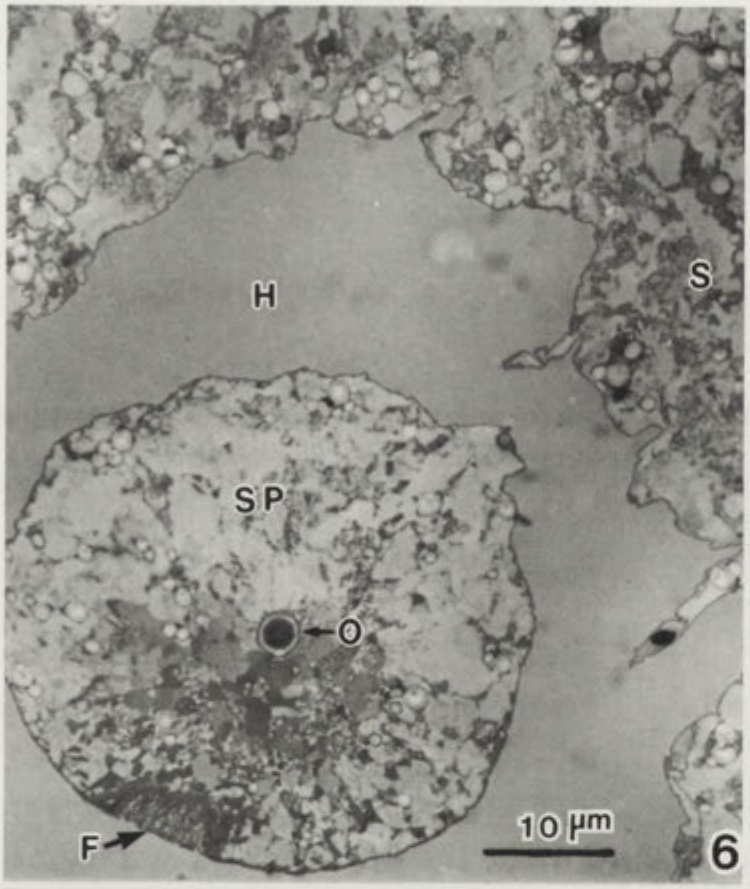

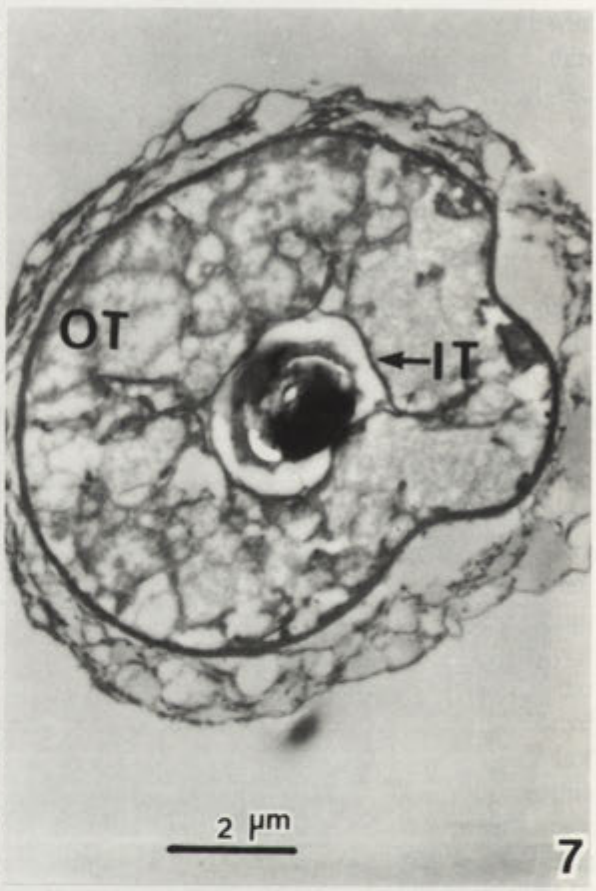

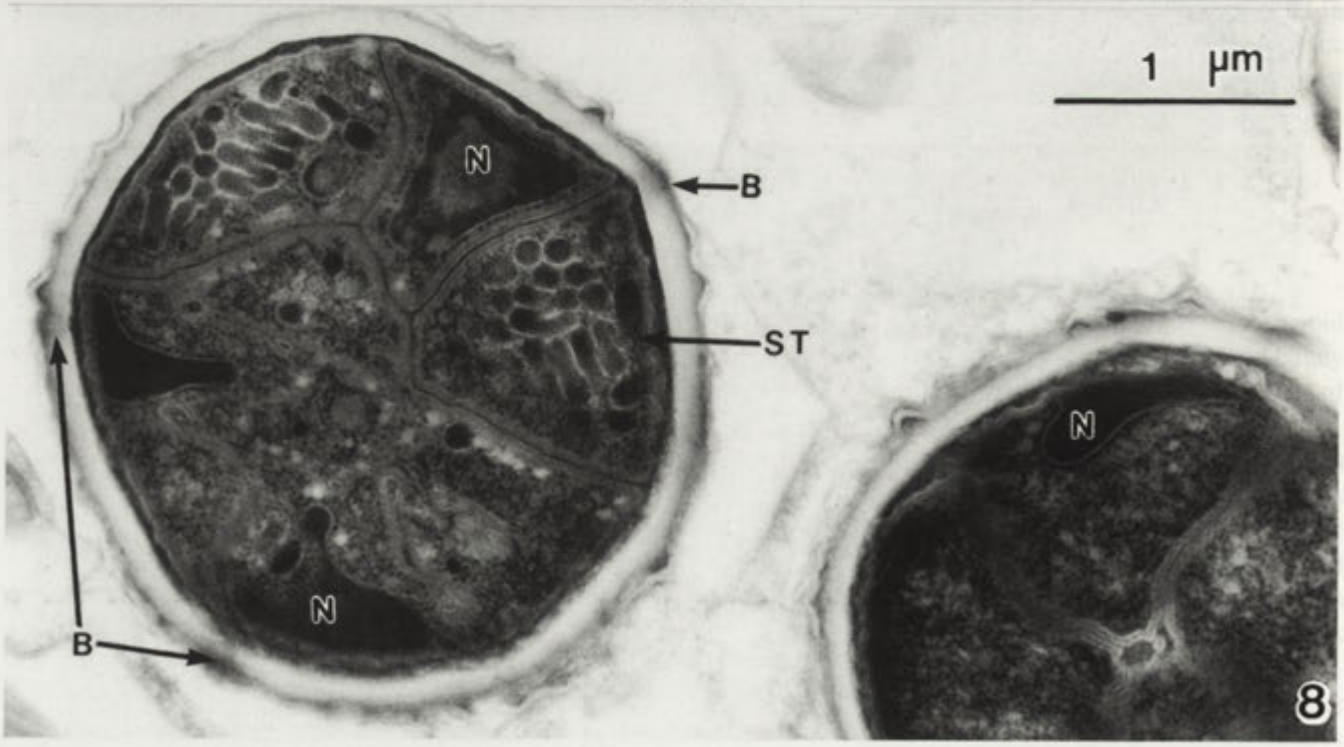

Figs. 6-7. Cross section of sporoduct of *G. korogi*. 6 – sporoduct cross section within a gametocyst, 7 – sporoduct cross section outside a gametocyst. SP- sporoduct, O- oocyst, F- fibrous structure, OT- outer tube, IT- inner tube

Fig. 8. Immature oocyst of *G. korogi*; ST- string-like structures, N- nucleus, B- breaks

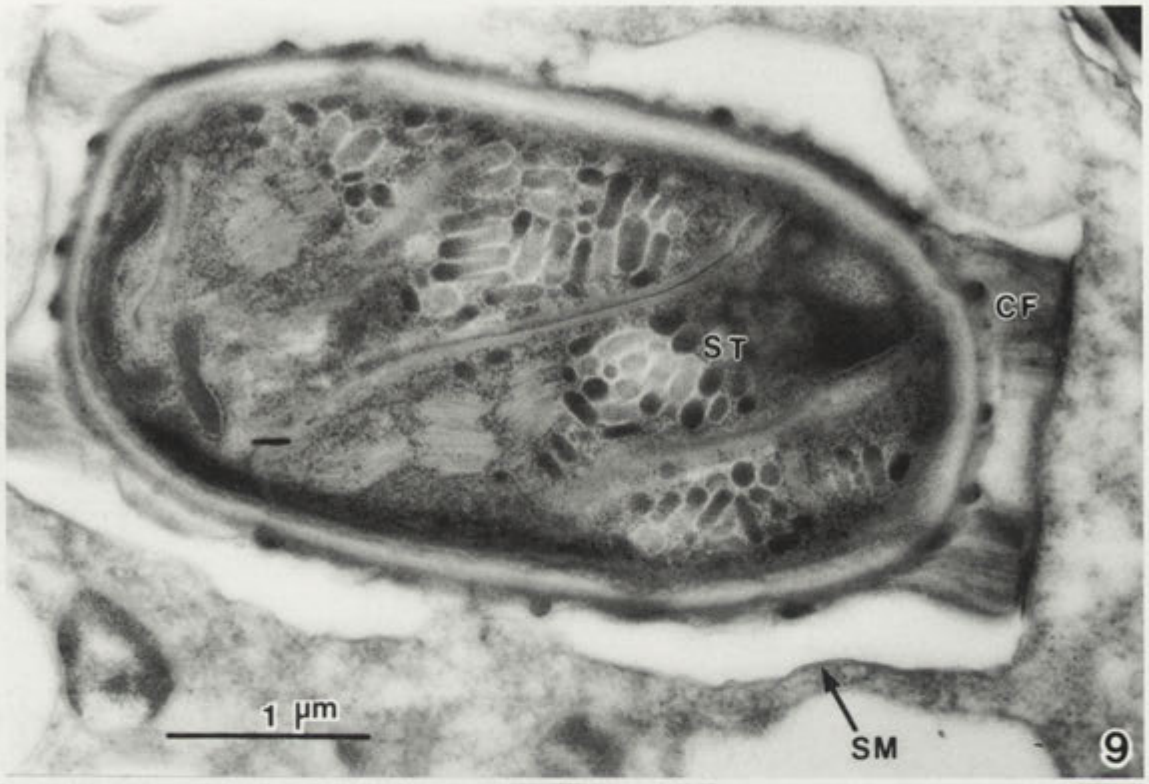

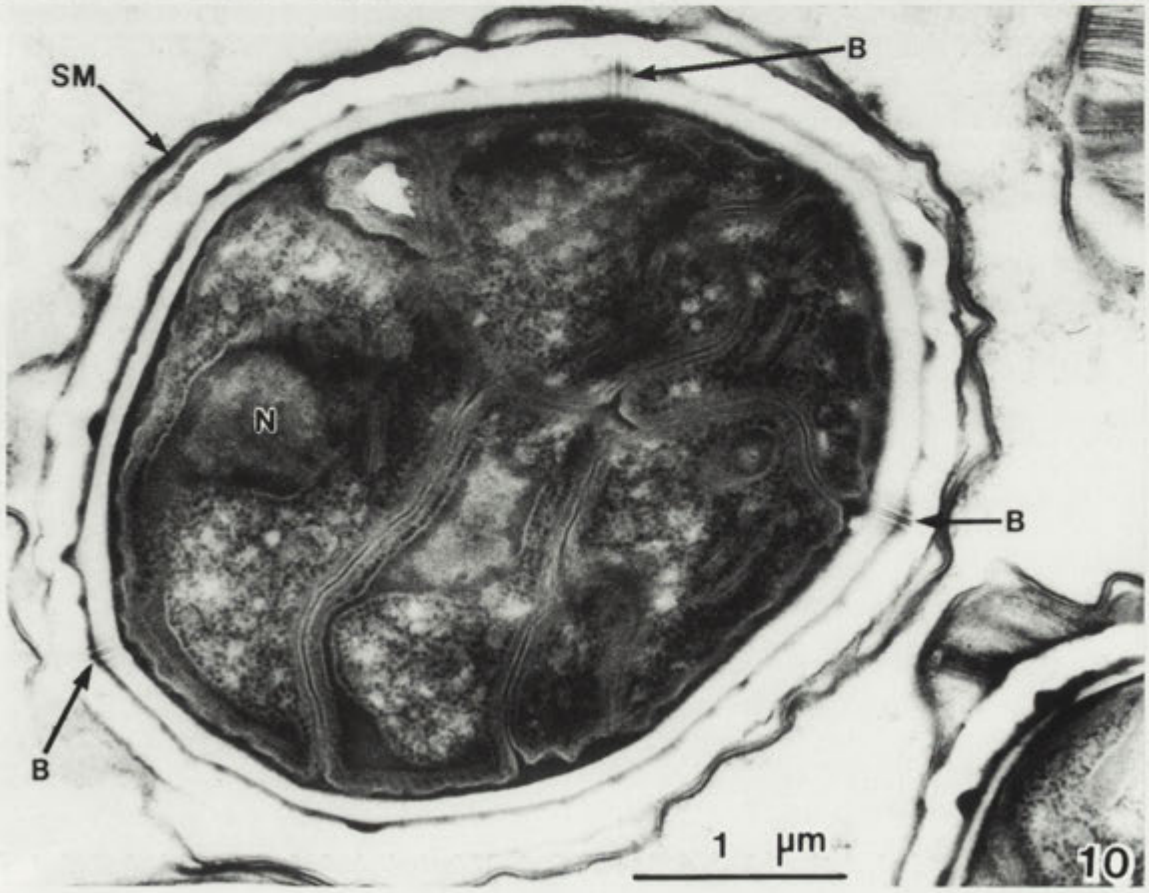

Figs. 9-10. Immature oocyst of *G. korogi*. 9 – immature oocyst-longitudinal section, 10 – immature oocyst-cross section. B- break, CF- circular folds, N- nucleus, SM- surrounding membrane, ST- string-like structures

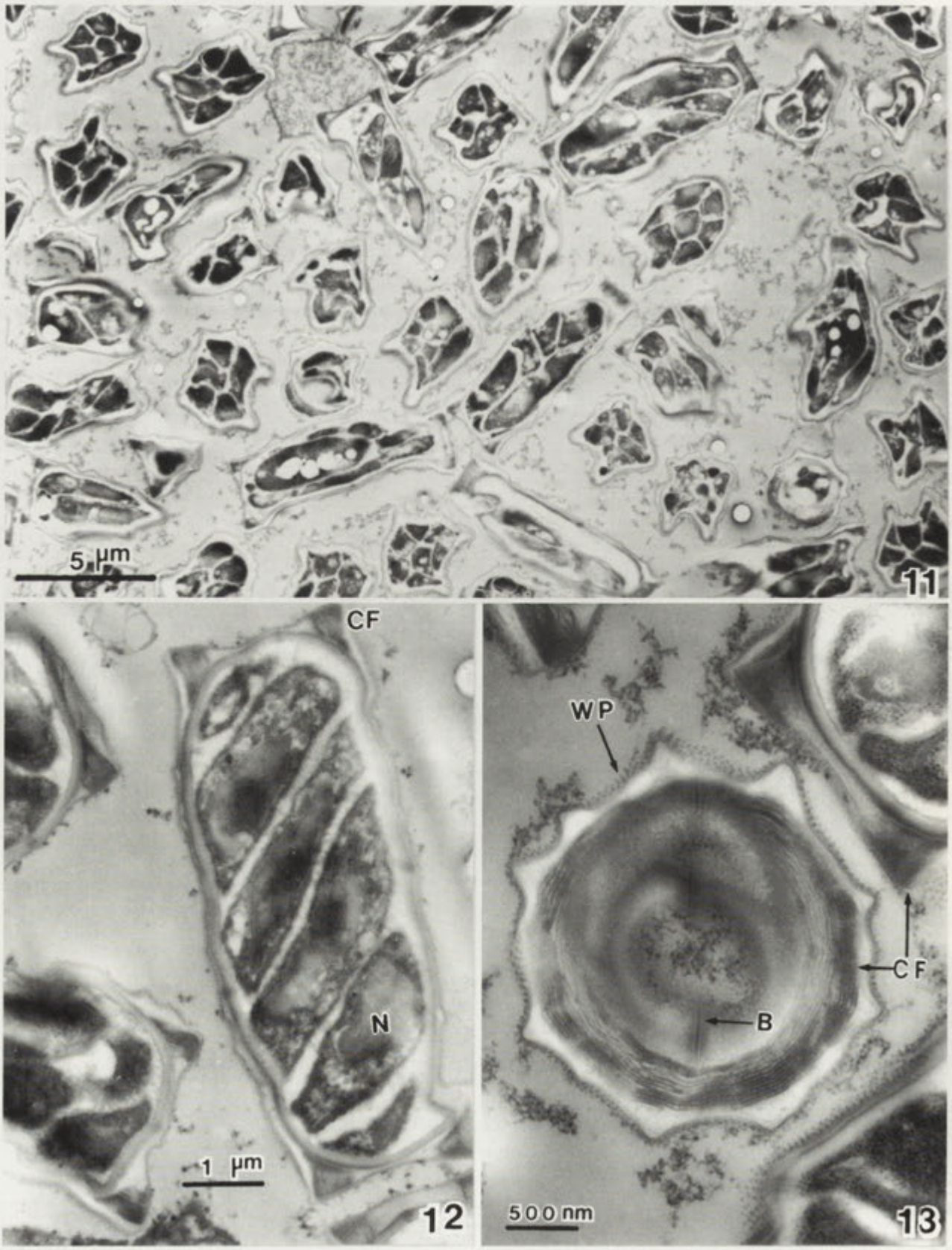

Figs. 11-13. Mature oocyst of *G. korogi*. 11 – many mature oocyst, 12 – mature oocyst longitudinal section, 13 – circular fold cross section. B- breaks, CF- circular folds, N- nucleus, WP- wart-like projections

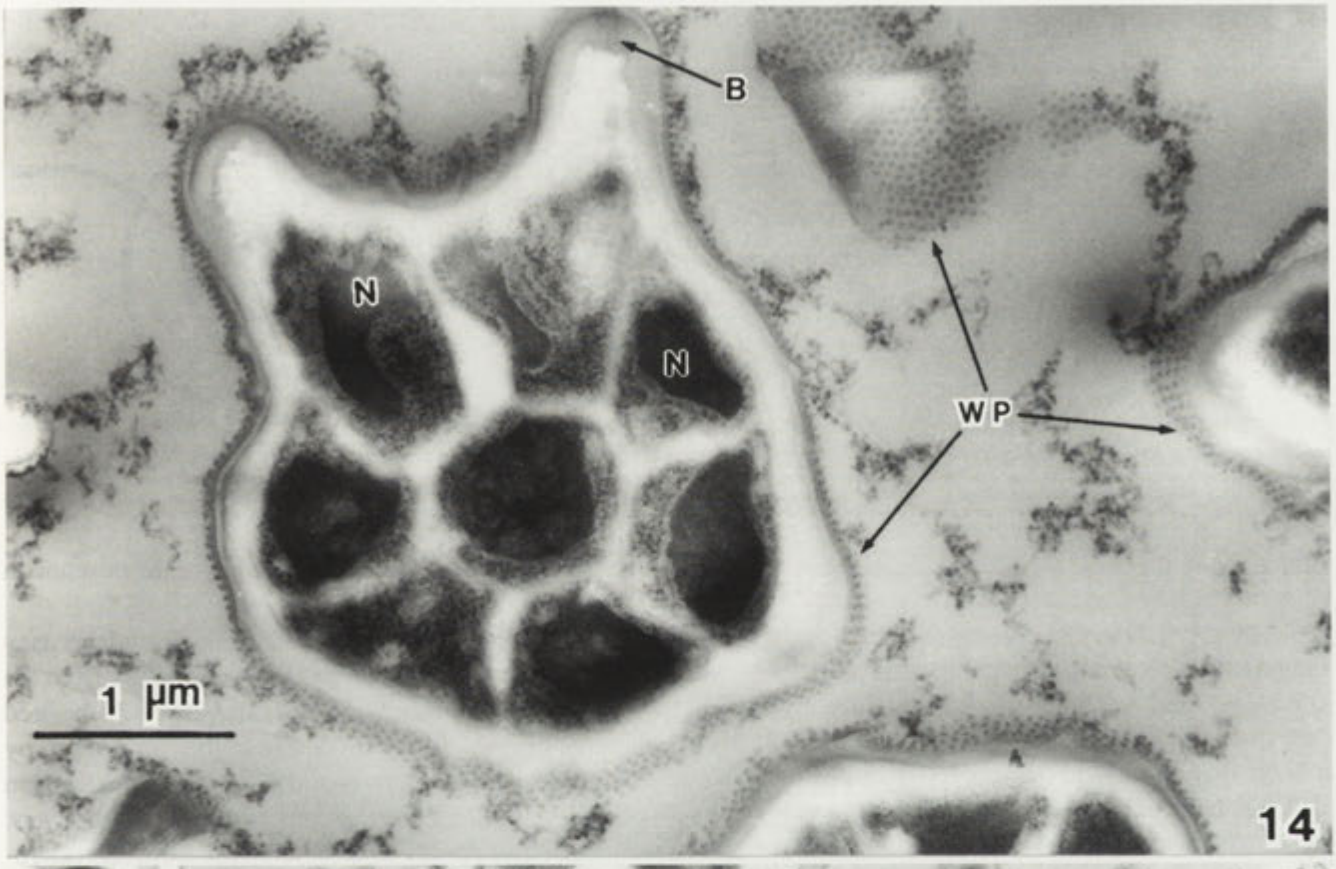

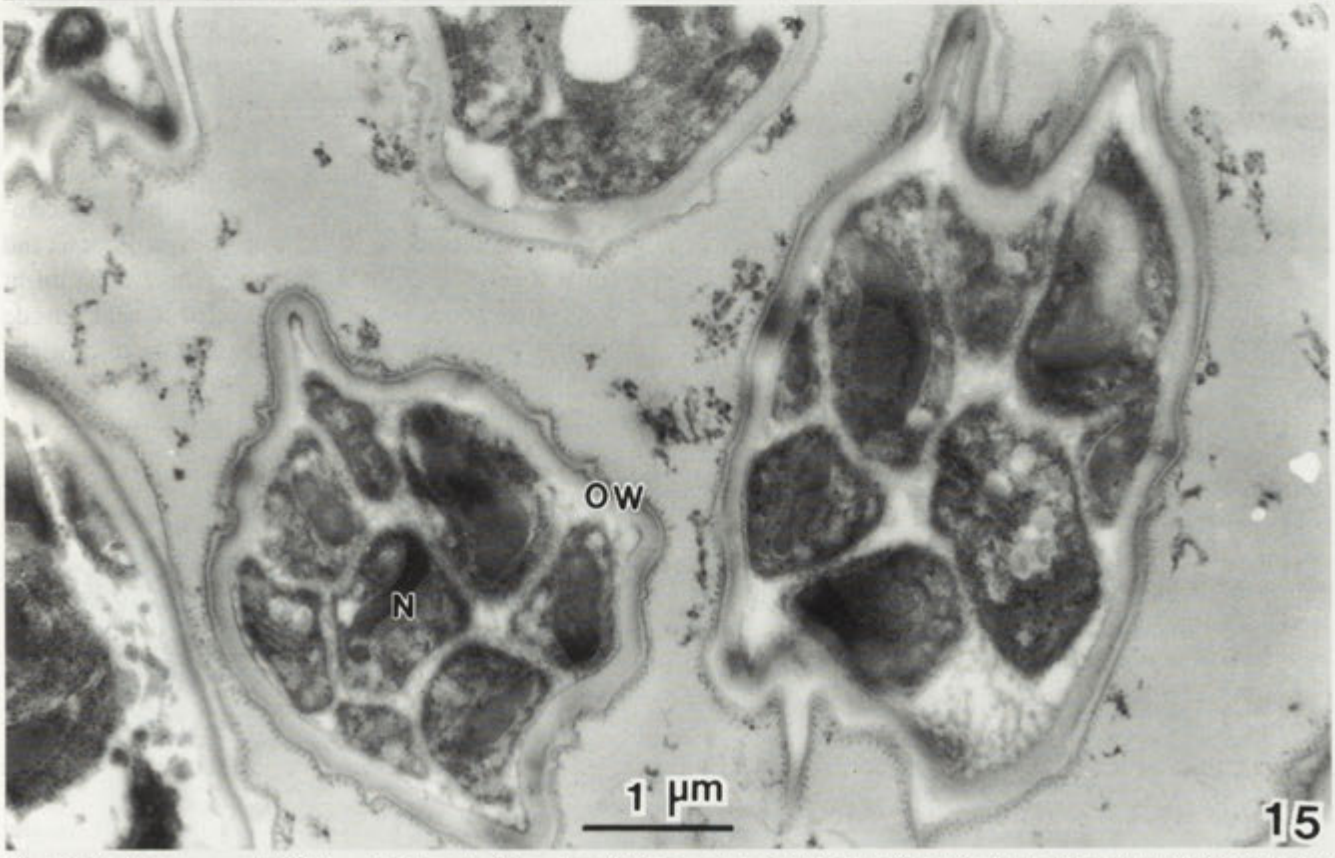

Figs. 14-15. Mature oocyst of *G. korogi*. B- breaks, N- nucleus, OW- oocyst wall, WP- wart-like projections on the surrounding membrane

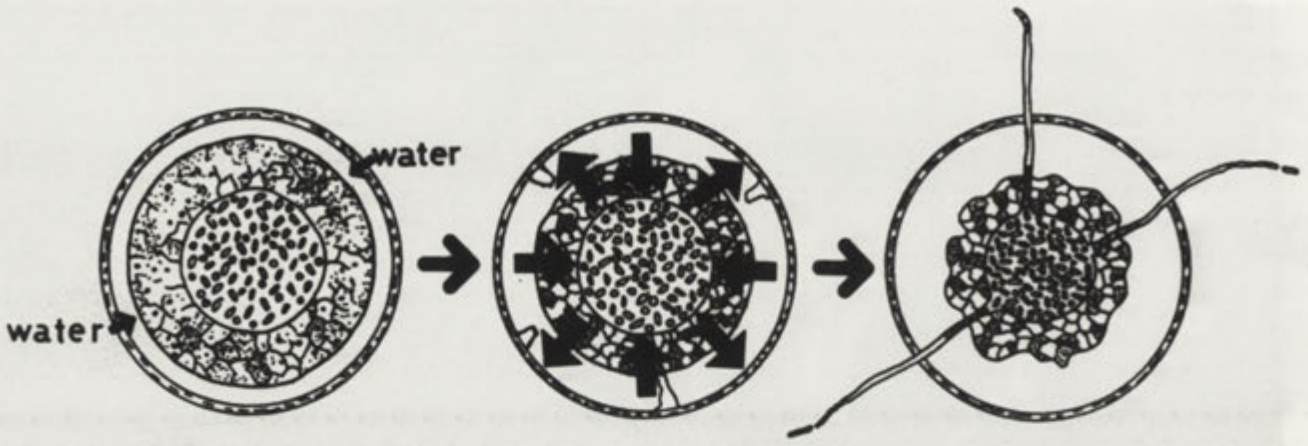

Fig. 16. Diagram of *Gregarina korogi* gametocyst maturation and oocyst discharge

Sporozoites

Oocysts contained 8 sporozoites, which at the beginning of the sporozoite formation, were closely packed and not regularly arranged (Figs. 8-10). In many oocysts, one sporozoite was in the center and the others were around it (Figs. 14, 15). Each sporozoite was covered with a homogeneous membrane and they were separated by a narrow space (Figs. 8-10). Upon maturation the sporozoites elongated and became more slender and appeared spindle- or crescent-shaped and separated from one another within the oocyst. Most sporozoites contained a nucleus but in some, no nucleus was present but elongate strands were observed. The strands had a helical structure and a vacuolated appearance (Figs. 8, 9).

DISCUSSION

The fine structure of gametocysts and oocysts of gregarines has been of interest to many people, but ultra thin sections of them have not been obtained until this time. The extended period of time utilized for infiltration of fixation fluid and embedding resin into the gametocysts and oocysts did not provide ideal results. However, the methods used resulted in thin sections of gregarine gametocysts, oocysts, and sporozoites which has allowed the description of previously unknown structures.

The gametocyst wall, which was composed of many layers, was secreted in several installments by gamonts at the beginning of gametocyst formation. The thick, multilayer and impervious nature of the wall may protect the gametocysts in the digestive tract of the host and in the external environment.

The homogeneous space and spongeform layer may play an important role to extrude the oocysts from the gametocysts at the end of maturation. It is hypothesized that the oocysts were extruded from the gametocysts by an increase in internal pressure caused by the absorption of water into the homogeneous and spongiform layers. This osmotic pressure increase compressed the centrosphere and forced the oocysts through the sporoducts. After extrusion of oocysts the centrosphere decreased in size. The proposed mechanics of the extrusion of the oocysts is illustrated in Fig. 16.

The oocysts were basically made up of two elements, a covering and sporozoites. The convering was composed of homogeneous walls, wart-like projections and circular folds. The thick homogeneous walls might protect sporozoites from a severe environment outside the digestive tracts of the hosts. Inspite of the thick walls, when mature oocysts enter the digestive tract of a

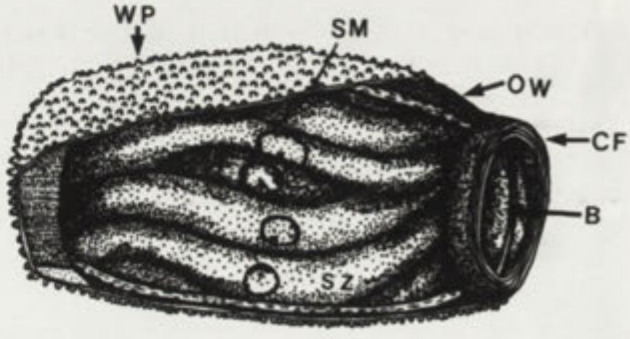

Fig. 17. Diagram of *Gregarina korogi* oocyst. B- break, CF- circular fold, OW- oocyst wall, SM- surrounding membrane, SZ- sporozoite; WP- wart-like projections

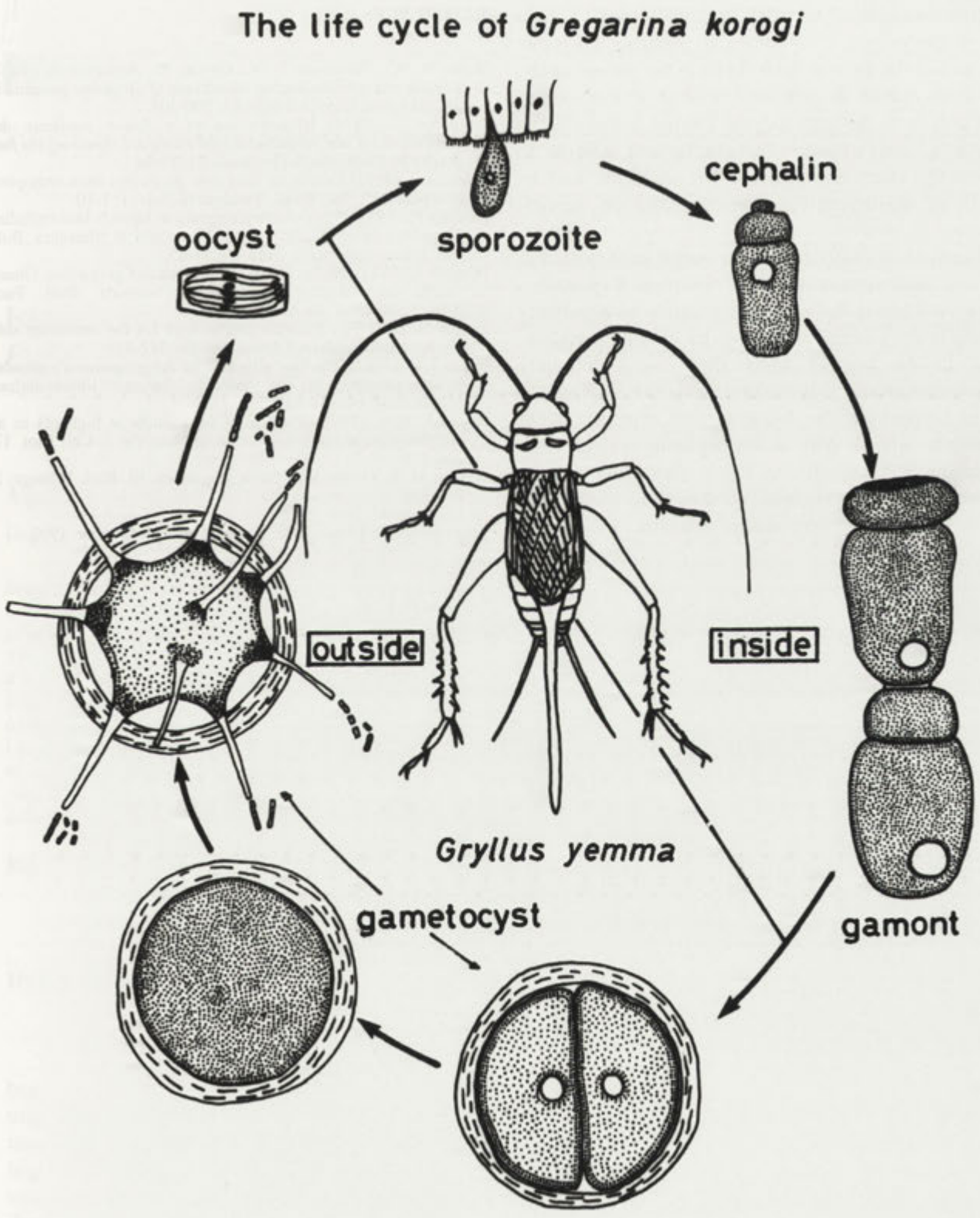

suitable host, the wall is easily destroyed by digestive fluids and the sporozoites escape from the oocysts Watson (1916). Electron micrographs revealed several ruptures (breaks) (probably 3) in the oocyst wall along the longitudinal axis. The oocyst wall probably ruptures along the breaks. The break may contribute to the destruction of the oocyst walls and the escape of the sporozoites. Using light microscopy, Watson (1916)

described a corona of very delicate spines or cilia at each end of the oocyst. The corona is probably the same structure as the circular folds found in the present study. The folds cause the oocysts to form chains during extrusion from the gametocysts. During our study, the discharged oocysts were very sticky and adhered to microscope slides and pipettes. The stickiness may be due to the small wart-like projections on the oocyst's surface.

A composite illustration of an oocyst is presented in Fig. 17. Many researchers have described 8 sporozites in oocysts, but it has not been possible to accurately determine the number of sporozoites with light microscopy. In the present study there were definitely 8 sporozites arranged in parallel along the longitudinal axis of the oocysts. The thin string-like structures in the sporozoites appear only at the beginning of sporozite formation and are present for a short time in the sporozites without a nucleus. We don't know what they are but they are of a very unique structure.

REFERENCES

Beam H. W., Tahmisian T. N., Devine R., Anderson E. (1957) Ultrastructure of the nuclear membrane of gregarine parasitic in grasshoppers. Exp. Cell. Res. 13: 200-204.

Desportes I. (1974) Ultrastructure et evolution nucléaire des trophozoites d'une grégarine d'ephéméroptére; *Enterocystis fungoides* M. Codreanu. J. Protozool. 21: 83-94.

Hoshide H. (1952) Studies on three new gregarines from orthoptera in Japan. Bull. Fac. Educ., Yamaguchi Univ. 1: 1-10.

Hoshide K. (1973) Notes on the gregarines in Japan 6, two cephaline gregarines from *Gryllus yemma* Ohamachi et Matsuura. Bull. Fac. Educ., Yamaguchi Univ. 23: 77-85.

Hoshide K.(1973) Studies on the fine structure of gregarines. Observation on *Ferraria cornucephala iwamusi*. Bull. Fac., Yamaguchi Univ. 23: 87-91.

Levine N. D. (1971) Uniform terminology for the protozoan subphylum Apicomplexa. J. Protozool. 18: 352-355.

Reger J. F. (1967) The fine structure of the gregarine Pyxinoides balani parasitic in the barnacle *Balanus tintinnabulum*. J. Protozool. 14: 488-497.

Reynolds E. S. (1963) The use of lead citrate at high pH as an electron-opaque stain in electron microscopy. J. Cell Biol. 17: 208-212.

Watson M. E. (1916) Studies on gregarines. Ill. Biol. Monogr. 2: 213-468

Received on 23rd June, 1992; accepted on 15th October, 1992

Acta Protozoologica (1993) 32: 27 - 32

ACTA
PROTOZOOLOGICA

Effect of Propranolol on the Duration of the Reversal Response in *Paramecium octaurelia* Induced by KCl and $BaCl_2$

Agnieszka UCIEKLAK, Jolanta PECHÉ, Anna ŁOPATOWSKA and Elżbieta WYROBA

Department of Cell Biology, Nencki Institute of Experimental Biology, Warszawa, Poland

Summary. The effect of the β-adrenoceptor antagonist l-propranolol on *Paramecium octaurelia* motor reactions was studied. Exposure to 75 μM and 100 μM of l-propranolol, shown previously to inhibit phagocytosis (Wyroba 1989b), caused shortening of both continuous ciliary reversal (CCR) induced by potassium and periodic ciliary reversal (PCR) induced by barium ions.
The observed effects were concentration- and time-dependent, being more pronounced in starved cells. Treatment with β-blocker evoked a 2-7 fold decrease in duration of CCR in starved cells: reaction was reduced by 55% after 20 min exposure to 75 μM drug and by 84% following 60 min incubation in 100 μM l-propranolol. A similar effect was observed in the case of PCR which was reduced by 22% to 61% depending on drug concentration and time of treatment. The examination of *Paramecium* reversal response was carried out at the l-propranolol doses blocking phagocytic activity of the cells which was monitored at the same time intervals. Simultaneous modulation of ciliary reversal and phagocytosis by l-propranolol suggest that transmembrane signalling associated with these two processes occurs via β-adrenergic system. Effect of β-blocker on *Paramecium* motor reactions is discussed in terms of its putative action on calcium channel gating mechanism.

Key words. *Paramecium octaurelia*, l-propranolol, ciliary reversal, phagocytosis.

INTRODUCTION

The free living ciliated protozoan *Paramecium*, has been used to study physiology and sensory behavior of unicellular organisms serving as a model system for investigation of a variety of processes related to the higher organisms, including membrane fusion, exocytosis, endocytosis and motility (Satir et al. 1989, Zieseniss and Plattner 1985, Wyroba 1987, Croce et al. 1990, Doughty and Dryl 1980). *Paramecium* exhibits several distinctive types of behavioral response following stimulation with inorganic cation salts (Kuźnicki 1966). In response to a higher concentration of potassium ions, *Paramecium* showed a characteristic reverse motion called "an avoiding reaction" (Jennings 1906).

In response to KCl the initial phase of the ciliary activity is termed "continuous ciliary reversal (CCR)". In solutions containing Ba^{2+} and Ca^{2+}, a different reaction, a periodic ciliary reversal (PCR), dominates in which the cells reverse their direction of swimming many times a minute (Janiszewski 1982). Ciliary reversal (CR) results from an activation of calcium conductance within the ciliary membrane and the influx of

Address for correspondence: A. Ucieklak, Department of Cell Biology, Nencki Institute of Experimental Biology, 3 Pasteura Str., 02-093 Warszawa, Poland.

external calcium ions into the intraciliary space (Dryl 1974).

β-adrenoceptor ligands have been found to interact with the cell membrane of *Paramecium* (Wyroba 1989a). Ciliates respond to β-receptor antagonists by complete inhibition of phagocytic activity (Giordano et al. 1985, Wyroba 1986) and to β-receptor agonists by its stimulation which is potentiated by phorbol ester and forskolin (Wyroba 1987, 1989a). When the phagocytic activity of the cells is blocked with l-propranolol, fluid phase uptake - quantitated with horseradish peroxidase - is increased: the total amount of the accumulated marker has been found to be twice higher than in the control (Wyroba 1991).

The effects of β-blockers, although differing in lipophilicity and membrane stabilizing activity, were found to be specific (Wyroba 1989b) and β-receptor sites were visualized in the *Paramecium* membrane using fluorescence microscopy (Wyroba 1989a). Modulation of endocytosis is not the only one physiological response of *Paramecium* to β-adrenergic ligands: preliminary experiments indicate that dichloroisoproterenolol and l-propranolol also affect swimming behavioral responses like ciliary reversal (Wyroba 1989a).

The aim of the present study was to analyze the effect of l-propranolol on the duration of the chemically-induced ciliary reversal responses in *P. octaurelia* in two physiological stages of the cells- starved and non starved. Behavioral and physiological experiments described in this paper show that l-propranolol modulates the ciliary reversal response and suggest involvement of membrane β-receptors in the regulation of calcium channel activity.

MATERIAL AND METHODS

Paramecium culture

Experiments were carried out on *Paramecium octaurelia* strain 299s, cultivated in axenic medium (Soldo et al. 1966) at 27° C. 5-day-old cell cultures were collected by centrifugation (MSE oil centrifuge, 600 x g) and washed twice with buffer solution (1 mM Tris/HCl, pH 7.6 + 1 mM $CaCl_2$). Collecting and washing of the ciliates were carried out under aseptic conditions. When starved cells were used, ciliates were left in sterile buffer for 24 h at 18°C. Cell density was 65,000-70,000 cells/ml. All procedures were performed at room temperature (21-23°C).

Treatment with l-propranolol

Ciliates were treated with the β-adrenergic blocker l-propranolol (Imperial Chemical Industries, U.K.) in Tris buffer at two concentrations (75 μM and 100 μM) shown previously to be effective in blocking endocytosis (Wyroba 1989b). At selected time points aliquots of cells were withdrawn from the incubation media to monitor phagocytic activity and to determine the duration of the ciliary reversal after exposure to KCl and $BaCl_2$. Prior to each experiment the physiological state of cells (shape, movement) and effectiveness of l-propranolol dose was checked.

Behavioral studies

The duration of ciliary reversal was determined by the exposure of l-propranolol-treated and control cells to cationic solutions in Tris buffer. Two types of behavioral responses were studied: continuous ciliary reversal (CCR) induced by 100 mM KCl and periodic ciliary reversal (PCR) induced by 1 mM $BaCl_2$. The motile behavior of ciliates was determined by stopwatch using a low magnification microscope.

The duration of ciliary reversal (CR) response was determined by observation of cells spinning in 50% of the population. The first series of the experiments was carried out on non-starved cells, and the second - on the ciliates starved for 24 hours. Mean times of CR evoked by 100 mM KCl or 1 mM $BaCl_2$, respectively, provided the control values.

Monitoring of phagocytic activity

To study the phagocytic activity cells were pulsed with polystyrene latex beads (0.8 μm in diameter, Serva, FRG) in the presence of l-propranolol. In all cases control was performed. At selected intervals (20, 30, 40 and 60 min), cells were withdrawn from the incubation media, fixed with Ca-buffered formalin and the number of digestive vacuoles (D.V.) in more than 50 cells was scored under the microscope. The ratio of the mean number of D.Vs. in the test sample - to their number in the appropriate control was calculated. Phagocytic activity of cells was estimated at the same time intervals at which ciliary reversal was examined.

RESULTS

Effect of l-propranolol treatment on the duration of the CCR induced by KCl

The total reversal response to KCl can be divided into two phases: continuous ciliary reversal (CCR) and partial ciliary reversal (PaCR). In this study we observed only continuous ciliary reversal (CCR). Starved and non-starved cells were treated with l-propranolol at two concentrations (75 μM and 100 μM) reported previously (Wyroba 1989b) to be effective in blocking phagocytosis.

The exposure to KCl showed a marked decrease in duration of CCR as a consequence of incubation in medium containing the β-blocker. Both β-blocker concentrations caused a decrease in duration of CCR, but the effect was more pronounced with 100 μM. The

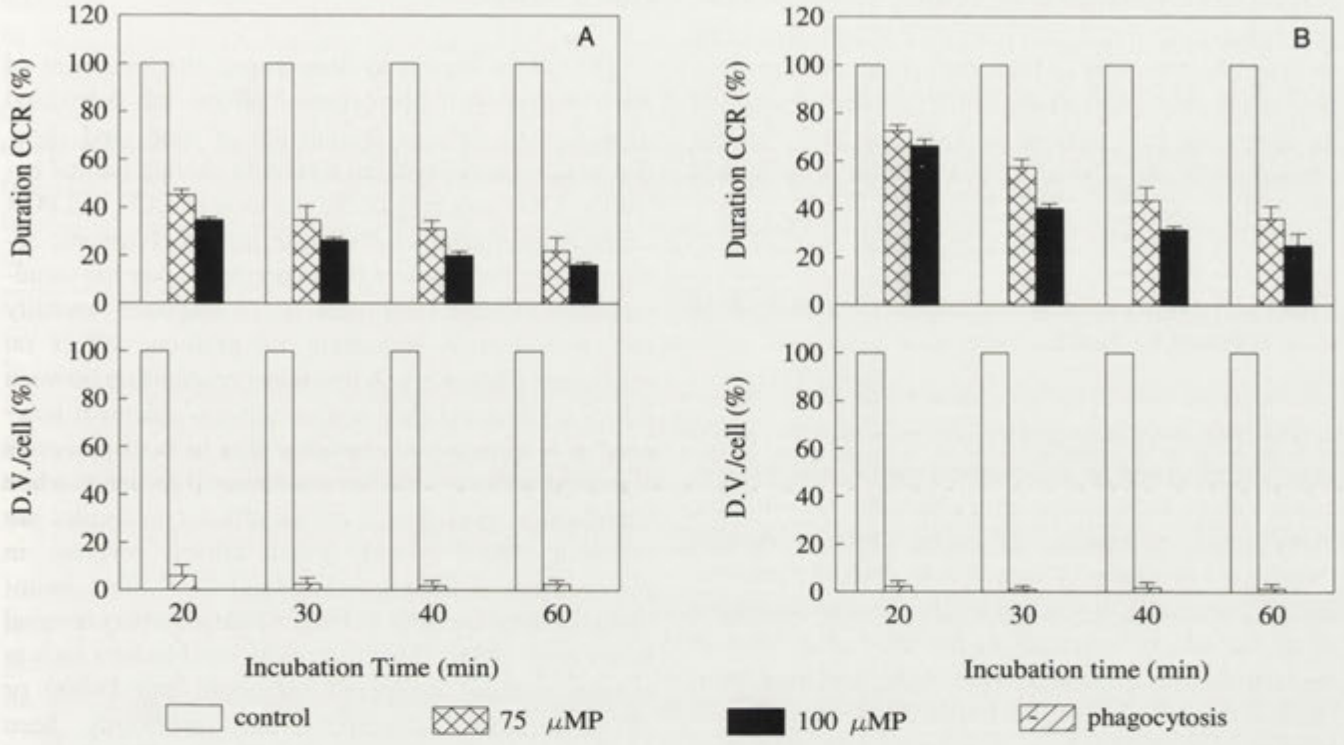

Fig. 1. Comparison of propranolol action on continuous ciliary reversal (above) and phagocytic activity (below) in starved (A) and non-starved (B) *Paramecium octaurelia* (shown as a percent of the control) in simultaneously carried out samples. Mean values and ±S.D. of 13 determinations at each concentration

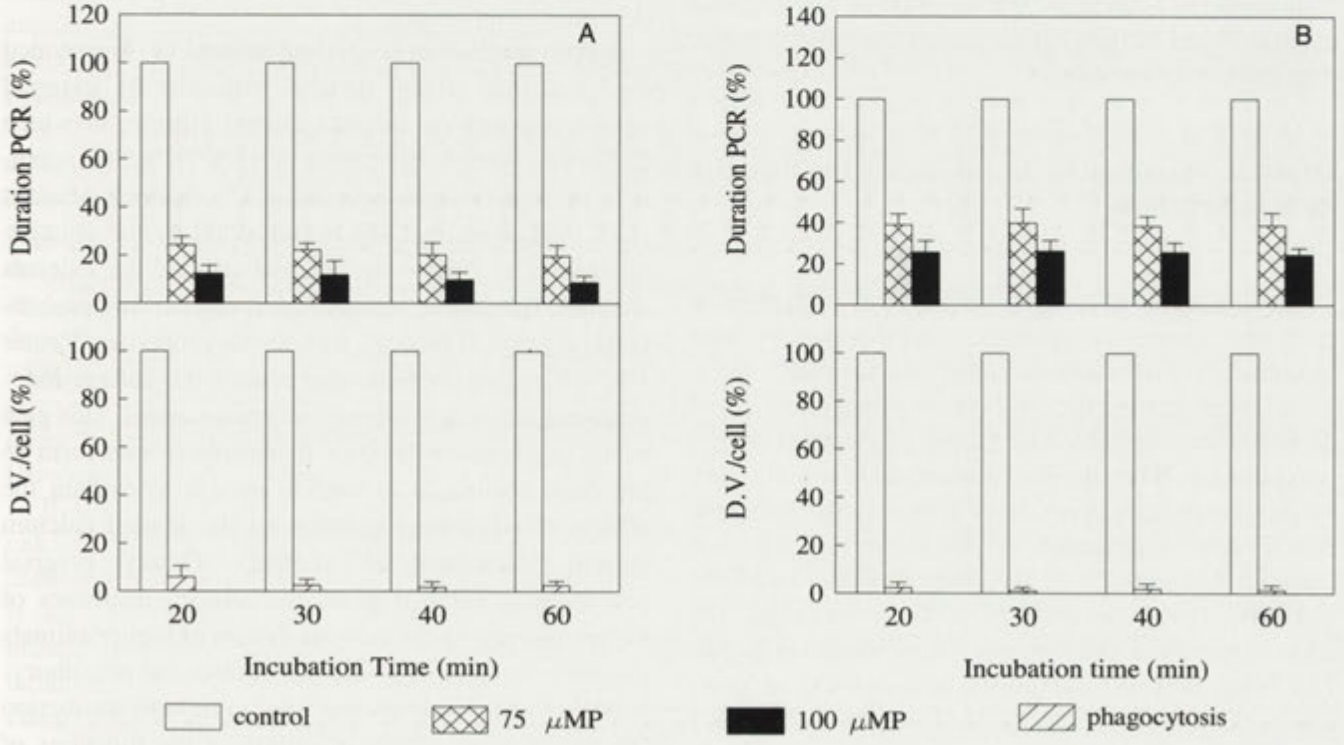

Fig. 2. Comparison of propranolol action on periodic ciliary reversal (above) and phagocytic activity (below) in starved (A) and non-starved (B) *Paramecium octaurelia* determined in simultaneously carried out samples (shown as a percent of the control). Mean values and ±S.D. of 16 determinations at each concentration

duration of CCR in starved cells treated with propranolol was between 45.0 and 16.1% of the control, depending on drug concentration and time of incubation (Fig. 1A). In non-starved cells duration of CCR in the presence of the β- bloker was reduced to 36.0 and 24.7% of the control at 75 and 100 μM concentration, respectively (Fig. 1B).

Effect of l-propranolol treatment on the duration of PCR induced by $BaCl_2$

The *Paramecium* characteristic response to barium ions was observed as a movement backwards and forwards with the cells reversing their direction of swimming many times a minute, so called "barium dance". Propranolol treatment of starved cells evoked a dose-related decrease of PCR reaction which was time-dependent up to 40 min of exposure to the drug (Fig. 2A). In non-starved cells a transient, short-lasting prolongation of "barium dance" was observed after 20 min exposure to l-propranolol followed by a gradual shortening of reaction related mainly to drug dose (Fig. 2B). Starved cells were more sensitive to barium ions following l-propranolol treatment than non-starved ones.

It should be pointed out that the effect of l-propranolol alone at 75 and 100 μM has not caused any ciliary reversal responses (data not shown).

Effect of l-propranolol treatment on the digestive vacuole formation

Monitoring of phagocytic activity was performed at each time interval in which behavioral responses were examined in simultaneously carried out samples.

All the diagrams (Figs. 1-2) demonstrate inhibition of digestive vacuole (D.V.) formation in *Paramecium* by l-propranolol. When the drug concentration was 100 μM, the phagocytic activity in starved cells declined during the first 20 min of treatment and the number of digestive vacuoles fell to 0-2% of the control; with 75 μM the number of D.Vs. was about 7% of the control (Figs. 1A, 2A). Non-starved cells responded similarly (Figs. 1B, 2B), being, however more susceptible to the drug, especially after 20 min of treatment. This phenomenon has been characterized in detail previously and seems to be related to lipid composition of the membrane (Wyroba 1989b).

DISCUSSION

The results presented demonstrate that treatment of *Paramecium* with l-propranolol affects the behavioral responses to cationic stimulation in time- and dose-dependent manner without markedly altering normal behavior. The shortening of the duration of CCR and PCR occurs concomitantly with impairment of phagocytic activity. Thus, the action of β-adrenergic blocker has simultaneously affected both types of cell response - motility and phagocytosis indicating its profound effect on membrane physiology. A functional relationship between ciliary reversal and phagocytosis remains unknown, however, it is tempting to speculate that in both processes signalling pathways involve membrane β-receptors while transduction mechanisms and/or effector molecules are different. Many drugs affect ciliary reversal in *Paramecium*. Trifluoroperazine and W-7 affect swimming behavior and abolish barium induced ciliary reversal (Otter et al. 1984). The effect of calcium blockers such as tertiary amines: verapamil, diltiazem and D-600 or dihydropiridines (nifedipine) has previously been reported by us (Ucieklak and Dryl 1990, 1991, Dryl and Totwen-Nowakowska 1985, Dryl and Łopatowska 1990). These drugs cause shortening of duration of K^+-induced CR in the similar range and manner as l-propranolol described in this paper.

Eckert and Brehm (1979) and Naitoh (1974) provided evidence that ciliary reversal induceds by external stimuli depends on calcium inward current, in which $Ca^{2+}$is the main charge carrier of a Ca^{2+}/K^+action potential, through voltage-operated Ca^{2+} channels. Eckert (1972) proposed that CR is controlled by the voltage-operated Ca^{2+} "gate", an integral part of the calcium channel. The gating, a complicated mechanism, probably has a group of proteins with dipole properties (Reuter 1983). Calcium channels also contain the voltage-independent gate, which is under receptor control. This gate exists in phosphorylated or dephosphorylated form as has been postulated in cardiac muscle to explain the effects of adrenergic agonists on the inward calcium current (Glossman et al.1982). Ciliary reversal resembles in some respects the sensory responses of higher animals. In the nervous system of higher animals calcium, calmodulin, cyclic nucleotides and phosphorylated proteins play important roles in signal transduction (Watanabe et al. 1990). A variety of the functions of metazoan cells are under control of β-adrenergic receptors. These are stimulated by β-adrenergic agonists and

inhibited by β-antagonists. Propranolol has been found to block the formation of the cleavage furrow during first division in sea urchin eggs. Nicotra and Schatten (1990) suggested that propranolol causes an impairment of the actin cytoskeleton thereby preventing an adequate response to the cleavage stimulus. Probably neurotransmitter monoamines play a role in regulation of actin microfilament organization and may modify some properties of actin or actin binding proteins normally controlled by modulating the levels of Ca^{2+} (Nicotra and Schatten 1990). Neurochemical sensitivity to adrenoceptive drugs has also been reported for the photobehavior of the dinoflagellate *Gymnodinium* (Forward 1977).Using radioligand binding assay, De Castro and Oliveira (1987) have characterized the β-adrenergic receptor, its dissociation constant and membrane localization in *Trypanosoma cruzi*. *Paramecium* responds to β-adrenergic ligands in a dose- and time-dependent manner and β-receptor sites have been mapped on its membrane (Wyroba 1986,1987,1989a,1989b).

In the present paper we report that β-adrenergic blocker shortens the ciliary reversal in a similar way to that we observed previously following action of calcium channel blockers. This may be due to the fact that propranolol affects the cell membrane in a way similar to amphipathic amines and local anesthetics. These drugs affect cells by asymmetric insertion into one face of the lipid bilayer (Surewicz 1982, Kubo et al. 1986, Rogers et al. 1986). The drugs possibly bind to a "protein receptor", indirectly affecting the Ca^{2+} "gate" and causing a modulation of ciliary reversal. Alternatively, since the calcium channel gate extends through the two halves of the lipid bilayer, the drugs affecting Ca^{2+} binding to the phospholipids in an asymmetric manner could produce membrane depolarization. Most likely propranolol interacts primarily with the lipid bilayer, an interaction that "senses" the potential difference across the membrane and communicates this information to a protein calcium channel gate (Browning and Nelson 1976).

β-adrenergic ligands have been found to modulate calcium channels in a variety of metazoan cells. In heart cells the positive inotropic effect of β-adrenergic agonist is due to an increased inward calcium current during the plateau phase of cardiac action potential (Curtis and Catterall 1985). Most likely, β-receptor regulation of calcium channels occurs by modulation of a gating mechanism. In fact, Yue et al.(1990) reported that in cardiac L-type Ca^{2+} channels a β-adrenergic agonist stimulates the calcium influx by modulation of channel gating.

It is tempting to speculate that l - propranolol modulates *Paramecium* calcium channels acting via β-adrenergic mechanisms. Some similarities between calcium channels in protozoan and metazoan cells have been recently discussed. The *Paramecium* calcium channel has many features in common with T-type channels in vertebrate tissues (Ehrlich et al. 1988).

Presented results also support the assumption that β-adrenergic ligands may act as modulators of calcium channel gating mechanism in *Paramecium*.

REFERENCES

Browning J.L., Nelson D.L. (1976) Amphipathic amines affect membrane excitability in *Paramecium*: role for bilayer couple. Proc. natn. Acad. Sci. USA 73: 452-456.

Croce A.C., Wyroba E., Bottiroli G. (1990) Uptake and distribution of hematoporphyrin-derivative in the unicellular eukaryote *Paramecium*. J. Photochem. Photobiol. B, 6: 405-411.

Curtis B.M., Catterall W.A. (1985) Phosphorylation of the calcium antagonist receptor of the voltage-sensitive calcium channel by cAMP-dependent protein kinase. Proc. natn. Acad. Sci. USA 82: 2528-2532.

De Castro S.L., Oliveira M.M. (1987) Radioligand binding characterization of β-adrenergic receptors in the protozoa *Trypanosoma cruzi*. Comp. Biochem. Physiol. 87C: 5-8.

Doughty M.J., Dryl S. (1980) Control of ciliary activity in *Paramecium*: an analysis of chemosensory transduction in eukaryotic unicellular organism. Progress in Neurobiology 16: 1-115.

Dryl S. (1974) Behavior and motor response of *Paramecium*. In: Paramecium - A current survey (Ed. J.W. Van Wagtendonk) Elsevier Sci. Publ. Comp., Amsterdam, 165-211.

Dryl S., Łopatowska A. (1990) Inhibition of potassium-induced ciliary reversal in *Fabrea salina* by inorganic and organic calcium channel blockers. Acta Protozool. 29: 173-178.

Dryl S., Totwen-Nowakowska I. (1985) Action of calcium blockers on potassium-induced reversed beat of cirri in *Stylonychia mytilus* Acta Protozool. 24: 291-296.

Eckert R. (1972) Bioelectric control of ciliary activity. Science 176: 473-481.

Eckert R., Brehm P. (1979) Ionic mechanism of excitation in *Paramecium*. Annu. Rev. Biophys. Bioeng. 8: 353-383.

Ehrlich B.E., Jacobson A.R., Hinrichsen R., Sayre L.M., Forte M.A. (1988) *Paramecium* calcium channels are blocked by a family of calmodulin antagonists. Proc. natn. Acad. Sci. USA 85: 5718-5722.

Forward R.B.Jr. (1977) Effects of neurochemicals upon a dinoflagellate photoresponse. J. Protozool. 24: 401-405.

Giordano P.A., Wyroba E., Bottiroli G. (1985) Internalization of cycloheptaamylose-dansyl chloride complex during labelling of surface membrane in living *Paramecium aurelia* cells. Bas. Appl. Histochem. 29: 121-133.

Glossman H., Ferry D.R., Lubbecke F., Mewes R., Hofmann F. (1982) Calcium channels: direct identification with radioligand binding studies. Trends Pharmacol. Sci. 3: 431-437.

Janiszewski J. (1982) Effect of various levels of external pCa on the barium-induced motor responses of *Paramecium caudatum*. Acta Protozool. 21: 221-226.

Jennings H.S. (1906) Behavior of the Lower Organisms. Columbia Univ.Press. New York.

Kubo M., Gardner M.F., Hostetler K.Y. (1986) Binding of propranolol and gentamicin to small unilamellar phospholipid vesicles. Biochem. Pharmac. 35: 3761-3765.

Kuźnicki L. (1966) Role of Ca^{2+} ions in the excitability of protozoan cell. Calcium factor in the ciliary reversal induced by inorganic cations in *Paramecium caudatum*. Acta Protozool. 4: 241-256.

Naitoh Y. (1974) Bioelectric basis of behavior in protozoa. Am. Zool. 14: 883-893.

Nicotra A., Schatten G. (1990) Propranolol, a β-adrenergic receptor blocker, affects microfilament organization, but not microtubules, during the first division in sea urchin eggs. Cell Motil.Cytoskel. 16: 182-189.

Otter T., Satir B.H., Satir P. (1984) Trifluoroperazine-induced changes in swimming behavior of Paramecium: evidence for two sites of drug action. Cell Motil. 4: 249-267.

Reuter H. (1983) Calcium channel modulation by neurotransmitters, enzymes and drugs. Nature 301: 569-574.

Rogers J.A., Cheng S., Betageri G.V. (1986) Association and partitioning of propranolol in model and biological membranes. Biochem. Pharmacol. 35: 2259-2261.

Satir B.H., Hamasaki T., Reichman M., Murtaugh T.J. (1989) Species distribution of a phosphoprotein (parafusin) involved in exocytosis. Proc. natn. Acad. Sci. USA 86: 930-932.

Soldo A.T., Godoy G.A., Van Wagtendonk W.J. (1966) Growth of particle bearing and particle free *Paramecium aurelia* in axenic culture. J. Protozool. 13: 492-497.

Surewicz W.K. (1982) Propranolol - induced structural changes in human erythrocyte ghost membranes. A spin label study. Biochem. Pharm. 31: 691-694.

Ucieklak A., Dryl S. (1990) Action of calcium channel blockers on potassium-induced ciliary reversal in *Paramecium octaurelia* (strain 299s). Acta Protozool. 29: 117-122.

Ucieklak A., Dryl S. (1991) Effect of organic calcium channel blockers on ciliary reversal in *Paramecium octaurelia* (strain 299s). Acta Protozool. 30: 157-160.

Watanabe Y., Hirano-Ohnishi J., Takemasa T. (1990) Calcium-binding proteins and ciliary movement regulation in *Tetrahymena*.In: Calcium as an intracellular messenger in eucaryotic microbes. (Ed. D.H. O'Day). American Society for Microbiology, Washington 343-361.

Wyroba E. (1986) Effect of β-receptor antagonist dichloroisoproterenol on *Paramecium* endocytosis. Acta Protozool. 25: 167-174.

Wyroba E. (1987) Stimulation of *Paramecium* phagocytosis by phorbol ester and forskolin. Cell Biol. Int. Rep. 11: 657-664.

Wyroba E. (1989a) Beta-adrenergic stimulation of phagocytosis in the unicellular eukaryote *Paramecium aurelia*. Cell Biol. Int. Rep. 13: 667-678.

Wyroba E. (1989b) Pharmacological specificity of beta-blockers induced inhibition of *Paramecium* phagocytosis. Acta Protozool. 28: 127-136.

Wyroba E. (1991) Quantitation of fluid phase uptake in *Paramecium*. I. Kinetics in the cells blocked in phagocytic activity. Cell Biol. Int. Rep. 15: 1207-1216.

Yue D.T., Herzig S., Marban E. (1990) β-adrenergic stimulation of calcium channels occurs by potentiation of high-activity gating modes. Proc. natn. Acad. Sci. USA 87: 753-757.

Zieseniss E., Plattner H. (1985) Synchronous exocytosis in *Paramecium* cells involves very rapid (1s), reversible dephosphorylation of a 65-kD phosphoprotein in exocytosis- competent strains. J. Cell Biol. 101: 2028-2035.

Received on 5th August, 1992; accepted on 4th December, 1992

Acta Protozoologica (1993) 32: 33 - 36

ACTA
PROTOZOOLOGICA

Activity of Prostaglandin Synthetase in *Tetrahymena rostrata* and *Tetrahymena pyriformis* GL-C

Leszek SZABLEWSKI

Deptartment of General Biology and Parasitology, Institute of Biostructure, Medical Academy, Warsaw, Poland

Summary. The activities of prostaglandin synthetase in two species of *Tetrahymena* (free-living, and a parasitic) at different growth phases were investigated. Differences in enzyme activity between examined species were evident. No difference in enzyme activity in relation to growth phase was noted.

Key words. Prostaglandin synthetase, *Tetrahymena rostrata, T. pyriformis* GL-C

INTRODUCTION

Prostaglandins (PGs) play an important role in the metabolic processes of organisms. They have been found in many taxonomic groups.

The synthesis of PGs depends on the presence of precursors and enzymes. Precursors of these compounds are unsaturated fatty acids of chain length C-18 to C-24 (Hadaś 1988, Mustafa and Srivastava 1989, Srivastava and Mustafa 1984, Zaorska 1986). Phospholipase A mediates the release of precursors from the phospholipid membrane. A phospholipase A_1 (E.C. 3.1.1.32), has been found in *Tetrahymena* (Florin-Christensen et al. 1986). A second stage is the formation of prostaglandins. PGs are synthesized by a multi-enzymatic microsomal complex, prostaglandin synthetase (E.C. 1.14.99.1). The prostaglandin synthesizing enzyme system was detected in *Tetrahymena* by the histochemical method (Szablewski and Hadaś 1991).

Erwin and Bloch (1963) found that the ratio unsaturated: saturated fatty acids depends on the age of the culture. In the early phases of growth the concentration of unsaturated fatty acids in cells is very low but increases with successive phases. If PG precursor concentration depends on the cultures age, is prostaglandin synthetase activity dependent on the growth phase? Is prostaglandin synthetase a constitutive or adaptative enzyme? Are there differences in activities in PG-synthetase from free-living and parasitic species of *Tetrahymena*? The present study has been designed to answer these questions.

MATERIAL AND METHODS

Ciliates. The experiments were performed on *Tetrahymena pyriformis* GL-C, amicronucleate strain isolated from a free-living form, and *T.rostrata* isolated from a parasitic form. The parasitic form was isolated from the renal organ of *Zonitoides nitidus*

Address for correspondence: L. Szablewski, Department of General Biology and Parasitology, Institute of Biostructure, Medical Academy, 5 Chałubińskiego Str., 02-004 Warsaw, Poland.

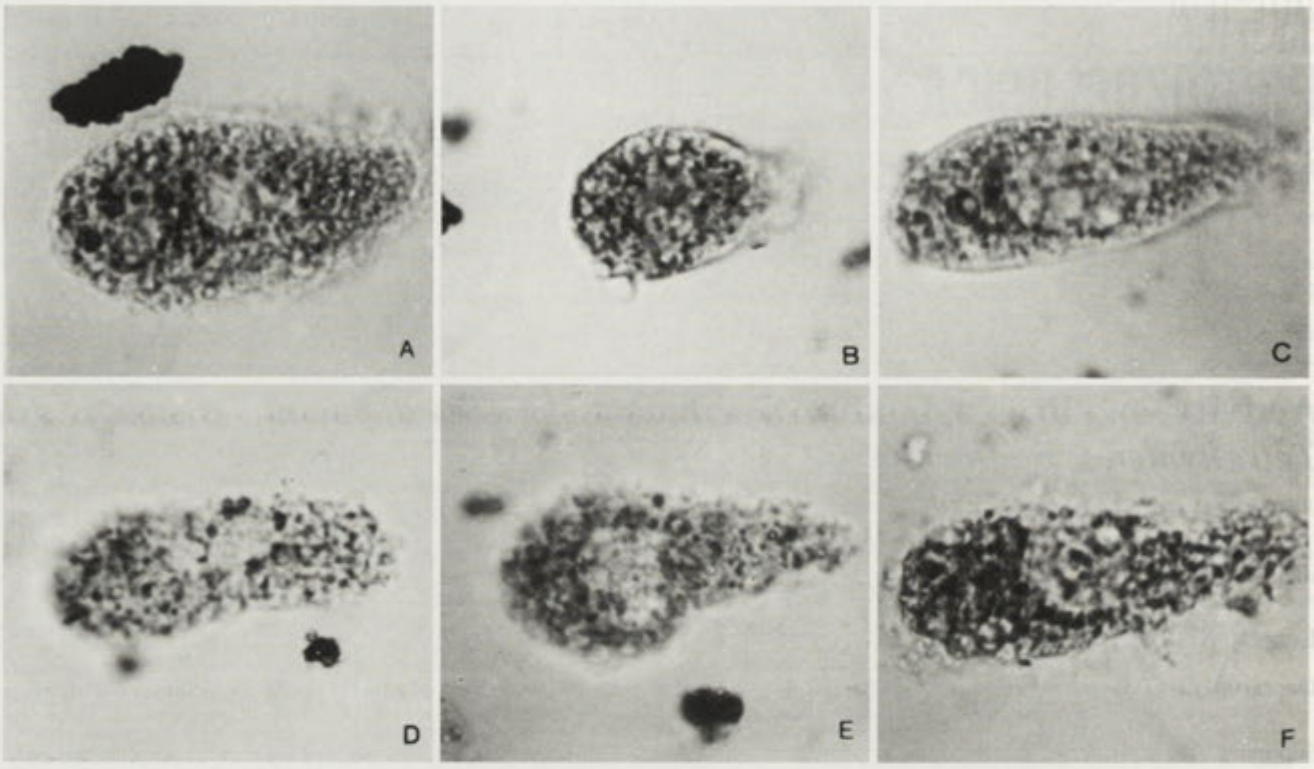

Fig. 1. The activity of prostaglandin synthetase in *Tetrahymena pyriformis* GL-C. Early log phase of: control (A), investigated cell (B). Late log phase of: control (C), investigated cell D). Stationary phase of: control (E), investigated cell (F)

(*Mollusca, Gastropoda*) and cultivated in the laboratory for about 10 years (Oleszczak and Szablewski 1992). Both free-living and parasitic forms were cultivated in a nutrient medium containing 1.5% proteose peptone + 0.1% yeast extract + salts. The salt containing medium was prepared according to the method of Plesner et al. (1964). Cells were grown in Erlenmeyer flasks containing 50 ml of medium at 25°C, and inoculated every day to fresh medium.

Ciliates used in this study were in the early log phase (4h after inoculation), late log phase (16 h after inoculation), and stationary phase (120 h after inoculation).

Localization of enzymes. The localization of prostaglandin synthetase was performed according to a partially modified method of Hadaś (1991). Cells were frozen (-25°C, 6 h) and then washed several times with cacodylic buffer. Fixation is not necessary because a loss in sensitivity of about 50% was noted during staining (Janszen and Nugteren 1971).

Histochemical reaction on the prostaglandin synthetase was performed by incubating the cells in a staining mixture containing 100 µM arachidonic acid, 1 mM 3,3'-diaminobenzidine and 2 mM potassium cyanide in 100 mM Tris-HCl buffer (pH 8.2). The reaction was stopped by rinsing the cells first with distilled water and then with cacodylic buffer. Samples were then embedded in 2% gelatin in 50% glycerin. Controls were stained with a mixture without arachidonic acid, or a mixture with 1 mM acetylsalicylic acid (a synthetase inhibitor).

Prostaglandin synthetase activity was assessed in the samples on the basis of colour intensity of the granule. Each sample then was photographed under the same conditions (time of exposure, magnification, lighting etc.).

RESULTS

Cells incubated with 100 µM arachidonic acid show a brown intracellular granule. Omission of substrate (arachidonic acid) or incubation of ciliates with 1 mM acetylsalicylic acid in control cells gave less intense staining in all ciliates (Figs. 1A, C, E; 2A, C, E). The slight residual browning observed in controls may arise from endogenous fatty acids formed from phospholipid in the cells during incubation (Janszen and Nugteren 1971).

No important differences were found in enzyme activity with respect to growth phase in the investigated species of *Tetrahymena*. This result was obtained in control cells and in the ciliates incubated with prostaglandin precursors (Figs. 1, 2). A comparison of brown granular products of enzyme activity in *T. pyriformis* GL-C and *T. rostrata* indicated a difference in activity of the enzyme systems. In all growth phases the activity of prostaglandin synthetase was higher in *T. rostrata* than in *T. pyriformis* (Figs. 1B, D, F; 2B, D, F).

DISCUSSION

The results indicate that *Tetrahymena* can convert potential precursors into prostaglandins, and that the appropriate enzymes are present.

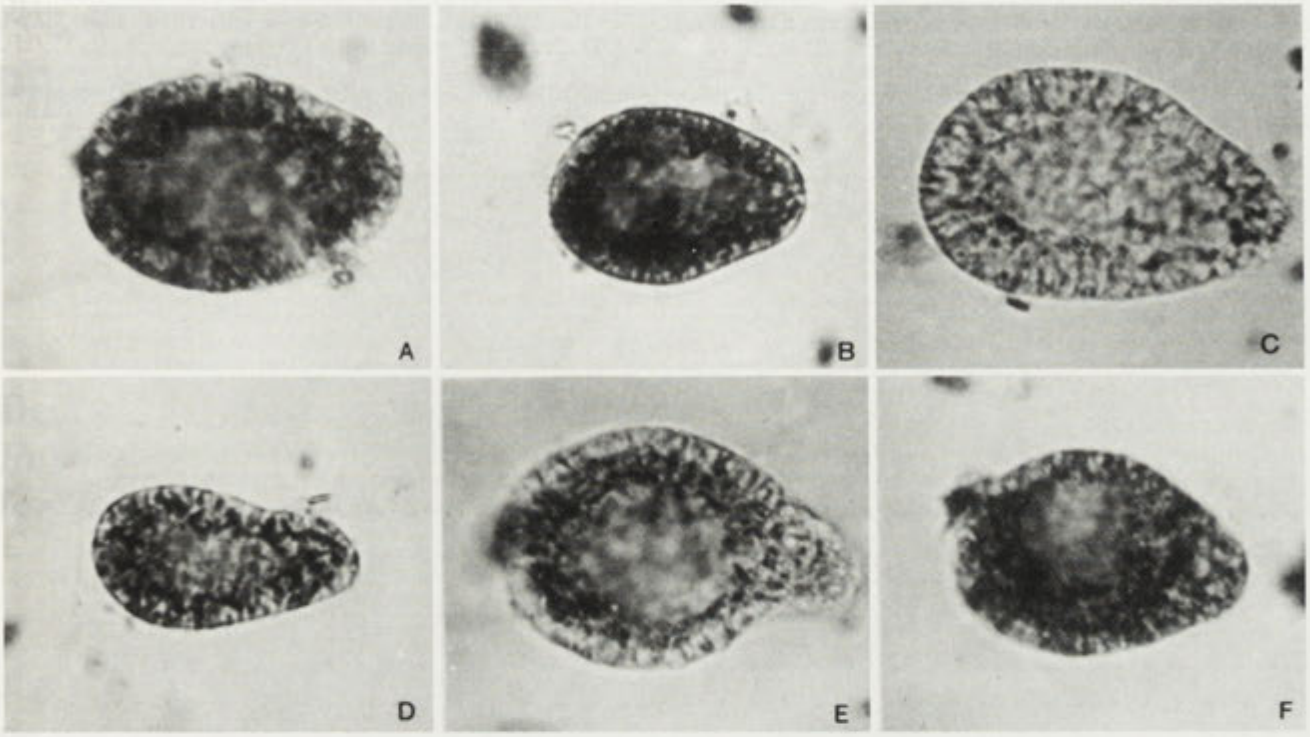

Fig. 2. The activity of prostaglandin synthetase in *Tetrahymena rostrata*. Early log phase of: control (A), investigated cell (B). Late log phase of: control (C), investigated cell D). Stationary phase of: control (E), investigated cell (F)

Unsaturated fatty acid concentrations in *Tetrahymena* depend on the growth phase (Erwin and Bloch 1963, Hill 1972). Prostaglandin synthetase activity, however, is the same at different phases of growth. These two facts suggest that the investigated enzyme has a constitutive character. This may be related to differences in prostaglandin concentrations at partial phases. This hypothesis is as yet unproven.

How can one explain the differences in prostaglandin synthetase activity between *T. rostrata* and *T. pyriformis* GLC? It may be important that the first species is parasitic and the latter is free-living. Misra et al. (1983) suggest that pathogenicity of amoeba depends on the presence of phospholipase. Hadaś (1987) has found differences in prostraglandin concentration in pathogenic and non-pathogenic strains of *Acanthamoeba*. He suggests that PGs play a role in the parasite pathogenicity. Although *T. rostrata* was cultivated for many years as a free-living form in proteose peptone, it nevertheless retained this feature. This may suggest that the ability to intensively synthesize PGs is important for parasites.

Acknowledgements. This study was supported by grant II d/9 from Warsaw Medical Academy.

REFERENCES

Erwin J., Bloch K. (1963) Lipid metabolism of ciliated Protozoa. J. Biol. Chem. 5: 1618-1624.

Florin-Christensen J., Florin-Christensen M., Rasmussen L., Knudsen J., Hansen H.O. (1986) Phospholipase A_1 and triacylglycerol lipase: two novel enzymes from *Tetrahymena* extracellular medium. Comp. Biochem. Physiol. 85B: 149-155.

Hadaś E. (1987) Prostaglandins of free-living amoeba from *Acanthamoeba* spp. Wiad. Parazytol. 33: 649-653 (in Polish).

Hadaś E. (1988) Biosynthesis of prostaglandins in pathogenic and non-pathogenic strains of *Acanthamoeba castellani*. Acta Protozool. 27: 61-66.

Hadaś E. (1991) Histochemical investigation of the synthetase of prostaglandin in pathogenic and non-pathogenic strains of *Acanthamoeba castellani* and infected host tissue. Acta Protozool. 30: 99-102.

Hill D.L. (1972) Biochemistry and Physiology of *Tetrahymena*. Acad. Press, New York and London.

Janszen F.H.A., Nugteren D. (1971) Histochemical localization of prostaglandin synthetase. Histochem. 27: 159-164.

Misra S.K., Sharma A.A., Mehdi H., Garg N.K. (1983) Phospholipase A and lipid contents in pathogenic and non-pathogenic *Acanthamoeba* sp. in relation to their virulence. Protistol. 19: 513-521.

Mustafa T., Srivastava K.C. (1989) Prostaglandins (eicosanonoids) and their role in ectothermic organisms. In: Advances in Comparative and Environmental Physiology, Springer-Verlag, Berlin, Heidelberg, 5: 158-207.

Oleszczak B., Szablewski L. (1992) Morpho-physiological characteristics of *Tetrahymena rostrata* (Ciliata). I. Changes during establishment of laboratory strains. Acta Protozool. 31: 39-42.

Plesner P., Rasmussen L., Zeuthen E. (1964) Techniques used in the study of synchronous *Tetrahymena*. In: Synchrony in Cell Division and Growth, (Ed. E. Zeuthen). Intersci. Publ., New York, 543-564.

Srivastava K.C., Mustafa T. (1964) Arachidonic acid metabolism and prostaglandins in lower animals. Mol. Physiol. 5: 53-60.

Szablewski L., Hadaś E. (1991) Prostaglandins of *Tetrahymena pyriformis* GL-C and *T. rostrata*. Acta Protozool. 30: 165-168.

Zaorska B. (1986) Prostaglandyny i inne eikozanoidy. PZWL, Warszawa (in Polish).

Received on 10th September, 1992; accepted on 28th October, 1992

Acta Protozoologica (1993) 32: 37 - 45

ACTA
PROTOZOOLOGICA

Description of Somatic Kineties and Vestibular Organization of *Balantidium jocularum* sp. n., and Possible Taxonomic Implications for the Class Litostomatea and the Genus *Balantidium*

J. Norman GRIM

Department of Biological Sciences, Northern Arizona University, Flagstaff, Arizona, USA

Summary. The ciliate *Balantidium jocularum* n.sp. was isolated from the intestinal lumen of the surgeonfish *Naso tuberosis*. This fish was from shallow marine waters off Lizard Island, Australia. The ciliate was studied by LM, SEM, and TEM. It is described with special attention on the kinetid organization of normal somatic, special dextr-oral somatic field, and right and left vestibular kineties. Some other features of the vestibulum are described. A slightly modified description of the class Litostomatea is proposed and taxonomic ramifications of the dextr-oral field discussed for the genus Balantidium.

Key words. *Balantidium*, specialized cilia, taxonomy, Litostomatea, vestibular structure.

INTRODUCTION

Within the past eight years it has become apparent that many marine, tropical, herbivorous fishes contain ciliated protozoa as intestinal symbionts (Diamant and Wilbert 1985; Grim 1985, 1988, 1989, 1992). These often include both vestibuliferan and nyctotheran (Grim 1992) ciliates.

Several species of surgeonfish from marine waters around Lizard Island, Australia (Great Barrier Reef) contain species of both *Balantidium* and the family Nyctotheridae; one of these fish, *Naso tuberosis* contained the rather unique symbiont, *Balantidium jocularum* sp. n. It has four somewhat different kinetal systems: normal somatic, specialized somatic forming a crescent-shaped field of about 7 rows of somatic kineties that is to the right of the posterior one-half of the vestibulum, and right and left vestibular. *Balantidium jocularum* is described herein, based on light, scanning electron, and transmission electron microscopy.

Address for correspondence: J. N. Grim, Department of Biological Sciences (Box 5640), Northern Arizona University, Flagstaff, Arizona 86011, USA.

MATERIAL AND METHODS

The host fish, *Naso tuberosis*, were collected by spear at 2m depth on the reef crest, off Lizard Island, Great Barrier Reef, Australia.

Protargol procedures. Specimens were fixed and shipped from Australia in non-EM grade (with methanol) marine formaldehyde. This is, by volume, 1 part 37% formaldehyde to 9 parts sea water. Staining procedures generally followed those noted previously (Grim 1988), including a soak in protargol, pH ca. 8.5, Au toning, and 2 h in sodium thio-sulfate. Some specimens were fixed in sea-water buffered Bouin's fluid; these were significantly smaller, appeared somewhat aberrant in form (author's judgment) and, consequently, were not used for the cellular dimensions in this report.

Electron microscopic procedures. Most specimens prepared for scanning electron microscopy were fixed in the non-EM grade formaldehyde. Specimens were freeze dried (Small and Marszalek 1969) and examined in an AMRAY 1000 SEM. Samples for transmission electron microscopic study were fixed as above, or in Karnovsky's aldehyde in diluted sea water = sea water: dist. water 1:3, with O.1M cacodylate buffer, pH 7.3. Specimens were rinsed in the diluted sea water and post fixed in 1% (W/V) osmium tetroxide, in dist water, buffered with O.1M cacodylate, pH 7.3. They were embedded in epoxy and examined in a JEM 7A, or JEM 1200EX II TEM.

RESULTS

Balantidium jocularum sp. n. (Figs. 1-10)

Host. *Naso tuberosis* Lacpéde, 1802. Family Acanthuridae.

Locality. Lizard Island, Great Barrier Reef, Australia. The island is 36 km from the coast of Queensland. 14° 38' S, 145° 24' E.

Habitat. Lumen of the intestines.

Description. *Balantidium jocularum*, fixed with sea water buffered 10% formalin, has an average length of 119.5 µm (86.3-160 µm, n=20) and width of 68.6 µm (47.5-97 µm, n=20). Cross sections through about mid-body and TEM examination revealed 189 body kineties. One hundred ten of these were judged to be located ventrally on the body and 79 kineties were dorsal. When viewed ventrally with the SEM, the vestibulum curves to the organism's right as it extends posteriorly. Its length was measured on a line parallel to the long body axis and averaged 44.4 µm (32-67.5 µm, n=20); thus, its length is 37% of the body length. Most vestibular kineties on the right side of the vestibulum are oriented toward the left-anterior of the body while those on the left side have rotated clockwise from inside the cell, and the anterior end (with respect to kinetid structures) of many extends toward the right-posterior of the organism. To the right of the posterior one-half of the vestibulum is a crescent-shaped (dextr-oral) field of 7 rows of cilia and 8 rows of elongated inter-kinetal ridges. Cilia in these rows are short and often adhere, but are not fused in TEM, forming groups of 2 or 3 cilia each. The kinety in the approximate center of the field has longer cilia than those flanking it. Most cells contained one macronucleus averaging 35.2 µm long (27-43.3 µm, n=20) and 17.1 µm wide (13.8-20 µm, n=20) and one micronucleus averaging 8.7 µm long (6-19.5 µm, n=14) and 4.96 µm wide (3-10 µm, n=14). The micronucleus always appeared adherent to the side of the macronucleus.

Syntype slide. A protargol stained slide with several specimens, USNM # 43114, is deposited in the International Protozoan Type Slide Collection, National Museum of Natural History, Smithsonian Institution, Washington, D.C.

Etymology. When *B. jocularum* is viewed with its long axis horizontal (Fig. 1), it appears smiling, and with an eye-brow above its mouth; thus, it appears jocular.

Ultrastructure of Kinetid Systems

Normal somatic kinetids. To the right of each kinetosome is a kinetodesmal fibril (Kd). It does not appear striated after Karnovsky's aldehyde fixation. It originates at the proximal end of kinetosomal triplet no. six and seven and extends right-anterior into the inter-kinetal ridge. Some, but not all, extend to at least the next kinetosome and thus, may overlap slightly with one other Kd fibril. Also, on the right side are two rows of convergent (Lynn 1981, Williams and Frankel 1973) postciliary microtubular ribbons (Pc); normally the most anterior row has four microtubules and the posterior has three (Figs. 9, 12). These ribbons bend toward the posterior and their microtubules stay close together; they continue to beyond the next posteriad kinetosome. Between three and six sets of Pc ribbons have been seen overlapping in different sections (Fig. 14). Five or six transverse microtubules (T1) originate on the left side near triplet no. three and four (Figs. 9, 13); these bend and extend about one kinetosome anteriad. Between these ribbons and the kinetosome is a thin sheet of electron opaque material. This species has anterior transverse microtubules (T2) arising near triplet no. five (Figs. 9, 11). Their long axis orientation parallels that of

Figs. 1-4. Scanning electron micrographs of *Balantidium jocularum* sp. n., fixed with non-EM quality formaldehyde. 1 - whole organism with curved vestibulum and dextr-oral ciliary field to the right (above in Fig.) the vestibulum, bar - 20 µm; 2 - higher mag. shows more clearly the organization of cilia and ridges of dextr-oral field (Df), closely packed cilia (C) of right side of vestibulum, and a shallow ridging (R) in the dorsal aspect of the vestibulum, bar - 10 µm; 3 - dextr-oral field - some cilia are in pairs (P) or triplets (T), and interkinetal ridges (OR) are much higher than "normal" somatic ridges (SR), bar - 1 µm; 4 - view of anterior vestibulum displays junction (arrows) of right and left transverse ribbons of microtubules, line (t) is transverse to the vestibulum, angles of microtubular ribbons from line t are shown, bar - 5 µm. inset: higher mag. of microtubular junction (arrows), bar - 1 µm.

Fig. 5. Light micrograph of *B. jocularum*; several rows of kineties in the dextr-oral field are darkly stained argentophilic lines (solid arrows), right margin of the vestibulum (open arrows) is below (in fig), bar - 10 µm.

Figs. 6-7. SEM of the same specimen at different orientations show how vestibular shape appears to change due to viewing direction, bar - 20 µm

the kinetosome in the anterior-posterior axis and the proximal ca. 130 nm of the cilium; however, they bend slightly to the organism's left. T2 microtubules have not been observed bending to run parallel to an interkinetal ridge. A nematodesmal-like bundle of at least eight microtubules extends from the proximal end of somatic kinetosomes. The proximal ends of these kinetosomes are surrounded by a fine microfibrilar network (Figs. 12, 14). This has been called the ectoplasmic - endoplasmic limit = eel (Noirot-Timothée 1958).

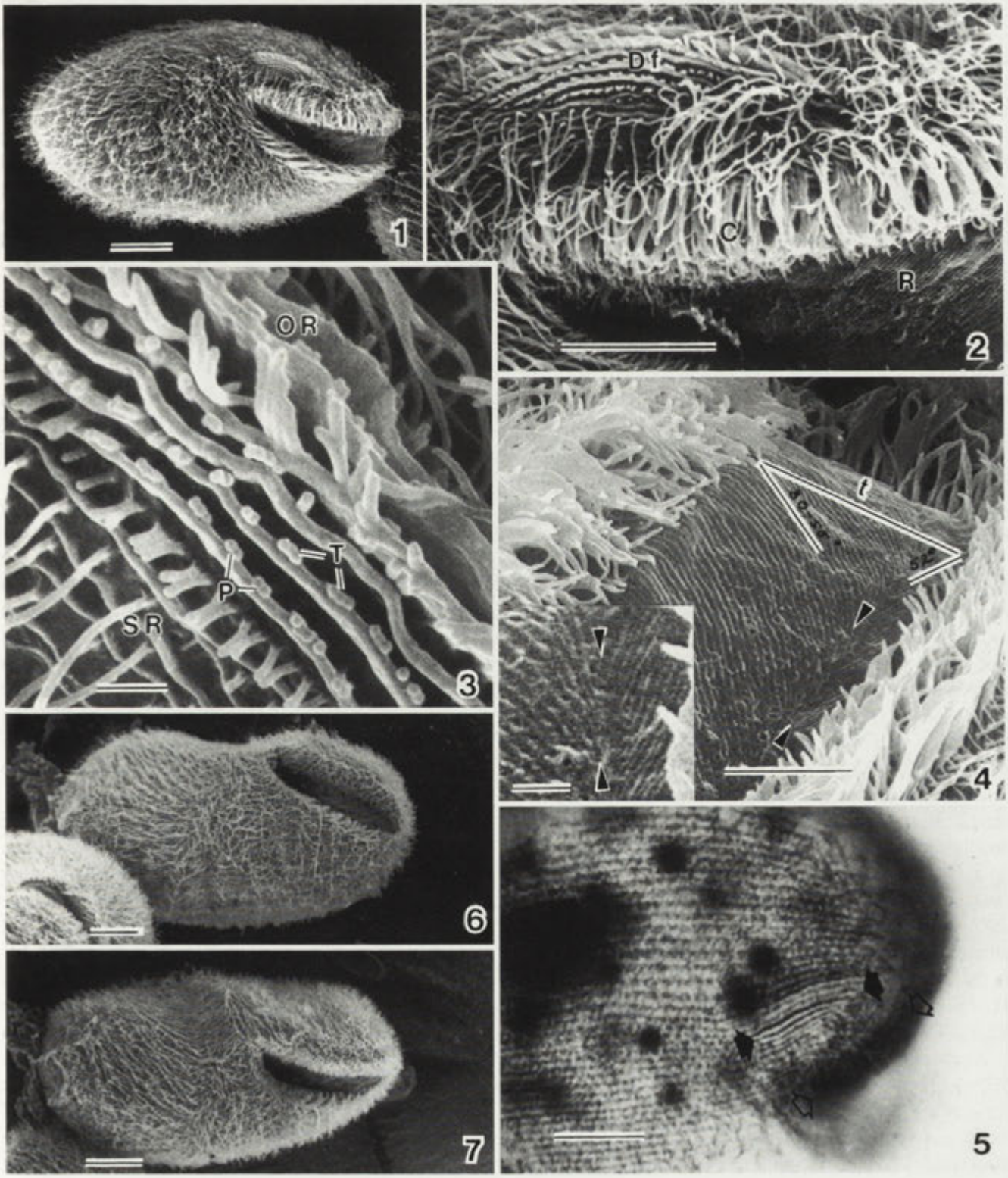

Dextr-oral ciliary field. This field (Figs. 2-3, 15) is separated from the right side of the vestibulum by several μm; from the vestibulum to the right, in sequence, there is a gap in some but not all specimens that has no visible cilia or ridges followed by 1-5 rows of normal appearing cilia with short ridges. The next row to the right is part of the field and contains quite short cilia that are spaced slightly closer than "normal" somatic cilia; some cilia here are adherent in SEM but not in TEM.

Within this field, some ridges are about as long as adjacent cilia. Some cilia appear to adhere to, or are very close to one ridge. About the fifth or sixth kinety to the right, within this field, has longer cilia than kineties to its right and left (Fig. 3). This has been observed in specimens collected from different fish, at different collection times. A field of this general description has been observed in several light microscopic preparations also (Fig. 5). In the SEM, it was sometimes covered by long body cilia of nearby kineties, thus can be difficult to see.

This field has been observed with the TEM in several specimens, each had approximately the same appearance and was in the same relative location. Cilia are closer together than other somatic kineties. Except for postciliary (Pc) microtubules, kinetid structures are similar to normal somatic kineties and only monokinetids have been observed. The contribution of Pc microtubules to interkinetal ridge cytoskeleton is different. Postciliary microtubules do not stay as the 4-3 row groupings, but form a single file in which intermicrotubular spacing is uniform (Fig. 15). In several specimens, the boundary between normal and dextr-oral kineties was apparent (Fig. 15). Transverse ribbon microtubules and Kd fibrils appear similar to those of normal somatic kineties. Kinetosomes of this field have nematodesmal microtubules which are long, extending deeply into the cytoplasm toward the cytopharynx. All cilia of the dextr-oral field had the 9 + 2 axonemal microtubules. Within and deep to the dextr-oral ridges are numerous vesicles and smooth endoplasmic reticulum; these are appreciably more concentrated than in the average normal somatic kineties; compare: Figs. 11, 15. Exo- or endocytosis may be occurring from the ridges (Fig. 15).

Surface of the vestibulum. Non-EM quality formaldehyde fixation and drying apparently caused some contraction and some loss of the plasma membrane (appears fragmented in the TEM) around the vestibular transverse microtubular ribbons. Consequently, ribbon orientations can be seen at the vestibular surface with the scanning electron microscope. These ribbons are perpendicular to the membrane and come from transverse ribbons of right and left vestibular cilia (Figs. 16, 18) and see (Grain 1966, Puytorac and Grain 1965). The origin and orientation of these ribbons are important criteria for modern ciliate phylogenetic schemes (Lynn 1981; Small and Lynn 1981, 1985). Transverse ribbons from the right side of the vestibulum extend toward the left at 30 to 55 degrees clockwise (viewed from outside the cell) from a plane transversing the vestibular long axis (Fig. 4). About 80% of the vestibular width toward the organism's left, the right microtubular ribbons meet (Fig. 4, arrow-heads) transverse ribbons originating at the left side of the vestibulum. Left ribbons are directed toward the right at an angle of about 52 degrees (counterclockwise) from transverse to the vestibulum (Fig. 4). The ribbons on the right are separated by about 260μm; those from the left have about 120μm spacing. Those differences are apparent in the TEM also. A slight groove or invagination is present at the line where microtubules meet (Fig. 4, arrows). It is more apparent in the TEM (Fig. 18), and has been observed also in the portion of the vestibulum that is within the cytoplasm.

Most specimens viewed in the light microscope appear to have a vestibulum that runs, straight, diagonally across the anterior body, thus, is not seen to curve to the right as in Fig. 1. It is important to future researchers to understand that this straight diagonal orientation appears when specimens of *B. jocularum* settle onto a substrate somewhat on their right-dorsal sides; they did this routinely in my L. M. preparations. This was true of the specimen in Fig. 6. When this specimen was tilted in the SEM chamber to give a ventral view, the curved vestibulum and the dextr-oral ciliary field, described here for the species, were seen (Fig. 7).

Right vestibular kineties. Cilia of these kineties are close together but not fused, viewed with the TEM (Figs. 16-17). Interkinetal ridges are less wide than either normal or dextr-oral somatic ridges. Kinetid units contain all the structures described for somatic kinetids, but microtubular components within interkinetal ridges differ somewhat. Kinetodesmal fibrils penetrate into ridges and may or may not associate closely with Pc microtubules. Some Kd fibrils extend a distance of two cilia to the "anterior" (Fig. 17), thus have some overlap. At the base of a kinetosome, there are at least five Pc microtubules, an anterior row of two and posterior of three. Only two or three of these microtubules penetrate into the ridge (Fig. 17). These microtubules extend to at

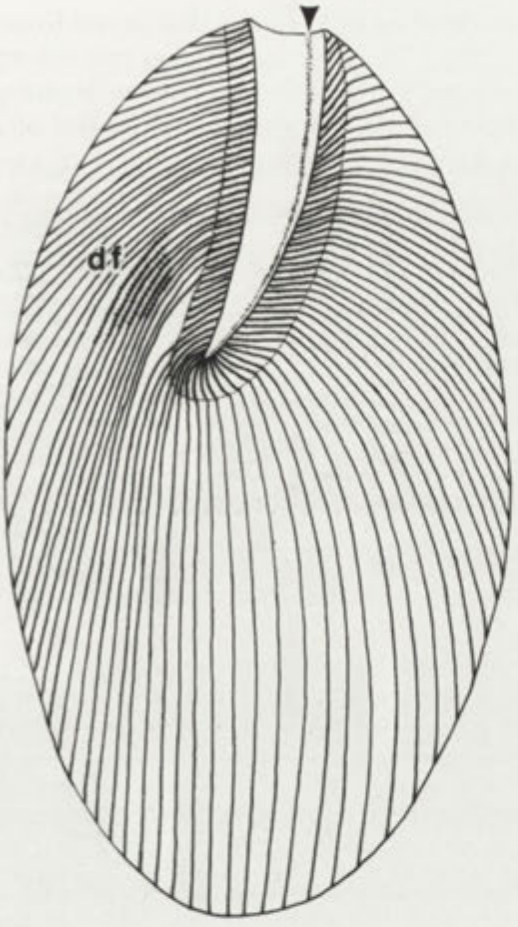

8

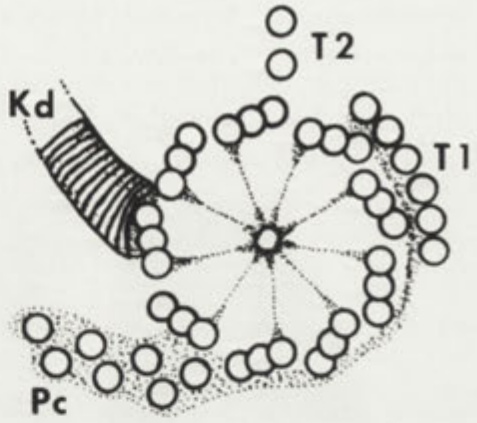

9

Figs. 8-9. Line drawings of *B. jocularum*. 8 - ventral view of whole organism. Vestibulum is curved to organism's right and has argentophilic feature (arrow-head) on left side; crescent shaped rows of cilia (df) to right of vestibulum is the dextr-oral field. At right-posterior of vestibulum, several rows of vestibular kineties are not contiguous with somatic kineties; 9 - somatic kinetid structures, viewed from outside the organism, possess kinetodesmal fibril (Kd), two rows of post ciliary microtubules (Pc), transverse microtubules (T1) at left of kinetosome and anterior transverse microtubules (T2)

least the next cilium posteriad. The T1 microtubular ribbon contains six Mts near the kinetosome but is reduced to three or four prior to ridge penetration (Fig. 16). T1 ribbons from adjacent kinetosomes usually associate into a file a short distance into the ridge (Fig. 16, inset). In some sections, at least one T2 microtubule extends into the ridge and bends slightly posteriad (Fig. 17), in other sections, none are seen. The bases of these kinetosomes are surrounded by an eel network and have nematodesmal microtubules which course to the left providing cytoskeleton deep to the vestibulum. The kinetosome closest to the vestibulum on the right side (of vestibulum) contributes its T1 microtubules to the long ribbons (files of 14-15 microtubules) that are perpendicular to and immediately beneath the vestibular plasma membrane (Fig. 16). There are other small ribbons of microtubules in this location (Fig. 16), there origin is unknown, but may be also from transverse ribbons (Furness and Butler 1985); perhaps they are T2 microtubules.

Left vestibular kineties. Kinetid organization, shape and composition of the ridges, nematodesmal microtubules and eel networks are similar to right vestibular kineties (Fig. 18), with the following exceptions:(1) because somatic kineties rotate clockwise (from inside the cell) as they approach the vestibulum, many vestibular kineties are acutally oriented toward the right-posterior of the body (see, Fig. 8), thus, have opposite polarity to those on the right side, (2) Kd fibrils have not been observed within a ridge, but at the base only, and (3) T1 microtubules of the first row of kinetosomes (at left edge of vestibulum) extend toward the right to underlie the vestibular floor.

DISCUSSION

Balantidium jocularum is judged, by the author, to be a new species because, (1) it has a field of specialized cilia to the right of the vestibulum, the dextr-oral field, (2) it has a distinct right-posterior curvature to the vestibulum and, (3) it does not possess body dimensions similar to any *Balantidium* species described from other marine, herbivorous fishes (Diamant and Wilbert 1985; Grim 1985, 1989, 1992); in fact, it is the first *Balantidium* reported from any species of the host genus, *Naso*. The author acknowledges that body dimensions (of any ciliate?) may vary depending upon the fixative (Choi and Stoeker 1989), time of day or year collected, and, in the case of gut symbionts, the specific chemical environment (food, etc.) of the gut.

Another genus of surgeonfish from the Lizard Island collection site contains the much smaller (119 μm vs 55 μm long *Balantidium zebrascopi* (Grim 1992). Its body

form, vestibular shape, and size differ significantly from *B. jocularum*. *B. zebrascopi* also appears to have a dextr-oral field (not described in Grim 1992); albeit, much smaller than that described here. "Abnormal cilia" have been reported in a "circum-vestibular region" of *B. caviae*, based on TEM studies (Paulin and Krascheninnikov 1973). Their precise location was not reported, thus, it is not known if they are possible homologues to the dextr-oral field. Perhaps some species of *Balantidium* have a derived, near-oral, ciliary structure that

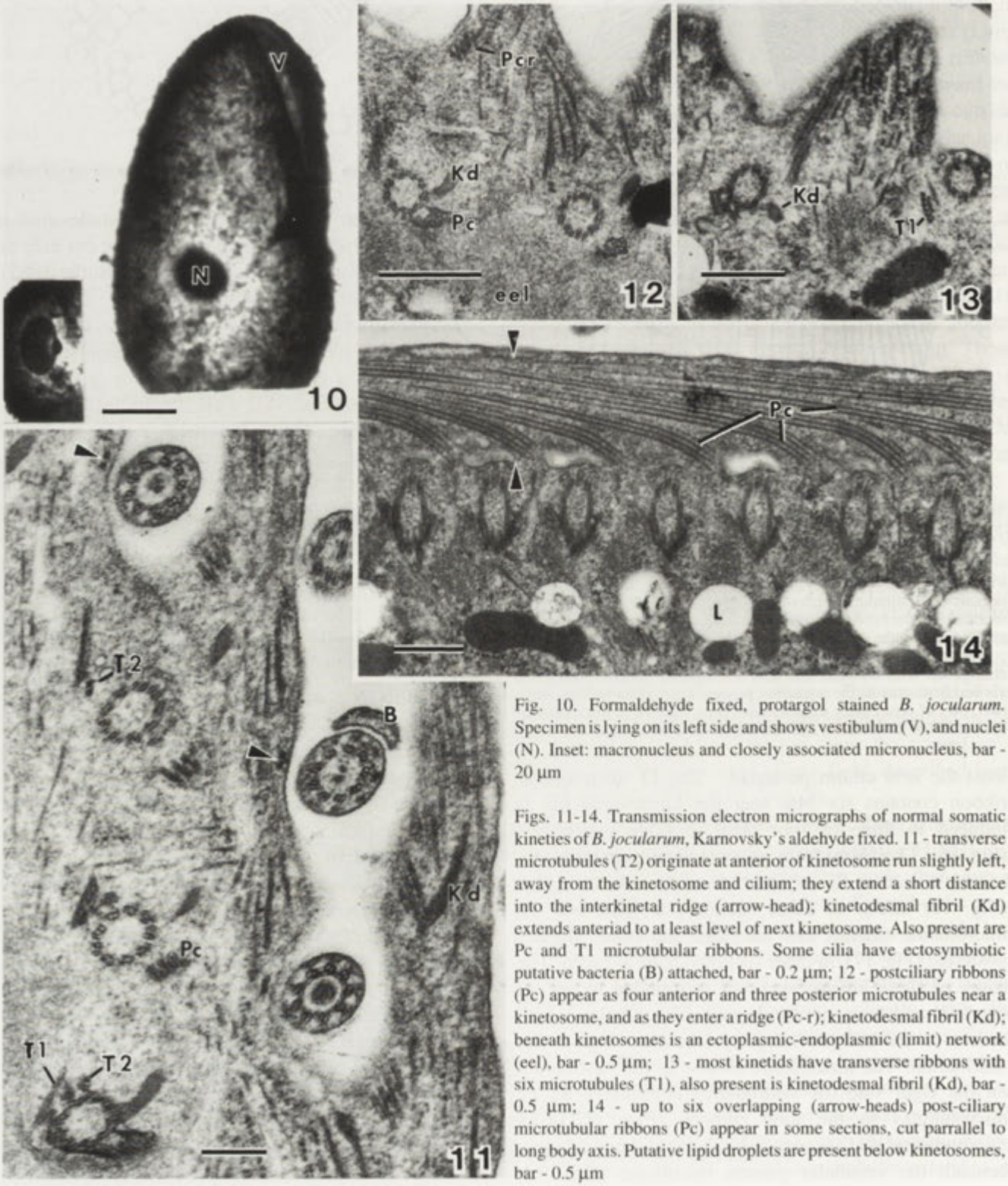

Fig. 10. Formaldehyde fixed, protargol stained *B. jocularum*. Specimen is lying on its left side and shows vestibulum (V), and nuclei (N). Inset: macronucleus and closely associated micronucleus, bar - 20 µm

Figs. 11-14. Transmission electron micrographs of normal somatic kineties of *B. jocularum*, Karnovsky's aldehyde fixed. 11 - transverse microtubules (T2) originate at anterior of kinetosome run slightly left, away from the kinetosome and cilium; they extend a short distance into the interkinetal ridge (arrow-head); kinetodesmal fibril (Kd) extends anteriad to at least level of next kinetosome. Also present are Pc and T1 microtubular ribbons. Some cilia have ectosymbiotic putative bacteria (B) attached, bar - 0.2 µm; 12 - postciliary ribbons (Pc) appear as four anterior and three posterior microtubules near a kinetosome, and as they enter a ridge (Pc-r); kinetodesmal fibril (Kd); beneath kinetosomes is an ectoplasmic-endoplasmic (limit) network (eel), bar - 0.5 µm; 13 - most kinetids have transverse ribbons with six microtubules (T1), also present is kinetodesmal fibril (Kd), bar - 0.5 µm; 14 - up to six overlapping (arrow-heads) post-ciliary microtubular ribbons (Pc) appear in some sections, cut parrallel to long body axis. Putative lipid droplets are present below kinetosomes, bar - 0.5 µm

represents a common specialization and their phylogenetic closeness.

The results of transmission and scanning electron microscopy suggest several possible functions for the dextr-oral field: (1) Secretion, possibly of mucus to aid in locomotion or enzymes for host cell degradation. Secretion should be facilitated by larger ridges - increase surface area, and their file of Pc microtubules could provide a continuous and possibly stronger cytoskeletal support to maintain the shape of this surface. The presence of SER and putative exocytosis further support a hypothesis of secretion. (2) Chemo-sensory. Plasma membranes of the ridges or the cilia may contain receptors for certain chemicals exuded by their food, thus used in chemo-taxis or orientation of the vestibulum for efficient feeding. (3) These cilia could be thigmotatic, thereby aiding in their attachment to host cells. The latter case seems unlikely since such attachment would probably partially hide the vestibulum from the intestinal luminal milieu.

There are possible concerns about fixation artifacts due to the use of non-EM quality formaldehyde. For example: are critical features described in SEM micrographs artifact only? Subsequent samples have been fixed with "normal" EM quality aldehyde and osmium procedures and the dextr-oral field appears the same, as are general body form, cilia, and interkinetal ridges. However, in the latter fixative, microtubular patterns in the vestibulum are not apparent.

For several years the author has puzzled over the occurrence of an argentophilic line on the left side of and parallel to the long axis of the vestibulum. This was observed in all protargol stains of several vestibuliferans (Grim 1985, 1988, 1989, 1992). This line is in the proper location to represent the boundary where right and left vestibular, transverse, microtubular ribbons meet, and also for the groove seen in the TEM. No other specialized structure (organelle) has been observed in this location by the author, based on both SEM and TEM studies of *B. jocularum*.

Evidence from several studies (Foissner and Foissner 1988, Grim 1988, Leipe and Hausmann 1989, Lynn and Nicholls 1985, Williams et al. 1981, others) is that T2 Mt penetrate into an interkinetal ridge perpendicular to the ridge long axis and almost parallel to the long axis of "their" kinetosome. Oriented in this way, they could provide more effective cyto-skeletal support to counter forces that could move a kinetosome parallel to its long axis. Also, possibly, the T2 Mt may provide support to the dorsal wall of the vestibulum. If this is true for *Entodinium*, T2 Mts would be the "Type II ribbons" (Furness and Butler 1985) which are a small sheet oriented parallel to the vestibular dorsal wall, and may have a small analogue in *B. jocularum* (Fig. 16).

Microtubular classes (Pc, T1, T2) that form the major cytoskeleton of interkinetal ridges are similar for all somatic kineties examined, but these are not similar to the ridges within vestibular kineties. In both normal somatic and dextr-oral ridges, the major microtubular cytoskeleton is from the overlapping Pc microtubules. Curiously, in the vestibular region it is T microtubules that appear to serve as the major skeleton. Perhaps there is a local (chemical?) influence that assures the elaboration of T microtubules for buttressing the vestibular wall and, at the same time, causes T ribbons of the nearby ridges to form a file of closely associated microtubules and inhibits Pc "normal"microtubule patterning.

Taxonomic implications. An important and useful character for most of the genera of the class *Litostomatea* is the presence of secondary transverse microtubules (T2); for brief reviews see (Lipscomb and Riordan 1990, Leipe and Hausmann 1989, Lynn and Nicholls 1985, Williams et al. 1981). These have been described in several haptorid and trichostomatid ciliates. Leipe and Hausmann (1989) have recently suggested a taxonomic revision of the class Litostomatea based, in part, on the presence or absence of these microtubules; however, new data challenge their proposals (Lipscomb and Riordan 1990).

Recently published characteristics of the class Litostomatea (Small and Lynn 1985) include "laterally directed kinetodesmal fibril(s) which do not overlap". In some species (genera?), the Kd fibril is laterally directed, e.g., *Spathidium* (Williams et al. 1981), *Lepidotrachelophylum* (Lynn and Nicholls 1985), others, and in other genera it is anteriorly directed, e.g., *Homalozoon* (Leipe and Hausmann 1989), *Vestibulongum* (Grim 1988), and *B. jocularum*. Kinetodesmal fibrils overlap very little in members of the class, with definite overlap of two to three Kds in the vestibular kineties of *B. jocularum*, and the somatic kineties of *V. corlissi* (though probably less than shown in Fig. 8 of Grim (1988). Thus, the description would be more accurate as: "right laterally or anteriorly directed kinetodesmal fibrils, rarely overlap but may do so in some kineties of some genera". Some or all of these ideas are being considered for a future redescription (Denis Lynn, pers. comm.).

There is evidence that several species of *Balantidium*: *B. jocularum*, *B. coli* (see: plate VI, Fig. 1

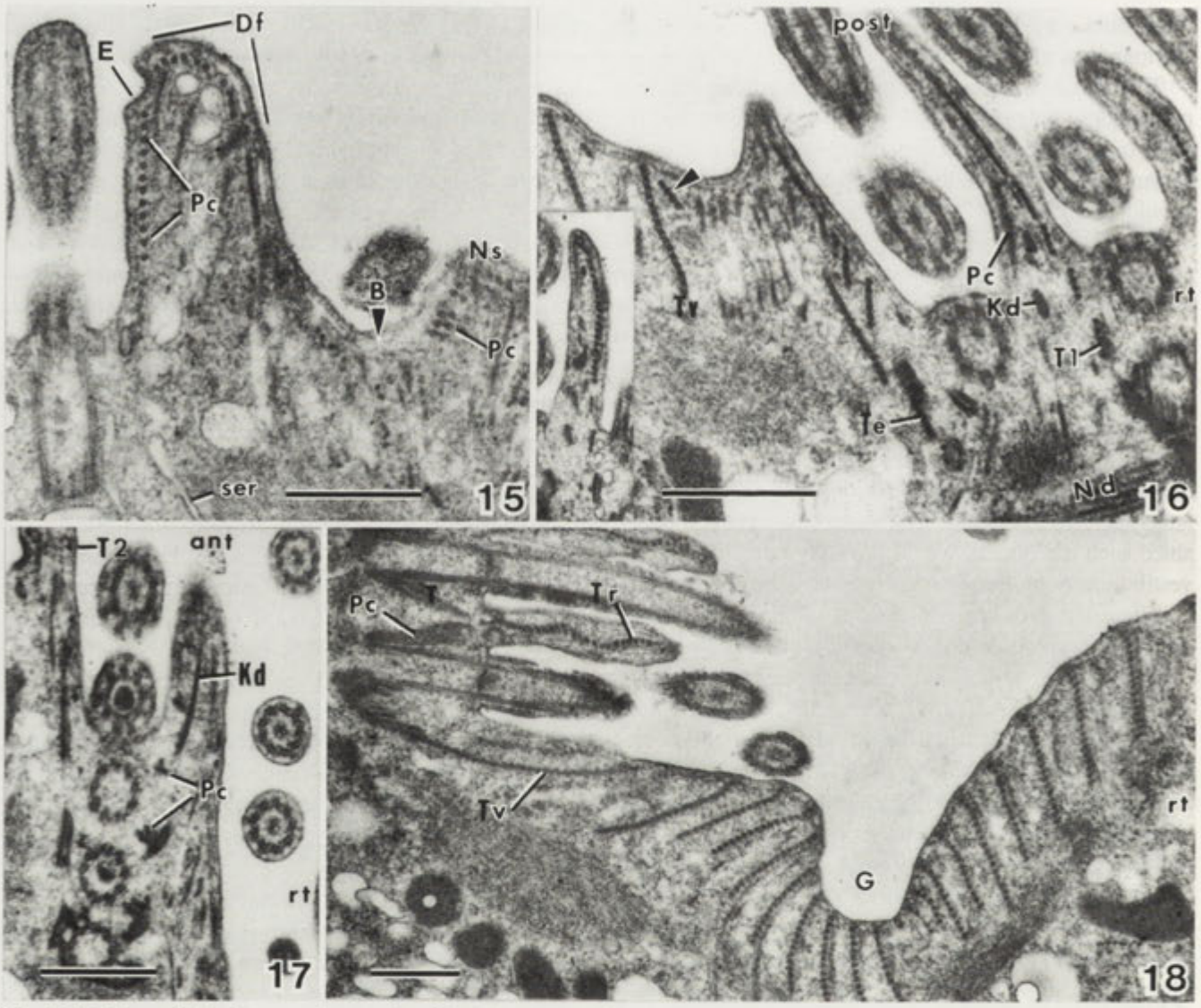

Figs. 15-18. Transmission electron micrographs of kinetid structures of *B. jocularum*. 15 - postciliary microtubules (Pc) within one ridge of dextr-oral field (Df) form into files; smooth endoplasmic reticulum (ser) and possible site of exocytosis (E) are present, normal somatic kineties and ridge (Ns) are separated from the dextr-oral field at B, bar - 0.5 µm. Figs. 16-17. Right vestibular kineties. 16 - kinetids have transverse (T1), postciliary (Pc), nematodesmal (Nd) microtubules, and kinetodesmal fibrils (Kd); transverse ribbons at edge (Te) of vestibulum contain additional microtubules and arch up to buttress the vestibulum (Tv); other microtubules here (arrow-head) may be T2. Transverse-diagonal section, view from outside, post - posterior side, rt - right side, bar = 0.5 µm. Inset = ridge with T1 microtubular file. 17 - internal view of cross section thru kinetosomes and cilia reveals that kinetodesmal fibrils (Kd) may extend ca. two kinetosomes anteriad, T2 microtubules arch slightly posteriorly into a ridge and Pc microtubles are reduced to three before entering the ridge; ant - anterior, rt - right side of organism, bar = 0.5 µm. 18 - left vestibular kineties, view is transverse section of vestibule, rt - cell's right side, anterior is toward the viewer. Transverse microtubules form files in ridges (Tr), and arch (Tv) to support the vestibular dorsal wall; post-ciliary microtubules (Pc) have not been seen to penetrate a ridge; near the left vestibular kineties is a groove (G) in the vestibular wall found throughout the length of the vestibule, bar = 0.5 µm

of Grain 1966), and *B. zebrascopi* have a dextr-oral field of "somatic" cilia. I have looked carefully for this field in protargol stained *B.prionurium* (Grim 1985) and not found it. Of course it is important to examine the type genus and species, *Balantidium entozoan* (Ehrenberg 1838) Claparède and Lachmann 1858, for this field of cilia. Possibly, then, the genus *Balantidium* should be split into two, however, more species of *Balantidium* must be examined for this field with both TEM and SEM. Thus far, no dikinetids have been seen in this field; if they are present, it may be a homologue to the brush of the haptorid ciliates. The SEM view of ridges and cilia within the field of *B. jocularum* are somewhat similar to the dorsal brush of *Prorodon* (Hiller and Bardele 1988).

Acknowledgment. I am pleased to thank Dr. Kendall Clements of James Cook University, Townsville, Australia, for his kind and very special efforts in collecting, fixing, and embedding samples; much of this work was done in the laboratory facilities of the Lizard Island Research Station. I also thank Marilee Sellers of NAU and Dr. John Corliss for technical and other assistance.

REFBRENCES

Choi J.W., Stoecker D.K. (1989) Effects of fixation on cell volume of marine planktonic protozoa. Appl. Env. Microbiol. 55: 1761-1765.

Diamant A., Wilbert N. (1985) *Balanditium sigani* sp. nov., a trichostome ciliate from Red Sea rabbitfish (Pices, Siganidae). Arch. Protistenkd. 129: 13-17.

Foissner W., Foissner I. (1988) The fine structure of *Fuscheria terricola* Berger et al., 1983 and proposed new classification of the subclass Haptoria Corliss, 1974 (Ciliophora, Litostomatea). Arch. Protistenkd. 135: 213-235.

Furness D.N., Butler R.D. (1985) The cytology of sheep rumen ciliates. III. Ultrastructure of the genus *Entodinium* (Stein). J. Protozool. 32: 699-707.

Grain J. (1966) Étude cytologique de quelques ciliés holotriches endocommensaux des ruminants et des équidés. Protistologica 2 (fasc. 1): 59-141, (fasc. 2): 5-51.

Grim J.N. (1985) *Balantidium prionurium* n. sp., symbiont in the intestines of the surgeonfish, *Prionurus punctatus*. J. Protozool. 32: 587-588.

Grim J.N. (1988) A somatic kinetid study of the pycnotrichid ciliate *Vestibulongum corlissi*, N. G., N. Sp. (Class: Litostomatea), symbiont in the intestines of the surgeonfish, *Acanthurus xanthopterus*. J. Protozool. 35: 227-230.

Grim J.N. (1989) The vestibuliferan ciliate *Balantidium acanthuri*, n. sp. from two species of the surgeonfish, Genus *Acanthurus*. Arch. Protistenkd. 137: 157-160.

Grim J.N. (1992) Description of two sympatric and phylogenetically diverse ciliated protozoa, *Balantidium zebrascopi*, n. sp. and *Paracichlidotherus leeuwenhoeki* n. gen., n. sp., symbionts in the intestines of the surgeonfish, *Zebrasoma scopas*. Trans. Amer. Micros. Soc. 111: 149-157.

Hiller S., Bardele C.F. (1988) *Prorodon aklitolophon*, n. spec. and the "dorsal brush" as a character to identify certain subgroups in the Genus *Prorodon*. Arch. Protistenkd. 136: 213-236.

Lipscomb D.L., Riordan G.P. (1990) The ultrastructure of *Chaenea teres* and an analysis of the phylogeny of the haptorid ciliates. J. Protozool. 37: 287-300.

Leipe D.D., Hausmann K. (1989) Somatic infraciliature in the haptorid ciliate *Homalozoon vermicular* (Kinetophragminophora, Gymnostomata) Ditransversalia N. Subcl. and phylogenetic implications. J. Protozool. 36: 280-287.

Lynn D.H. (1981) The organization and evolution of microtubular organelles in ciliated protozoa. Biol Rev. 56: 243-292.

Lynn D.H., Nicholls K.H. (1985) Cortical microtubular structures of the ciliate *Lepidotrachelophylum fornicus* Nicholls & Lynn, 1984 and phylogeny of the litostomate ciliates. Can. J. Zool. 63: 1835-1845.

Noirot-Timothée C. (1958) L'ultrastructure de la limite ectoplasme-endoplasme et des fibres formant le caryphore chez les ciliés du genre *Isotricha* Stein (Holotriches Trichostomes). C.R. Acad Sci. 247: 692-695.

Paulin J.J., Krascheninnikov S. (1973) An electron microscopic study of *Balantidium caviae*. Acta Protozoologica. 12: 97-104.

Puytorac P. de, Grain J. (1965) Structure et ultrastructure de *Balantidium xenopi* s.p. nov. Cilié trichostome parasite du Bactracien *Xenopus fraseri* Boul. Protistologica. 1 (fasc. 2): 29-36.

Small E.B., Marszalek D.S. (1969) Scanning electron microscopy of fixed, frozen and dried protozoa. Science. 163: 1964-1965.

Small E.B., Lynn D.H. (1981) A new macrosystem for the phylum Ciliophora Doflein, 1901. BioSystems 14: 387-401.

Small E.B., Lynn D.H. (1985) Phylum Ciliophora. In: Illustrated Guide to the Protozoa. (Eds. J.J. Lee, S.H. Hutner, E.C. Bovee). Society of Protozoologists, Lawrence, Kansas, 393-575.

Williams N.E., Frankel J. (1973) Regulation of microtubules in *Tetrahymena*. I. Electron microscopy of oral replacement. J. Cell Biol. 56: 441-457.

Williams D.B., Williams B.D., Hogan B.K. (1981) Ultrastructure of the somatic cortex of the gymnostome ciliate *Spathidium spathula* (O. F. M.). J. Protozool. 28: 90-99.

Received on 2nd June, 1992; accepted on 21st October, 1992

Acta Protozoologica (1993) 32: 47 - 62

ACTA
PROTOZOOLOGICA

On the Biology of *Pallitrichodina rogenae* gen. n., sp. n. and *P. stephani* sp. n. (Ciliophora: Peritrichida), Mantle Cavity Symbionts of the Giant African Snail *Achatina* in Mauritius and Taiwan

Jo G. VAN AS and Linda BASSON

Department of Zoology-Entomology, University of the Orange Free State, Bloemfontein, South Africa

Summary. During a research visit to the Indian Ocean island of Mauritius, specimens of the giant African snail, *Achatina fulica* Bowdich, 1822 and *A. panthera* (Férussac, 1821) were found to host two species of trichodinids (Ciliophora: Peritrichida). These trichodinids displayed characteristics such as an adoral spiral of 270°, a horseshoe-shaped macronucleus, a complex microfibrillar system and an infundibulum which does not conform to any of the existing genera in the family *Trichodinidae*. These species are described as *Pallitrichodina rogenae* gen. n., sp.n. and *P. stephani* sp.n. Collections were made at 16 sampling localities throughout the island. It was found that all specimens of achatinids examined were infested, that both species of trichodinids occurred sympatrically on the same host and that hosts of all sizes were infested. Experiments on transmission revealed that cross infestation takes place when snails are in close proximity in an aquatic medium. The morphology of *P. rogenae* is described by means of scanning electron microscopy which revealed the true shape of the elements of the adhesive disc. On a subsequent visit to Taiwan (Republic of China), specimens of *A. fulica* were found to be infested by *P. rogenae*. A theory is put forward on the origin and distribution of these trichodinds from Africa.

Key words. *Trichodinidae, Pallitrichodina*, molluscan symbionts, *Achatina*, ciliophoran.

INTRODUCTION

Among the variety of animal groups acting as hosts for trichodinid ciliophorans are molluscs from marine, freshwater as well as terrestrial environments. Various species of the genus *Trichodina* Ehrenberg, 1830 have so far been recorded from the mantle cavity of aquatic snails (Raabe and Raabe 1959, 1961; Raabe 1965; Shtein 1974). So far, however, only representatives of one genus, *Semitrichodina* Kazubski, 1958, have been described from the mantle cavity of terrestrial snails, i.e. *S. sphaeronuclea* (Lom, 1956) and *S. convexa* Kazubski, 1961 by Lom (1956) and Kazubski (1958, 1961).

During a research visit to the island of Mauritius, specimens of the giant African snail *Achatina* were examined and found to host large populations of trichodinids in the mantle cavity.

The first published record of *Achatina* on Mauritius was that by Bosc (1803) who recorded the occurrence of *A. fulica* Bowdich, 1822 on this island. This snail was purposely introduced into Mauritius as a remedy for an ailment of the then governor's wife. Accounts of its introduction to this island was also given later by

Address for correspondence: J. G. Van As, Department of Zoology-Entomology, University of the Orange Free State, P.O.Box 339, Bloemfontein, South Africa.

Beaquart (1950), Mead (1961) and Purchon (1968). Later a second species, *A. panthera* (Férussac, 1821) was introduced in 1847 (Benson 1858).

After studying the trichodinids from *Achatina*, we came to the conclusion that both *A. fulica* and *A. panthera* were infested with two species of trichodinids which are described here-in. These trichodinids displayed characteristics such as an adoral spiral of 270°, a horseshoe-shaped macronucleus, a complex microfibrillar system and an infundibulum which does not conform to any of the existing genera in the family Trichodinidae. A new genus was created to accommodate these species which are described below. During the study in Mauritius, information was collected on infestation statistics and experiments were carried out to determine how transmission takes place. Preserved material was also used for studying the morphology by scanning electron microscopy.

During a recent research visit to Taiwan (Republic of China), we found specimens of *A. fulica* distributed widely on this island. These achatinids also hosted a trichodinid which upon examination proved to be the same as one of the species found on Mauritius.

Data collected in this study was used in presenting a possible explanation of the origin of these trichodinids on the island of Mauritius and its subsequent distribution to Taiwan.

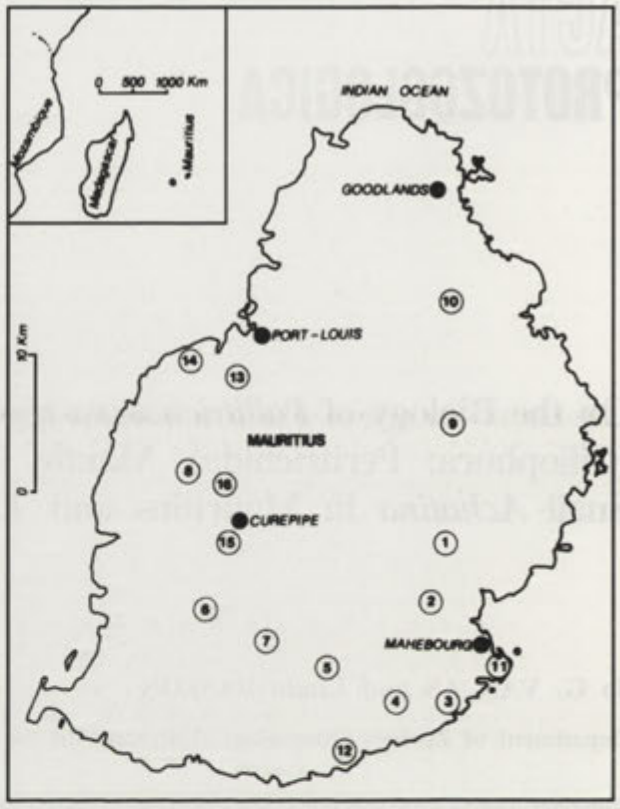

Fig. 1. Map of the Indian Ocean island Mauritius indicating sampling localities where specimens of achatinids were collected. 1 - Ferney, 2 - Riche en Eau, 3 - Mon Tresor, 4 - Savannah, 5 - Britannia, 6 - Makabee Forest, 7 - Grand Bassin, 8 - La Ferme, 9 - F.U.E.L., 10 - Mon Loisir, 11 - Pointe Desny, 12 - Bel Air, 13 - Port Louis, 14 - Pointe aux Sables, 15 - Curepipe, 16 - Vacoas

MATERIAL AND METHODS

Specimens of *Achatina* were collected from 16 different localities on Mauritius (Fig. 1). Localities are numbered from one to 16 which are used in the species descriptions. After establishing that the highest infestation occurs on the moist "neck" region by dissecting the snail, we examined different methods of rapidly collecting a representative sample of trichodinids without having to dissect the host. When the snail was fully extended and firmly attached to a smooth surface, the shell was lifted and gently twisted, following the direction of the whorls. In this way the columella of the shell is lifted away from the foot exposing the "neck" region. By using a glass microscope slide a smear of the area could then be made. A drop of tap water was added to the mucus and spread over the glass slide. These slides were scanned using a dissecting microscope. The level of infestation was divided in a four point scale; * - less than 10 trichodinids, ** - 10 to 100, *** - 100 to 250 and **** - more than 250 trichodinids. Each snail was measured and identified either as *A. fulica* or *A. panthera*.

From each sampling locality, we tried to collect both snail species, but in some cases only *A. fulica* was collected and in others only *A. panthera*. In total 153 specimens were examined, ranging from less than 20 to more than 150 mm in total length.

Slides were kept from each locality for later processing in the laboratory. Smears were processed in the same way as described by Basson et al. (1983). Descriptions are based on both air-dried smears impregnated with silver nitrate in order to study details of the adhesive disc and haematoxylin-stained specimens for studying the nuclear apparatus. All measurements are presented in micrometres and follow the uniform specific characteristic system proposed by Lom (1958). Detailed descriptions of the denticles are presented in accordance with the method proposed by Van As and Basson (1989) and follow the sequence as indicated in Van As and Basson (1992). Minimum and maximum values are given, followed in parentheses by the arithmetic mean, standard deviation and number of specimens measured. In the case of the number of denticles and number of radial pins, the mode is given instead of the arithmetic mean. Body diameter is measured from impregnated specimens as the adhesive disc plus border membrane.

A modified Protargol impregnation method as suggested by Wilbert (1975) was used to reveal the fine details of the infraciliature and microfibrillar system.

For scanning electron microscopy (SEM), material collected as described above was fixed in formalin, washed in tap water, dehydrated in a series of ethanols, transferred to amyl acetate and critical point dried. Additional specimens were prepared as described by Van As and Basson (1989). Sputter coating was done with gold and specimens were examined in a JEOL WINSEM at 5-10 kV.

Some laboratory experiments were carried out to examine methods of transmission. As it is difficult to separate the methods from the results, the methodology will be described together with the results under the heading Observations on Transmission.

Table 1

Biometrical data of *Pallitrichodina rogenae* gen.n., sp.n. and *P. stephani* sp.n. from different localities

	P. rogenae n.sp.			*P. stephani* n.sp.	
Locality	Brittania	Ferney	Nankang and Peikang Rivers	Ferney	Curepipe
Country	**Mauritius**	**Mauritius**	**Taiwan**	**Mauritius**	**Mauritius**
Host	*A.fulica*	*A.panthera*	*A.fulica*	*A.panthera*	*A.fulica*
Body diam.	32.0-44.5 (37.2±3.1)	35.0-46.0 (40.8±2.9)	35.0-44.0 (40.2±2.8)	45.5-57.0 (52.1±3.4)	44.0-61.0 (52.6±4.6)
A.d.diam.	27.5-37.5 (31.9±2.6)	28.0-43.5 (34.3±1.2)	30.0-36.0 (33.6±1.8)	39.0-49.0 (43.7±2.8)	38.0-52.5 (45.4±4.3)
B.m.width	2.0-3.5 (2.6±0.4)	3.0-4.5 (3.4±0.4)	2.5-6.5 (3.4±0.8)	3.0-6.0 (4.2±0.9)	3.0-5.0 (3.8±0.5)
D.r.diam.	14.0-21.0 (17.0±1.9)	12.5-20.0 (16.5±1.7)	15.5-21.0 (17.9±1.4)	21.0-30.0 (25.1±2.5)	20.5-29.5 (24.5±2.5)
D.no.	19-22 (21)	18-22 (20)	18-24 (20)	24-29 (26)	25-30 (27)
R.p.d.	7-9 (8)	8-10 (8)	7-10 (9)	6-10 (8)	8-10 (9)
D.l.	5.0-6.5 (5.8±0.5)	4.0-7.0 (5.5±0.7)	5.0-6.5 (5.7±0.4)	6.0-8.0 (6.8±0.5)	6.0-8.5 (7.2±0.7)
B.l.	2.0-3.5 (2.6±0.3)	3.0-4.0 (3.3±0.3)	2.0-3.0 (2.6±0.4)	2.5-5.5 (4.0±0.8)	3.5-6.0 (4.9±0.7)
C.p.w.	1.0-3.0 (1.5±0.5)	1.5-2.5 (2.0±0.3)	1.0-2.0 (1.5±0.4)	2.0-3.0 (2.2±0.4)	2.0-3.0 (2.4±0.3)
R.l.	1.0-3.0 (2.2±0.6)	2.0-3.0 (2.7±0.4)	1.5-3.0 (2.1±0.3)	2.5-5.0 (3.7±0.9)	3.5-5.5 (4.6±0.7)
D.s.	5.0-7.5 (6.3±0.5)	6.5-9.0 (7.9±0.6)	5.5-7.0 (6.2±0.5)	8.0-12.0 (9.8±1.5)	10.0-13.5 (11.6±0.9)
Ma.shape	C-shaped	C-shaped	horshoe to C-shaped	horseshoe-shaped	not studied
Ma.e.d.	28.0-55.5 (38.7±5.1)	27.0-47.5 (36.7±4.9)	28.0-55.5 (38.7±5.1)	39.0-48.0 (42.3)	
Ma.th.	4.0-7.0 (5.5±0.8)	3.5-7.0 (5.5±0.9)	4.0-7.0 (5.3±0.8)	4.5-7.0 (5.5)	
Ma.x.	13.0-25.5 (20.8±3.6)	8.5-30.0 (21.2±6.0)	13.0-25.5 (20.8±3.6)	24.5-30.0 (26.7)	
Mi.shape	oval	round to oval	round to oval	not detected	
Mi.width	1.0-3.0 (2.0)	1.0-3.5 (2.1±0.5)	3-4		
Mi.length	2.0-5.0 (3.5)	2.5-4.5 (3.2±0.6)	5-7		
Y pos.	$^{+}$Y $^{-}$Y^{1} $^{-}$Y	$^{-}$Y $^{+}$Y	$^{-}$Y^{1}		
Y value	3.0-18.0 (10.5)	0-31.0 (8.6±8.3)	0-14		
Ad.z.	320°	320°	295-345°	300°	300°
n^1	25	24	25	18	17
n^2	24	24	24	17	-
n^3	3	25	3	-	-
Ref.mat.		87/05/14-01	88/11/01-08		87/06/19-01
Typ.mat.	87/05/26-01 87/05/26-02 87/05/19-01			87/05/14-01 87/05/14-02 87/05/23-01	

Abbreviations: A.d. - adhesive disc, Ad.z - adoral zone, B.l. - blade length, B.m. - border membrane, C.p.w. - central part width, diam. - diameter, D.l. - denticle length, D.no. - denticle number, D.r. - denticle ring, D.s. - denticle span, e.d. - external diameter, Ma. - macronucleus, Mi. - micronucleus, n^1 - number of silver impregnated specimens measured, n^2 - number of macronuclei measured, n^3 - number of micronuclei measured, Ref.mat. - reference material, R.l. - ray length, R.p.d. - number of radial pins per denticle, th. - thickness, Typ.mat. - type material, Y pos. - Y position of micronucleus, x. - length of sector between terminations of macronucleus

Type-material of the new genus and species described in this paper is deposited in the collection of the National Museum in Bloemfontein, South Africa, while additional reference material is in the collection of the authors.

RESULTS

Pallitrichodina gen. n.

Diagnosis

Member of the family Trichodinidae Claus, 1874 with adhesive disc comprising denticles with well-developed blades, central parts and rays. Adoral spiral more than 180°, but less than one full circle. A very distinct microfibrillar system is present, which is closely associated with distinct body indentations, corresponding to microfibrils attached to the periphery of the body adoral to adhesive disc. Infundibulum situated at right angle to adhesive disc. Macronucleus C- or horseshoe-shaped. Symbionts in the mantle cavity of terrestrial molluscs.

Pallitrichodina rogenae gen. n., sp. n.

Hosts and localities: Mantle cavity of *Achatina fulica*; Sites 1, 2, 4, 5, 6, 7, 8, 9, 10, 13, 14, 15, 16. Mantle cavity of *Achatina panthera*; Sites 1, 2, 3, 5, 6, 10, 11, 12, 14.

Type-specimens: Holotype, slide 87/05/26-01, and paratype, slide 87/05/26-02 and 87/05/19-01, in the collection of the National Museum, Bloemfontein, South Africa.

Type-host and locality: *A. fulica*, Britannia(5).

Etymology: This species was named after Dr. Rogene Thompson who acted as our host during our visit to Mauritius.

Biometrical data is summarized in Table 1.

Description

Pallitrichodina rogenae is a small to medium-sized trichodinid with a cup-shaped body. The adoral cilia is in the form of a closed C-shape, which is situated almost at the highest point of the body (Figs. 9A, D). The beginning of the adoral zone and the point where it disappears into the infundibulum is at the same level. The adoral ciliary ring is spaced perfectly in the middle of the adoral surface. The ciliary apparatus is composed of a distal septum separating the cilia from the body (Figs. 9A, B, D). On the inner margin of the septum, a single row, the haplokinety begins out of phase with three rows of inner cilia, the polykinety (Figs. 9B, 14A, B). The haplo- and polykineties are separated by a groove. The cilia of the four rows appear to be of the same length and thickness. Both the haplo-as well as the polikinety dip into the infundibular funnel, the haplokinety extending further along the outer lip whilst the polikinety plunges directly into the funnel. Both kineties perform a spiral of 1.5 turns before reaching the cytostome (Figs. 14A, B). Thus both rows are mutually shifted out of phase while continuing their counter clockwise spiral down the funnel. No germinal row was observed. When entering the infundibulum the polikinety widens forming a peniculus of which the number of rows could not be distinguished. The haplokinety is supported by a short impregnable band situated near the last spiral of the haplokinety. No C-shape structure was observed at the inner end of the infundibulum. The infundibulum is situated at a right angle to the adhesive disc. As the adoral cilia enters the infundibulum, the cilia performs a spiral of 1.5 turns before reaching the cytostome (Fig. 9C).

Directly adoral to the ciliary girdle characteristic body indentations are clearly visible. These indentations are also distinct in live specimens and is also visible in some haematoxylin stained material (Fig. 10A). They vary in number between 15 and 21 and correspond to microfibrils which are most likely attached at the point of indentation. The complex microfibrillar system consists of three interlinking rings (Figs. 9E, F, 12). The aboral ring, the longer, consists of a circular band at the level and parallel to the adhesive disc. This ring consists of radially and evenly spaced projections tapering from a broad basis proximally to a sharp distal point which corresponds to the body indentations. Each of these projections consists of three distinct fibrils. The smaller adoral ring of the microfibrillar system is formed by the adoral zone which is linked to the aboral circle via vertical bands of fibrils. The whole fibrillar system forms the shape of a top hat (Figs. 9F, 12).

The cytoplasm of *P. rogenae* is characterized by granular inclusions of a consistent size which can clearly be seen in both Protargol impregnated and haematoxylin stained material (Figs. 9F, 10A).

The aboral ciliary complex consists of three groups of cilia. On the adoral side the marginal cilia consists of a single row of long cilia well spaced, wedged between two septa (Fig. 10B). The outer ciliary ring consists of

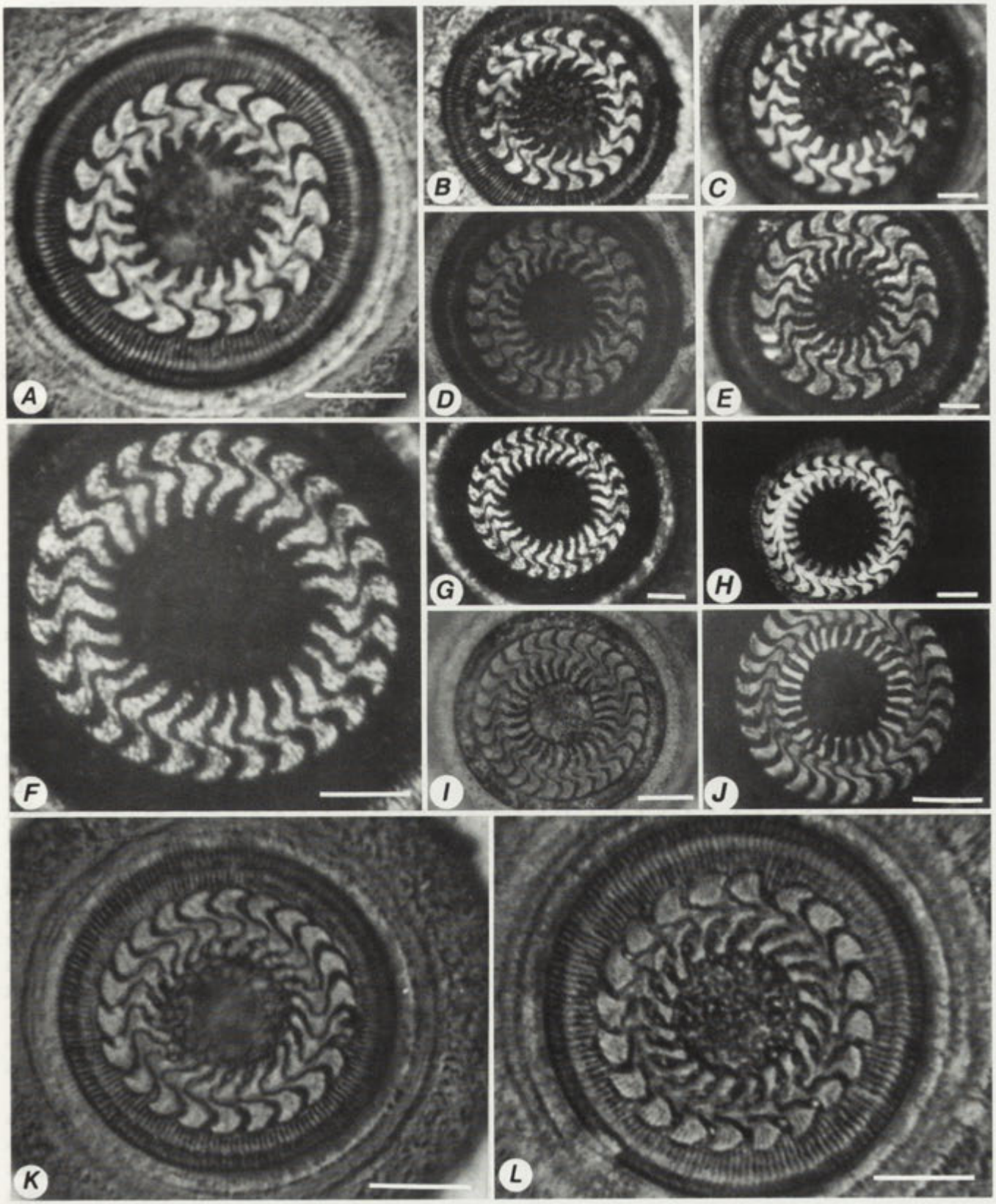

Fig. 2. Photomicrographs of silver impregnated specimens of adhesive discs of trichodinid species. A-C - *Pallitrichodina rogenae* sp.n. from *Achatina fulica*, Ferney; D,E - *P. rogenae* from *A. panthera*, Ferney, F - *P. stephani* sp.n. from *A. panthera*, Ferney, G,H - *P. stephani* from *A. panthera*, Savannah, I,J - *P. stephani* from *A. fulica*, Ferney, K,L - *P. rogenae* from *A. fulica*, Nankang-Peikang Rivers, Taiwan. Scale-bar: 8.5 µm (A, F, K, L), 6 µm (B-E, G-J)

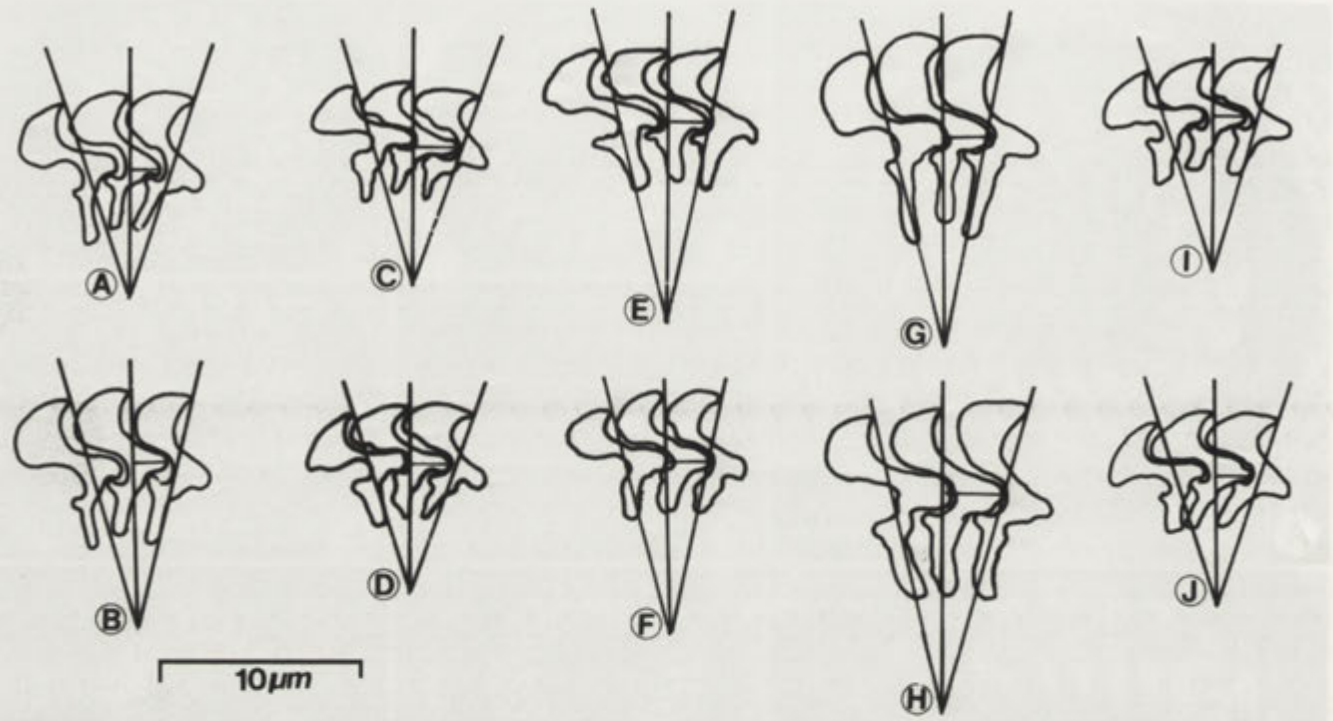

Fig. 3. Microscope projection drawings of the denticles of trichodinids. A,B - *Pallitrichodina rogenae* from *Achatina panthera*, Mauritius, C,D - *P. rogenae* from *A. fulica*, Mauritius, E,F - *Pallitrichodina stephani* sp.n. from *A. panthera*, Mauritius, G,H - *P. stephani* from *A. fulica*, Mauritius, I,J - *P. rogenae* from *A. fulica*, Taiwan

11 rows of which those closer to the marginal cilia are longer with consecutive rows becoming increasingly shorter (Fig. 10C). The inner ciliary ring consists of a single row of short cilia separated from the outer cilia by a septum.

The border membrane in *P. rogenae* is broad and frequently characterized by a ridge near the outer perimeter (Figs. 10C, D). This ridge is sometimes clearly visible in silver impregnated stains (Fig. 2A). It would appear that the border membrane may display some flexibility at this point, but not to the same degree as at the hinged point where it is connected to the radial pins of the striated membrane. No evidence was, however, found of a hinge-like structure at this point in dissolved specimens (Fig. 10F). The striated membrane stretches to the central part of the denticle on the adoral side and consists of well developed radial pins linked together by platelets forming a continuous band on the distal perimeter of the blade (Figs. 10E, F). In some specimens the distance between the distal point of the blade and border membrane is notably greater than other specimens. This accounted for considerable variation in adhesive disc diameter (See Fig. 6). The distal edges of these pins have a broad joint-like surface at which point articulation with the peripheral pins of the border membrane is facilitated (Fig. 10E). Two to three peripheral pins are joined to each of the radial pins in the striated membrane.

The denticles in the ring are wedged tightly together leaving very little space in between (Fig. 10D). The centre of the adhesive disc is the same in texture as the rest of the adhesive disc. The blade is broad and sickle-shaped (Figs. 2A-E, 3A-D). The distal surface slopes down towards a prominent apex. The tangent point is sharp, situated mostly higher than the distal surface (Fig. 3C). The anterior margin and apex are angular, the apex extending to and sometimes beyond the y+1 axis. The blade apophysis is prominent, forming a smooth articulation surface with the adoral side of the central part (Fig. 11B). The posterior margin forms a shallow curve in relation to y the axis. The deepest part corresponds to the apex of the blade. The blade connection, although appearing thin in some specimens, is well developed, but short. Considerable variation was noted between different specimens.

The notch on the central part is not visible as a groove of articulation with the previous denticle is situated on the adoral surface. In SEM micrographs (Fig. 11A), this articulation surface is revealed as a groove. The central part is well developed, sharply pointed to round, fitting tightly into the preceding denticle. The central conical part, although not visible in

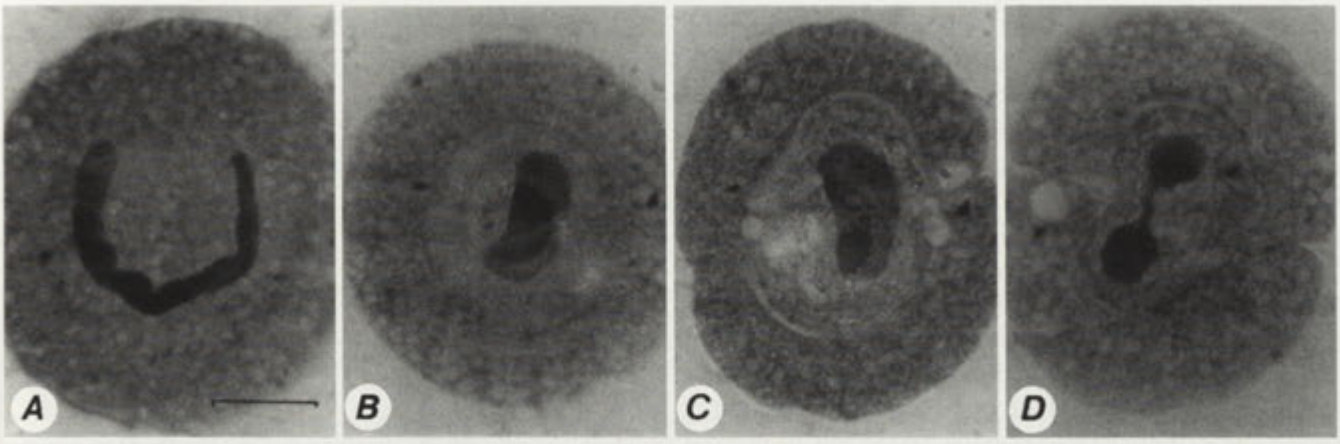

Fig. 4. Photomicrographs of haematoxylin stained nuclear material of *Pallitrichodina rogenae* sp.n. from *Achatina fulica*, Mauritius. A - vegetative macronucleus, B-D - stages in the process of binary fission, D - cell in final stage of division. Scale-bar: 17 µm

silver impregnated specimens, is strongly developed and tapers to a sharp point (Fig. 11A). When viewed from the adoral side it is clear that the adoral surface of the central part is considerably broader and extends further in a posterior direction than is the case for the aboral surface (Fig. 11A). The distal and proximal sides of the central part has a deep groove which facilitates a secure connection between the consecutive denticles. At the same time this groove and the corresponding opening of the preceding denticle could serve as an articulation surface which could allow twisting movements of individual denticles whilst maintaining the circular structure of the denticle ring.

The apex of the central part extends to the y-1 axis. The section above the x axis slopes downwards, with the section below almost parallel to the x axis. In some silver impregnated specimens, the indentation on the bottom section of the central part is visible. In SEM micrographs, however, no indentation is visible as the articulation with the ray apophysis is situated on the adoral surface of the blade (Fig. 11D). In Fig. 11A where dislodged denticles can be seen from a distal view, it is clear that the blades and rays are flattened in an aboral-adoral way and the central part is wider.

The ray connection is not clearly distinguishable from the rest of the ray in most specimens. The ray apophysis is strongly developed, triangular in shape and directed in a straight line towards the following denticle. The point of the apophysis extends past the ray of the following denticle. The shape of this projection could only be exposed by SEM studies. When the denticle ring is intact, the strongly developed ray apophysis is not always visible in all silver impregnated specimens. The true shape of this apophysis can clearly be seen in specimens where the denticle ring is dislodged. In a adoral view of the denticles, this very strong apophysis which we normally refer to as the ray apophysis is seen (Fig. 11B). It is in fact a protrusion of the central part rather than the ray. Most likely this will also apply to other species where a so-called ray apophysis is present. For taxonomic descriptive purposes, however, we suggest that the term ray apophysis referring to this structure should remain in use. The rays show some variation in shape and size. They are short, robust and terminate in flat blunt points. The rays are mostly straight, but in some specimens projected in an anterior direction. All specimens examined by SEM, have broad rays wedged tightly together. This in particular was not always evident in silver impregnated specimens where the rays in many specimens appeared thin (Fig. 2B), most likely the result of impregnation differences.

The ratio of the denticle above to the denticle below the x axis is one to slightly more than one (1.05-1.3).

Pallitrichodina stephani sp. n.

Hosts and localities: Mantle cavity of *Achatina fulica*; Sites 2, 4, 5, 6, 7, 10, 13, 15, 16. Mantle cavity of *A. panthera*; Sites 1, 2, 3, 4, 5.

Type-specimens: Holotype, slide 87/05/14-01 and paratype, slides 87/05/14-02 and 87/05/23-01, in the collection of the National Museum, Bloemfontein, South Africa.

Type-host and locality: *A. panthera*, Ferney(1).

Etymology: This species was named after the young Stephan Van As in acknowledgement for his enthusiastic collection of snails on Mauritius.

Biometric data is summarized in Table 1.

Description

Pallitrichodina stephani is a medium-sized trichodinid with a cup-shaped body. General morphology such as the adoral ciliary zone, infundibulum, microfibrillar system and locomotor fringe are the same as that described for *P. rogenae* above.

The centre of the adhesive disc is the same in texture as the rest of the adhesive disc. The shape of the denticles show considerable variation in different specimens (Figs. 2F-J, 3E-H). The blade is sickle-shaped, sometimes with the distal part of the blade broader than the proximal part. The distal surface in some specimens is parallel to the border membrane, in others the distal surface slopes down towards the apex. The anterior margin is angular, in some specimens the anterior margin is rounded. The prominent apex extends to and sometimes beyond y+1 axis. The blade apophysis is present and in some specimens even prominent. The curve of the posterior margin is deep, with the deepest point opposite the apex. The blade connection is thin and extended. The central part is robust with the apex of the central part sloping downwards appearing almost hook-like. The section above the x axis is curved with a rounded tip and the section below forms a slightly concave curve. Although it appears as if a notch is present, SEM revealed that the aboral section of the central part does not have a notch, as the articulation surface with the ray apophysis is on the adoral side of the central part (Figs. 11C, D).

The ray connection is short and indistinct. The ray apophysis is strongly developed, situated high on the ray, triangular in shape with the tip obscured by the central part of the following denticle. The rays are broad and stout with flat blunt points.

The ratio of the denticle above to the denticle below the x axis is more than one (1.25-1.4).

***Pallitrichodina rogenae* - Taiwan (Figs. 2K,L, 3I-J)**

Specimens of *Achatina fulica* examined from two out of three localities in Taiwan (Republic of China) hosted trichodinids in the mantle cavity which upon examination proved to be representatives of *P. rogenae*. The infested snails were found in the Taipei area and Nankang and Peikang Rivers in the central part of Taiwan. Snail specimens from the third locality at the Feitsui Reservoir high in the mountains were found not

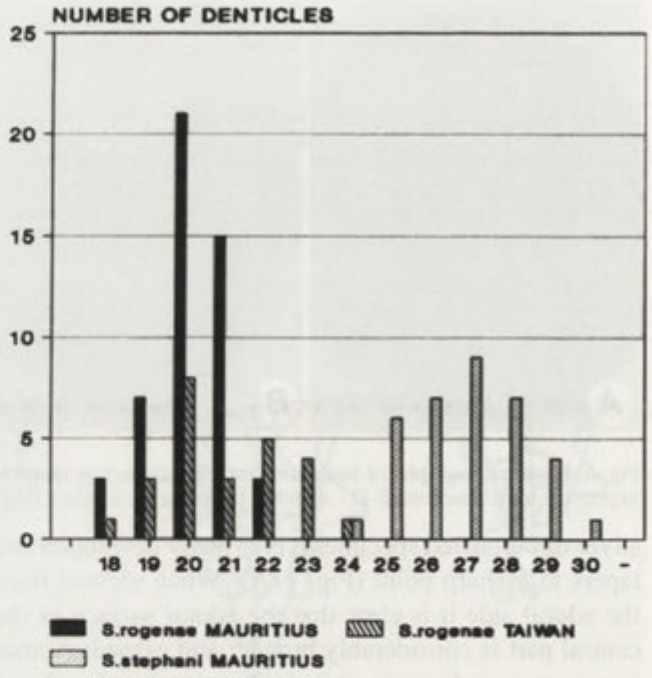

Fig. 5. Histogram of the frequency of denticle numbers of individual specimens of *Pallitrichodina rogenae* sp.n. from Mauritius and Taiwan as well as *P. stephani* sp.n. from Mauritius

to be infested. The morphometrical data of *P. rogenae* from Taiwan is included in Table 1 for comparative purpose. These body measurements all fall within the range recorded for *P. rogenae* from Mauritius. Adhesive disc (Fig. 6), denticle ring (Fig. 7) and denticle span (Fig. 8) were almost identical with that recorded for the type population. The number of denticles also corresponded to that of the type population (Fig. 5). No specimens of *Semitrichodina stephani* were found on any of the examined hosts.

Taxonomic Remarks

So far the only trichodinids collected from terrestrial molluscs were assigned to the genera *Trichodoxa* Sirgel, 1983 and *Semitrichodina* Kazubski, 1958. Representatives of the genus *Trichodoxa* were reported from the genital system of *Trachycystis* species by Sirgel (1983). This genus is characterized by a single row of cilia in the locomotor fringe as well as a border membrane adorned by stout spines on its circumference. These features were not found in the present material which further differed from *Trichodoxa* in general body shape, as well as the position of the adoral spiral in relation to the adhesive disc.

In the case of *Semitrichodina* the adoral spiral is notable abridged, completing only half a turn and slanted

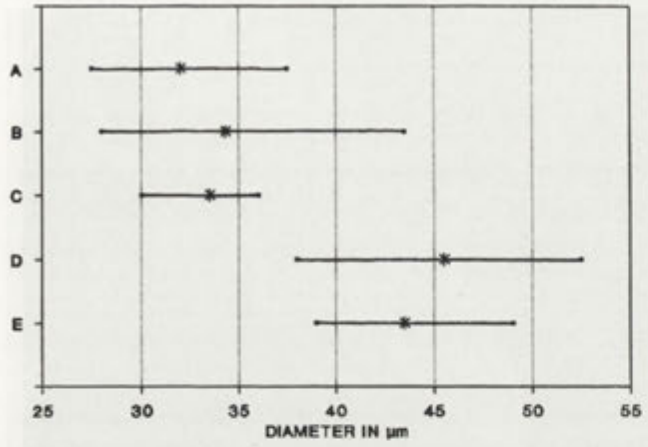

Fig. 6. Diagrammatic representation of the range of adhesive disc diameter of different populations of *Pallitrichodina* species. A - *P. rogenae* sp.n. from *Achatina fulica*, Mauritius, B - *P. rogenae* from *A. panthera*, Mauritius, C - *P. rogenae* from *A. fulica*, Taiwan, D - *P. stephani* sp.n. from *A. fulica*, Mauritius, E - *P. stephani* from *A. panthera*, Mauritius

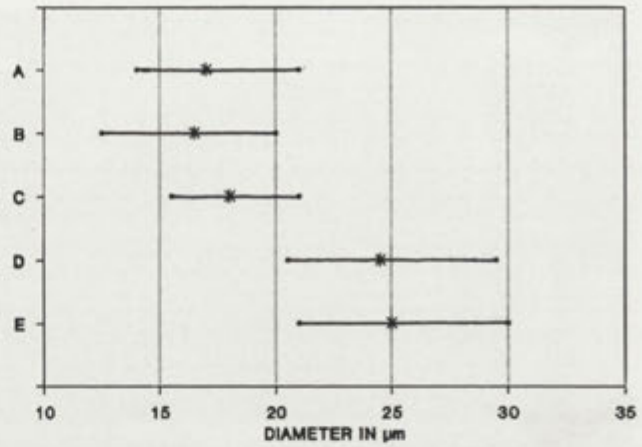

Fig. 7. Diagrammatic representation of the range of denticle ring diameter of different populations of *Pallitrichodina* species. A - *P. rogenae* sp.n. from *Achatina fulica*, Mauritius, B - *P. rogenae* from *A. panthera*, Mauritius, C - *P. rogenae* from *A. fulica*, Taiwan, D - *P. stephani* sp.n. from *A. fulica*, Mauritius, E - *P. stephani* from *A. panthera*, Mauritius

at an angle in relation to the adhesive disc. The macronucleus is ovoid to spherical. In both species of the present material specimens were found with nuclear material representing different stages of division (Figs. 4A-D). The vegetative nucleus, however, was always horse-shoe or C-shaped (Fig. 4D). The micronucleus was only detected in some specimens. The position varied from +Y to -Y as well as -Y[1]. This variation in position is most likely the result of the different ways in which specimens flattened when preparations were made, rather than a variation in its actual placement. The infundibulum of *Semitrichodina*, unlike our material, is parallel to the adhesive disc. The infundibulum of *Semitrichodina* makes two full turns with a well developed impregnable band, while in our material the infudibulum completes a spiral of 1.5 turns with a weakly developed impregnable band. *Semitrichodina* is characterized by a third kinety which is absent in *Pallitrichodina*. No mention is made of a microfibrillar system in any of the descriptions of *Semitrichodina* (Lom 1956; Kazubski 1958, 1960, 1961, 1981; Raabe and Raabe 1961) whilst this is prominent in the present material.

The difference between our material and those described for *Semitrichodina* and *Trichodoxa* in our opinion warrants the creation of a separate genus to accomodate these trichodinids.

Despite the resemblance in morphology between *P. rogenae* and *P. stephani* as mentioned above, the two species differ significantly in a number of important characteristics (See Table 1; Figs. 5-8). The number of denticles varies between 24 and 30 with a mode of 27 in *P. stephani*, which is outside the upper range of that recorded for *P. rogenae* (See Fig.5). Although both species display a very prominent ray apophysis which is similar in shape, the shape of the blades are different. In the case of *P. stephani* the blades are mostly broad and most specimens have a more prominent distal surface, where in the case of *P. rogenae* the distal blade surface is not distinguishable from the rest of the blade surface. The most important difference in denticle morphology is to be found in the central part. Although this structure is of robust nature in both species, the apex of *P. stephani* slopes downwards to almost form a hook-like shape at the point where it articulates with the following denticle (Figs. 11C, D). The central part in *P. rogenae* is rounded and straight (Fig. 10D).

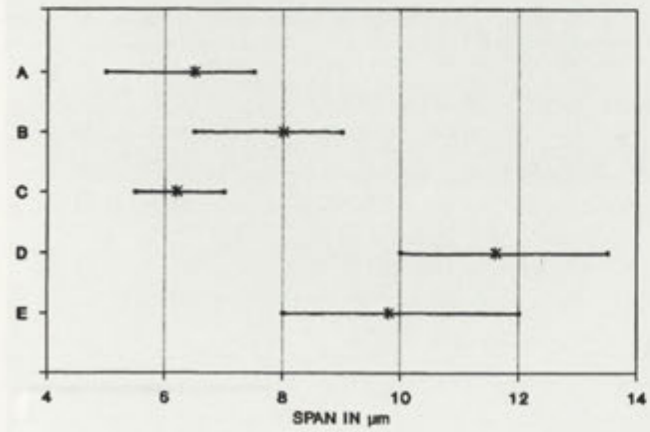

Fig. 8. Diagrammatic representation of the range of denticle span of different populations of *Pallitrichodina* species. A - *P. rogenae* sp.n. from *Achatina fulica*, Mauritius, B - *P. rogenae* from *A. panthera*, Mauritius, C - *P. rogenae* from *A. fulica*, Taiwan, D - *P. stephani* sp.n. from *A. fulica*, Mauritius, E - *P. stephani* from *A. panthera*, Mauritius

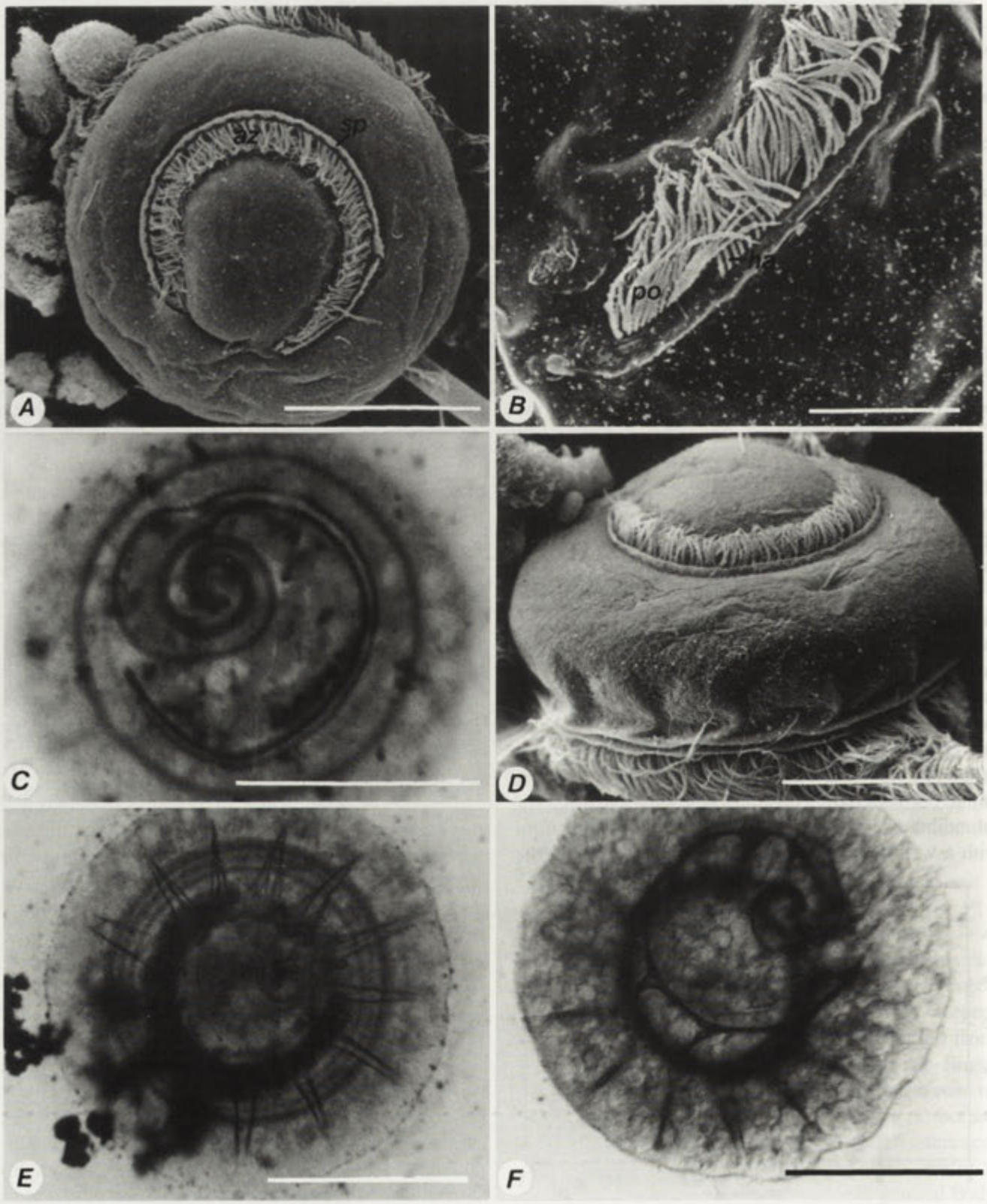

Fig. 9. Scanning electron micrographs (A,B,D) and photomicrographs of Protargol stained specimens (C,E,F) of *Pallitrichodina rogenae* sp.n. (A-E) and *P. stephani* sp.n. (F) from Mauritius. A - showing adoral ciliary zone (sp), B - point of origin of adoral zone with polikinety (po) beginning out of phase with haplokinety (ha), C - infraciliature, D - body showing indentations, E - microfibrillar system showing aboral ring, F -microfibrillar system showing adoral zone, vertical bands and aboral ring slightly out of focus. Scale-bar: 20 µm (A, C-F), 5 µm (B)

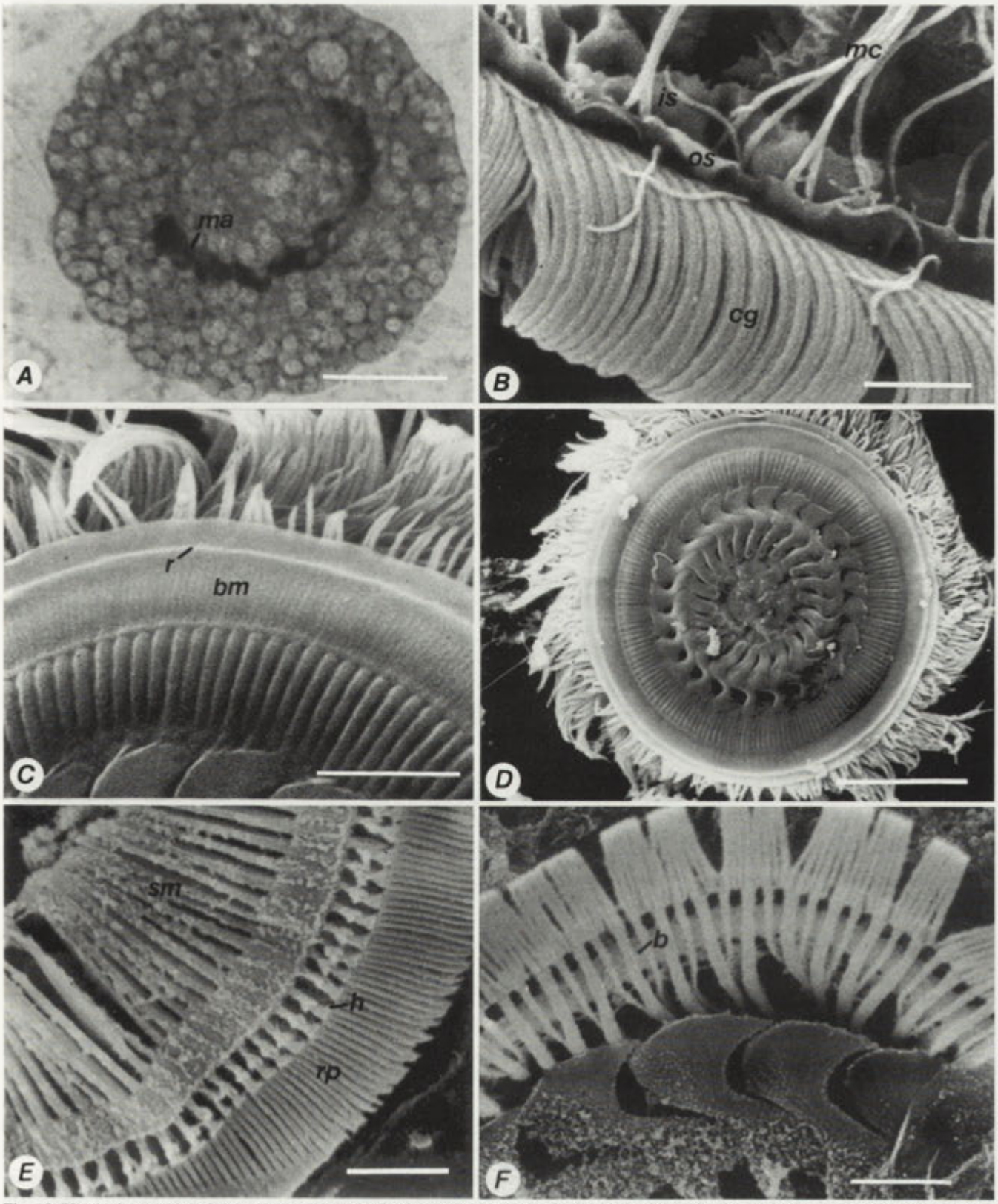

Fig. 10. Photomicrographs of haematoxylin stained specimen (A) and scanning electron micrographs (B-F) of *Pallitrichodina rogenae* sp.n. form Mauritius. A - macronucleus with rest of body filled with granular inclusions, B - ciliary girdle, C - border membrane, D - adhesive disc, E - adoral view of striated embrane, F - straited membrane with denticles from aboral side. Abbreviations: b - band of interlinking platelets, bm - border membrane, cg - ciliary girdle, h - hinge, is - inner septum, mc -marginal cilia, os - outer septum, r - ridge, rp - peripheral pins. Scale-bar: 2.5 µm (B,C,E,F), 15 µm (A,D)

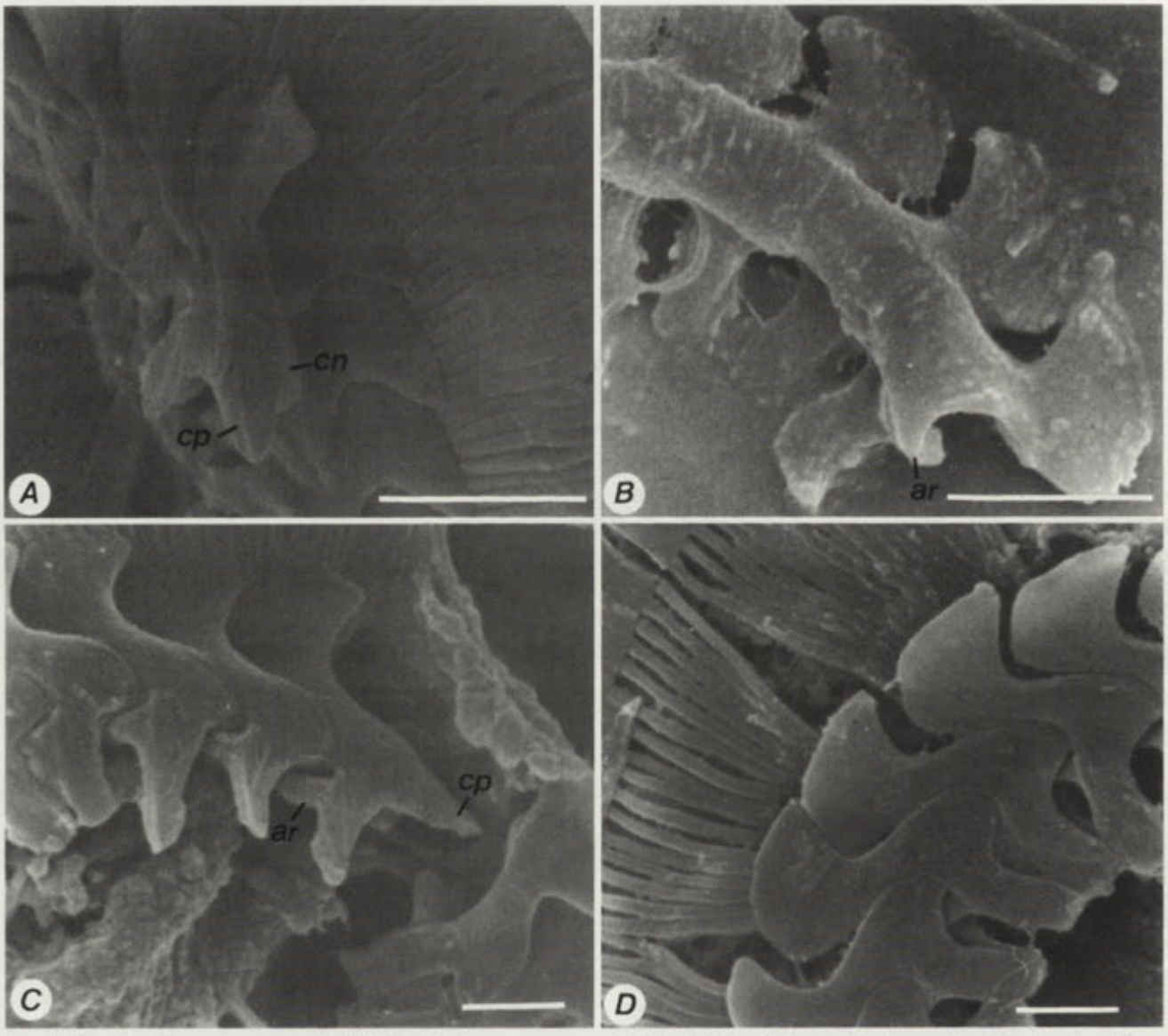

Fig. 11. Scanning electron micrographs of *Pallitrichodina rogenae* sp.n. (A,B) and *P. stephani* sp.n. (C,D) from Mauritius. A - aboral view of dislodged denticles, B - adoral view of broken denticle ring, C - aboral view of broken denticle ring, D - aboral view of denticles. Abbreviations: ar - ray apophysis, cn -adoral section of central part, cp - central conical part. Scale-bar: 3 µm

So far the only reference to any other trichodinid collected from an achatinid is that by Fantham (1924) who reported the occurrence of *Trichodina achatinae* Fantham, 1924 in the receptaculum seminis of *Achatina zebra* from southern Africa. This paper, however, does not provide sufficient data for any meaningful comparison. It is however, highly unlikely that our material is the same as Fantham's as he clearly states that he did not find any specimens in any other organ than the receptaculum seminis. Until we had the opportunity to collect more material from *A. zebra*, it would not be possible to make any further comments on the species described by Fantham (1924).

Infestation Statistics

Specimens of *Achatina fulica* and *A. panthera* occurred at most of the localities sampled (Table 2). At Mon Tresor (no. 3), Pointe Desny (no. 11) and Bel Air (no. 12) only *A. panthera* was collected. These localities are all at sea level. In the high lying localities (380 metres and above), only *A. fulica* was collected. The fact that *A. panthera* was absent from these localities, correlates with the observation by Mead (1961). He suggests that when *A. panthera* was introduced into Mauritius this snail successfully spread and became the dominant species on the lower lying areas forcing

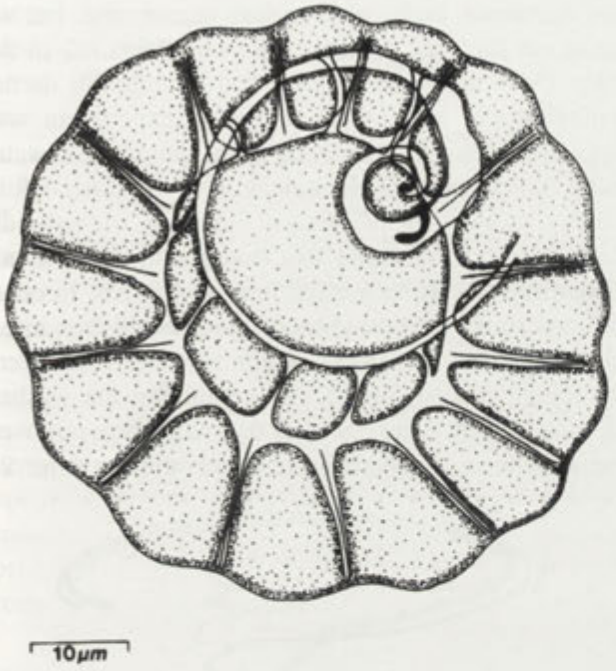

Fig. 12. Microscope projection drawing of Protargol impregnated specimens of the infraciliature and microfibrillar system of *Pallitrichodina stephani* sp.n. from Mauritius

A. fulica to inhabit the higher lying areas above 300 metres where this snail is the dominant species today.

Both species of trichodinids were found widespread throughout the island. *Pallitrichodina rogenae* was, however, clearly the dominant species and were found in different localities to be the only species. In only one population of snails examined, i.e. Savannah (no. 4) *P. stephani* alone was collected from *A. panthera*.

Although a total of more than 150 specimens of achatinids were examined, not a single specimen could be found without a trichodinid infestation. There was no pattern concerning different levels of infestation in smaller and larger specimens (Fig. 13) and infestations occurred throughout the full range of snails from less than 20 mm up to 140 mm in shell length. Specimens which bore high infestations (****) occurred amongst all length groups. Low levels of infestation (*) also occurred on larger as well as smaller specimens. In the size range 41 to 50 mm of which the most specimens of *Achatina* were examined, very high (****) and high infestations (***) were found in almost equal numbers, with slightly less individuals with medium (**) to low (*) infestations. In total more achatinids carried high to very high infestations than low to medium infestations. These results suggest that a very effective mechanism of transmission exists which is not related to age of snail specimens.

Observation on transmission

The lack of uninfested *Achatina* necessitated the use of other terrestrial molluscs in order to examine the modes of transmission. A snail commonly found on Mauritius is the introduced predator *Euglandina rosae*. This snail proved to suit our purpose ideally. A number of specimens of this snail were dissected and they were found to be uninfested by trichodinids.

Concerning transmission, our hypothesis was that cross infestations will take place when snails are in physical contact or that transmission can take place in an aquatic medium. Although there are differences in the pattern of precipitations at the different sampling localities, the island in general has a very high rainfall. We often observed achatinids in pools of water and at different occasions found achatinids floating in canals and streams. Part of our hypothesis was that such conditions as well as the moist conditions in undergrowth and decaying vegetation where achatinids feed, could also serve as medium for transmission.

In order to study the survival of trichodinids away from their host in water, the following procedure was followed: Trichodinids were collected from the mantle cavity of achatinids by making smears as described

Table 2

Summary of data collected on infestation of achatinid snails by trichodinids on Mauritius

Locality	Altitude in metres above sea level	*Achatina fulica*		*Achatina panthera*	
		Pallitrichodina rogenae	*P.stephani*	*P.rogenae*	*P.stephani*
1	40	*	x	*	*
2	40	*	*	*	*
3	SL	No snails collected	*	*	
4	40-80	*	*	x	*
5	200	*	*	*	*
6	400	*	*	No snails collected	
7	560	*	*	No snails collected	
8	120-160	*	x	-	-
9	160	*	x	-	-
10	80	*	*	*	x
11	SL	No snails collected	*	x	
12	40	No snails collected	*	x	
13	40-80	*	*	No snails collected	
14	40	*	x	*	x
15	560	*	*	No snails collected	
16	380	*	*	No snails collected	

SL - sealevel, x - trichodinid species not found, * - trichodinid species found, - snails were collected and found to be infested, but no species identification of trichodinids was possible

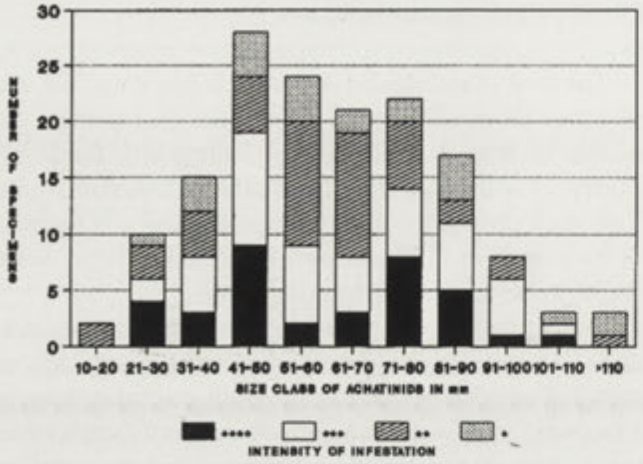

Fig. 13. Staggered histogram of intensity of infestation found in different size classes of achatinid snails in Mauritius. No distinction was made between the two achatinid or trichodinid species. * - less than 10 trichodinids, ** - 10-100, *** - 100 -250, **** - more than 250 trichodinids

under Methods. These trichodinids were transferred to a Petri dish filled with tap water and observed every 10 minutes for an hour and thereafter every hour for 12 hours. At every observation trichodinids were found swimming actively. No change in their mobility was observed even after 12 hours. From this we concluded that trichodinids could survive for extended periods in water which could affect transmission if they are washed off their host and susceptible hosts are present.

The next question was to determine whether achatinids and their trichodinid symbionts could survive in water for extended periods. Mead (1961) reported that achatinids could survive for up to 48 hours in water even when the dissolved oxygen has been driven off by boiling the water prior to inundation of snails.

We placed five achatinid snails in a sealed container filled with water. After 12 hours all the snails were still alive and upon examination it was found that they still all hosted active trichodinids. The inundated snails secreted mucus which covered their feet and part of the shells. Trichodinids were also found free swimming within this mucus. From this we concluded that not only can trichodinids survive extended inundated conditions, they will be found outside the mantle cavity in the mucus which will provide ideal conditions for transmission. Although this is a possibility of transmission, it is unlikely that this would be the normal route by which achatinids be infested and should rather be regarded as the exception.

We examined the mucus trials left by achatinids when moving about. Ten snails were left to roam about in a moist plastic tray overnight. The next morning the tray was examined under a dissecting microscope, but we could not find any evidence of trichodinids left in the trials. From this we concluded that trichodinids do not spontaneously leave their host. The experiment was repeated, but this time spraying the achatinids with water using Pasteur pipettes. Examination of the water left in the tray, revealed the presence of numerous trichodinids. With this we concluded that under rainy conditions, trichodinids could be washed from their hosts. In order to establish whether these trichodinids could then infest other hosts, five specimens of uninfested *E. rosae* were left roaming about in the tray containing the washed off trichodinids. After one hour the snails were removed and examined. They all hosted trichodinids. After 24

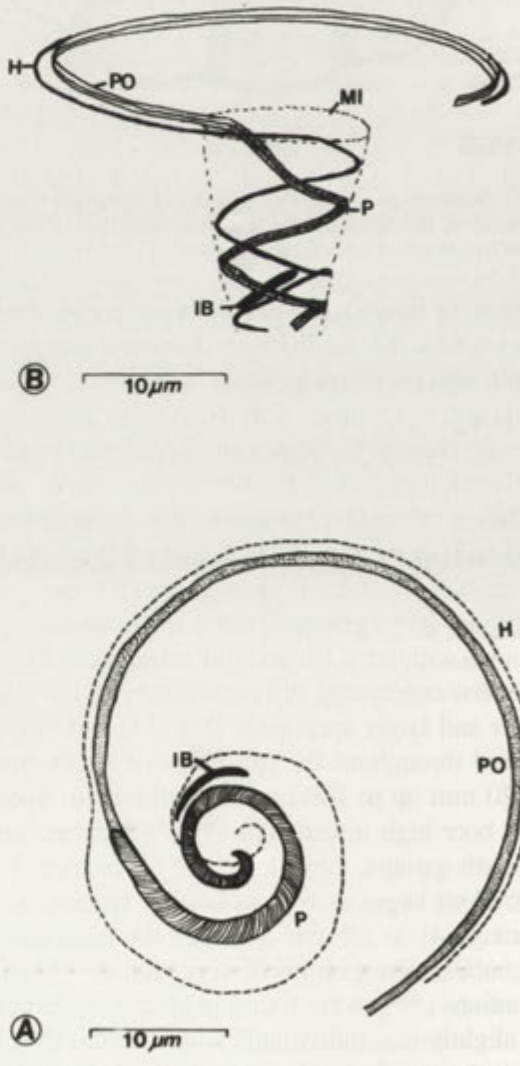

Fig. 14. Drawings from Protargol impregnated specimens of the infraciliature of *Pallitrichodina rogenae* sp. n. from Mauritius. A - microscope projection drawing of an adoral view, B - schematic presentation of a lateral view. Abbreviations: H - haplokinety, IB - impregnated band, MI - mouth of infundibulum, P - peniculus, PO -polikinety

hours all snails still hosted small numbers of trichodinids and after 48 hours one of the specimens still hosted a small number of ciliates. After 72 hours, however, the snails were all free of trichodinids.

In order to establish whether cross infestations could take place merely by physical contact, five uninfested *E. rosae* snails were placed in a glass aquarium containing 20 infested achatinids. One week later these snails were removed and examined. They were found to host populations of trichodinids. These snails were removed and maintained separate and after 48 hours no trichodinids could be found. The fact that *E. rosae* collected from different localities in Mauritius did not host any trichodinids suggested that this snail is not a suitable host for these trichodinids to establish a viable infestation. *E. rosae* left together with achatinids were probably reinfected continuously as when they were removed the infestation only lasted for two days.

Our conclusions concerning transmission are that cross infestation probably occurs in different ways. The trichodinids are capable of swimming for extended periods in moist conditions where they will reinfest a slow moving snail when passing over this area. When snails are in close proximity as we often found in the undergrowth, transmission will be direct. It is therefore not surprising that the level of infestation of achatinids in Mauritius is so high that we could not find any uninfested snails on the island.

We have so far only examined about 50 achatinids from different parts in southern Africa, but has yet been unable to find any infested snail there. We have, however, not so far had the opportunity to examine either *A. fulica* or *A. panthera* from their endemic areas from the East coast of Africa.

CONCLUDING REMARKS

The trichodinids from *Achatina* in Mauritius are clearly two different and distinct species. They are, however, closely related and most likely share a common ancestor. The fact that these two trichodinids now share common hosts on Mauritius, does not necessarily imply that both trichodinids share these hosts in their endemic area of distribution in East Africa. According to Bequaert (1950) *A. panthera* and *A. fulica* do not occur sympatrically in Africa and although the snails are also found in Madagascar it is not clear whether this forms part of their natural range of distribution. It is most likely that these snails were introduced to Madagascar by man.

It is a well documented fact that *A. fulica* was introduced to the island of Mauritius from Madagascar close to the turn of the previous century and that it rapidly established viable populations spread throughout the island (Bosc 1803). It is furthermore well documented that *A. panthera* only arrived at Mauritius approximately 47 years after *A. fulica*. During the same year *A. fulica* was introduced to India from Mauritius. It is safe to presume that the specimens of *A. fulica* which left Mauritius had no contact with the newly introduced *A. panthera*.

Although this needs to be confirmed, our information suggests that *Pallitrichodina rogenae* originates from its original host *A. fulica* from East Africa, whilst *P. stephani* is originally a parasite of *A. panthera* from Africa. If our deductions are correct, this will explain the absence of *P. stephani* in Taiwan as the original introduction to this island originated from snail stock which left Mauritius before the introduction of *A. panthera* and its parasite *P. stephani*.

Acknowledgements. The authors wish to express their appreciation to the Camaron Production Company PTY LTD, Mauritius for their logistic support and permission to sample on sugar estates during our research in Mauritius. We are also grateful to Dr. Rogene Thompson for her interest and support in this study. This project was carried out with the financial support of the Foundation for Research Development, Republic of South Africa.

REFERENCES

Basson L., Van As J.G., Paperna I. (1983) Trichodinid ectoparasites of cichlid and cyprinid fishes in South Africa and Israel. Syst. Parasitol. 5: 245-257.

Benson W.H. (1858) Note sur la transportation et la naturalisation au Bengale de l'*Achatina fulica* de Lamarck. J. de Conchyl. 7: 266-268.

Bequaert J.C. (1950) Studies in the Achatininae, a group of African land snails. Bull. Mus. Comp. Zool., Harvard 105: 1-216.

Bosc L.A.G. (1803) Agatine, Achatina. In: Nouveau Dictionnaire d'Histoire Naturelle Appliquée aux Arts...par une Société de Naturalistes et d'Agriculteurs, (Ed. C. Deterville). Paris.

Fantham H.B. (1924) Some parasitic Protozoa found in South Africa-VII. S. Afr. J. Sci. 21: 435-444.

Kazubski S.L. (1958) *Semitrichodina* gen. nov. *sphaeronuclea* (Lom, 1956) (Peritricha-Urceolariidae) in *Schistophallus orientalis* Cless. (Pulmonata-Zonitidae) in Poland. Bull. Acad. Polon. Sci., Sér. Biol. Sci. 6: 109-112.

Kazubski S.L. (1960) Materialy k poznaniju fauny paraziticeskih infuzorij nazemnyh molljuskov Karpat, Flora i fauna Karpat, (Sbornik rabot). Izd. AN SSSR, Moskva, 220-223.

Kazubski S.L. (1961) *Semitrichodina convexa* sp. n. (Urceolariidae) from land snail *Cochlodina laminata* (Mont.). Acta Parasit. Pol. 9: 273-278.

Kazubski S.L. (1981) Further investigation on morphological variability of *Semitrichodina sphaeronuclea* f. *macrodentata* (Lom) (Ciliata, Peritrichida), a parasite of land snails. Acta Protozool. 20: 385-392.

Lom J. (1956) Beiträge zur Kenntnis der parasitischen Ciliaten aus Evertebraten I. Arch. Protistenk. 101: 277-288.
Lom J. (1958) A contribution to the systematics and morphology of endoparasitic trichodinids from amphibians, with a proposal of uniform specific characteristics. J. Protozool. 5: 251-263.
Mead A.R. (1961) Comparative genital anatomy of some African Achatinidae (Pulmonata). Bull. Mus. Comp. Zool., Harvard 105: 217-292.
Purchon R.D. (1968) The biology of the Mollusca. 1 ed. Pergamon Press, Oxford.
Raabe Z. (1965) The parasitic ciliates of gastropods in the Ohrid Lake. Acta Protozool. 3: 311-320.
Raabe J., Raabe Z. (1959) Urceolariidae of molluscs of the Baltic Sea. Acta Parasitol. Pol. 7: 453-465.
Raabe J., Raabe Z. (1961) Urceolariidae from fresh-water and terrestrial molluscs in Poland. Acta Parasitol. Pol. 9: 141-152.
Shtein G.A. (1974) Morphological patterns of ciliates of the family Urceolariidae (Peritricha, Mobilia) from some marine invertebrates. Zool. Zh. 53: 965-973 (in Russian).
Sirgel W.F. (1983) A new ciliate genus *Trichodoxa* n.g. (Ciliata, Peritricha, Mobilina, Trichodinidae) with two new species from the genital system of terrestrial pulmonates. J. Protozool. 30: 118-125.
Van As J.G., Basson L. (1989) A further contribution to the taxonomy of the Trichodinidae (Ciliophora: Peritrichia) and a review of the taxonomic status of some ectoparasitic trichodinids. Syst. Parasitol. 14: 157-179.
Van As J.G., Basson L. (1992) Trichodinid ectoparasites (Ciliophora: Peritrichida) of freshwater fishes of the Zambesi River system, with a reappraisal of host specificity. Syst. Parasitol. 22: 81-109.
Wilbert N. (1975) Eine verbesserte Technik der Protargolimprägnation für Ciliaten. Mikrokosmos 6: 171-179.

Received on 9th January, 1992; accepted on 9th September, 1992

Acta Protozoologica (1993) 32: 63 - 66

ACTA
PROTOZOOLOGICA

Trichodina trendafilovi sp. n. and *Trichodina puytoraci* Lom, 1962 (Ciliata: Urceolariidae) from Freshwater Fishes in Bulgaria

Ginka GRUPCHEVA

Institute of Zoology, Bulgarian Academy of Sciences, Sofia, Bulgaria

Summary. *Trichodina trendafilovi* sp. n. is described from the skin of *Carassius auratus gibelio* from the Batak Dam and the Ovcharitza Dam. Mean diameter of the body of a medium sized *T. trendafilovi* is 62 µm, adhesive disc 43 µm, denticulate ring 29 µm, the number of the denticles 27-40. The slightly curved blades with broadly rounded tips are longer then the thorns slightly curved backward. The central area of the adhesive disc is slightly and unevenly impregnated with grainy appearance. A large population of *Trichodina puytoraci* is reported from the skin of *Alburnus alburnus* from the Ovcharitza Dam. *T. puytoraci* may found its way into the inland freshwater Ovcharitza Dam with the introduction of breeding specimens of *Mugil cephalus*. Photomicrographs and morphometric data are presented for both *Trichodina* species.

Key words. *Trichodina*, Urceolariidae, freshwater fishes, Bulgaria.

INTRODUCTION

Trichodina puytoraci from the skin of *Alburnus alburnus* (L.) and *Perca fluviatilis* L. and *Trichodina* sp. from the skin of *Carassius auratus gibelio* (Bloch) were recorded in the course of research on protozoan parasites of fishes in the Ovcharitza Dam (Grupcheva 1987). As the two species were found in a very small numbers, in the years after the publication more specimens were sought to clarify the taxonomic position of *Trichodina* sp. and to confirm hosts and location of *T. puytoraci*.

MATERIAL AND METHODS

Throughout the entire investigation period (1982-1991) a total of 78 specimens of *Alburnus alburnus* 111 specimens of *Perca fluviatilis* and 166 specimens of *Carassius auratus gibelio* were examined in the Ovcharitza Dam. In the period from 1986 to 1990 56 specimens of *Carassius auratus gibelio* were examined from the Batak Dam.

Address for correspondence: G. Grupcheva, Institute of Zoology, Bulgarian Academy of Sciences, boul. Tzar Osvoboditel 1, 1000 Sofia, Bulgaria.

Air dry smears from the skin, gills and nasal pits were impregnated with 2% aqueous solution of $AgNO_3$ (Klein's dry silver impregnation technique). Some of the preparations were fixed in Schaudinn's fluid, hydrolysed in 5 N HCl (at room temperature) and subsequently stained with Giemsa after the method of Robinov-Piekarski (Jirovec 1958).

Measurements of the adhesive disc and nuclear apparatus were made according to Lom (1958) and Arthur and Lom (1984a). All measurements are given in µm.

RESULTS

Trichodina puytoraci Lom, 1962 (Figs. 1-3)

Host. *Alburnus alburnus*
Location. Skin, very rarely in the nasal pits
Locality. Ovcharitza Dam

The report of this species (Grupcheva 1987) was based on several specimens from *A. alburnus* and only one from *P. fluviatilis*. In the follow-up study *T. puytoraci* was not found in *P. fluviatilis*, but many specimens were found in *A. alburnus*. Eight fish (47%) were infected in 1987 and 3 fish (21.4 %) were infected in 1988. For the whole investigation period a total of 13 specimens (16,7%) of *A. alburnus* were infected. All findings were in the spring.

The dimensions of 68 measured specimens are presented on Table 1. A comparison with the original description of the species from *Mugil cephalus, M. auratus* and *M. saliens* (Lom 1962) show almost identical data of diameter of the body, adhesive disc and denticulate ring, while the averages of the blade, central part, thorn and length of the denticles are below the single value from the host *M. cephalus*, although they with the exception of the length are within the limits of *A. alburnus* population. The general impression is that denticles of the population of *T. puytoraci* from *A. alburnus* are smaller. Diameter of macronucleus measured only from 3 specimens is below the limits given by Lom (1962) from M. cephalus. The average of the number of the denticles is below from those in Mugilidae and the limits of variation are lower. The granules in the central area of the adhesive disc in some specimens appear as light spots (Figs. 1, 2) while in the others they correspond partially (Fig. 3 - the central granule) or completely to the original description.

According to the key of the genus *Trichodina* (Stein 1984) the thorns of the denticles of *T. puytoraci* are longer than the blades, but we believe that the blades are longer although in some cases they are equal with the thorns. According to the original description (Lom 1962) they are also equal. Comparing the data of population from the skin of *A. alburnus* and those from the gills of Mugilidae (Lom 1962) it may be said *T. puytoraci* could be referred to a species with low variability.

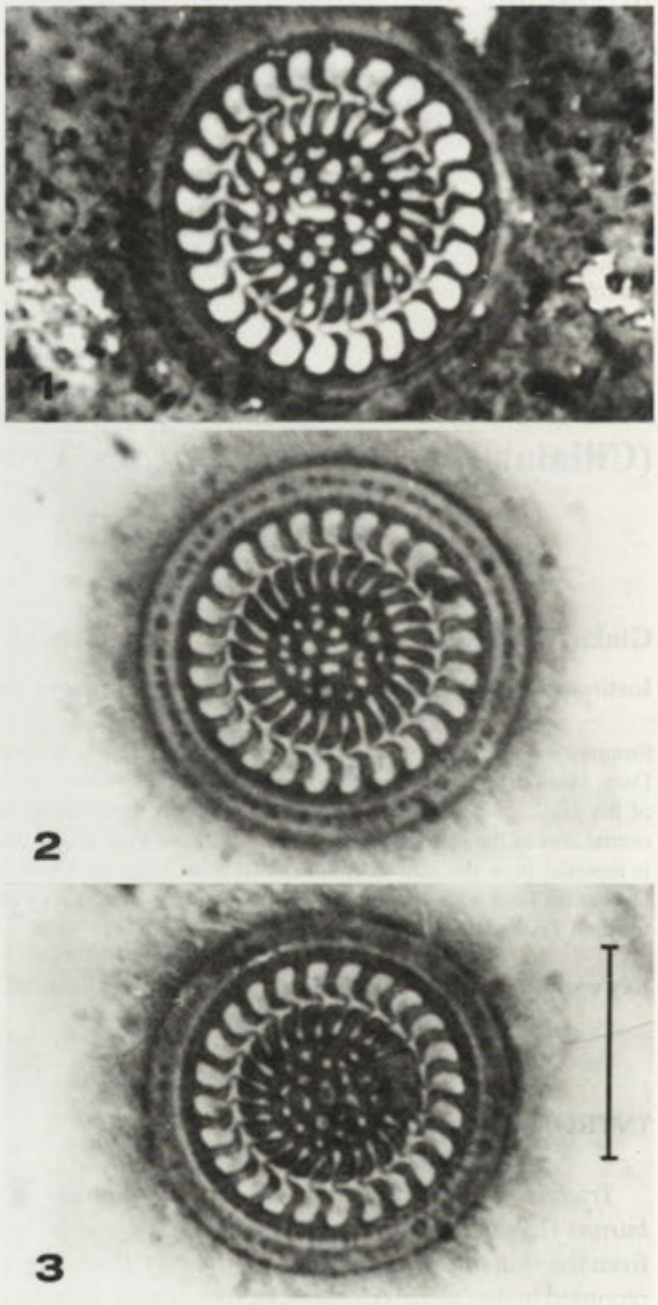

Figs. 1-3. Different specimens of *Trichodina puytoraci*. Scale bar: 20 µm

***Trichodina trendafilovi* sp. n. (Figs. 4-6)**

Host. *Carassius auratus gibelio*
Location. Skin
Locality. Batak Dam and Ovcharitza Dam

Very rare species. During the whole period of investigation only single specimens were found on 7 fish (4,2%) in the Ovcharitza Dam and on 3 fish (5,4%) in the Batak Dam, always in the spring. Usually it occurs with *T. reticulata, T. nigra* or *T. acuta*.

A medium sized *Trichodina trendafilovi* (Table 1) can be characterized only by the appearance of the adhesive disc. The denticles possess slightly curved blades with broadly rounded tips. The thorns are also slightly curved backward, their length is smaller than those of the blades. The number of the denticles is relatively high (27-40), they are situated close each to other especially in their central part. The central area of the adhesive disc is slightly and unevenly impregnated and with a slightly grainy appearance. Some variations

Table 1

Morphometric data of *Trichodina puytoraci* and *Trichodina trendafilovi* sp. n.

	Trichodina puytoraci	*Trichodina* trendafilovi sp.nov.
Number of specimens	68	20
Diameter of:		
body	45(37-62)	62(49-71)
adhesive disc	32(27-38)	43(36-53)
denticulate ring	20(17-25)	29(22-40)
macronucleus	20-23	
Number of:		
denticles	24(20-27)	31(27-40)
radial pins/denticle	7(6-8)	7.4(6-8)
Dimensions of a denticle:		
blade	3.9(3.4-4.8)	4.8(4.1-5.6)
central part	1.4(1-2)	2.1(2-3.1)
thorn	3.4(2.9-4.6)	3.6(2.9-4.8)
length	4.5(2.9-5.3)	5.3(4.3-6.6)
span	8.8(7.6-10.4)	10.5(9.1-12.2)
Width of the border membrane	3.5(2.9-4.1)	4.2(3.6-5.1)

are observed in the dimensions of the body and the adhesive disc and the shape of the denticle, the last one is to a great degree in the connection with the success of the impregnation. Dimensions of the nuclear apparatus cannot be reported due to difficult stainability in this species.

Compared with other *Trichodina* species *T. trendafilovi* reveals some similarities only in a few instances. In blade shape it is very close to *T. modesta* Lom, 1970 and *T. siluri* Lom, 1970, but according to the original description (Lom 1970) the first of them has smaller dimensions of the body and lower number of the denticles and the second one has longer thorns than the blades. In the structure of the central area of the adhesive disc, the number and the morphology of the denticles, especially their central part, *T. trendafilovi* closely resembles specimens described by Aschurova and Stein (1972) as *Trichodina strelkovi f. badachschanica*, later synonymized with *Trichodina nigra* Lom, 1961 (Stein 1984), which however has higher number of the radial pins per denticle (10-12), larger dimensions of the denticles and different shape of the thorns. *T. trendafilovi* by the dimensions of the body and adhesive disc, by the shape of the blades resembles also *T. borokensis* Arthur et Lom, 1984, but it has larger dimensions of the denticles and equal length of the blades and the thorns (Arthur and Lom 1984b). *T. trendafilovi* is similar in number of the denticles to many *Trichodina* species e.g. *T. pediculus* Ehrenberg, 1938, *T. izyumovae* Arthur et Lom, 1984, *T. tenuidens* Faure-Fremiet, 1943, *T. elegini* Schulman-Albova, 1950, *T. mutabilis* Kazubski et Migala, 1968, *T. mutabilis* illustrated by Lom (1970)

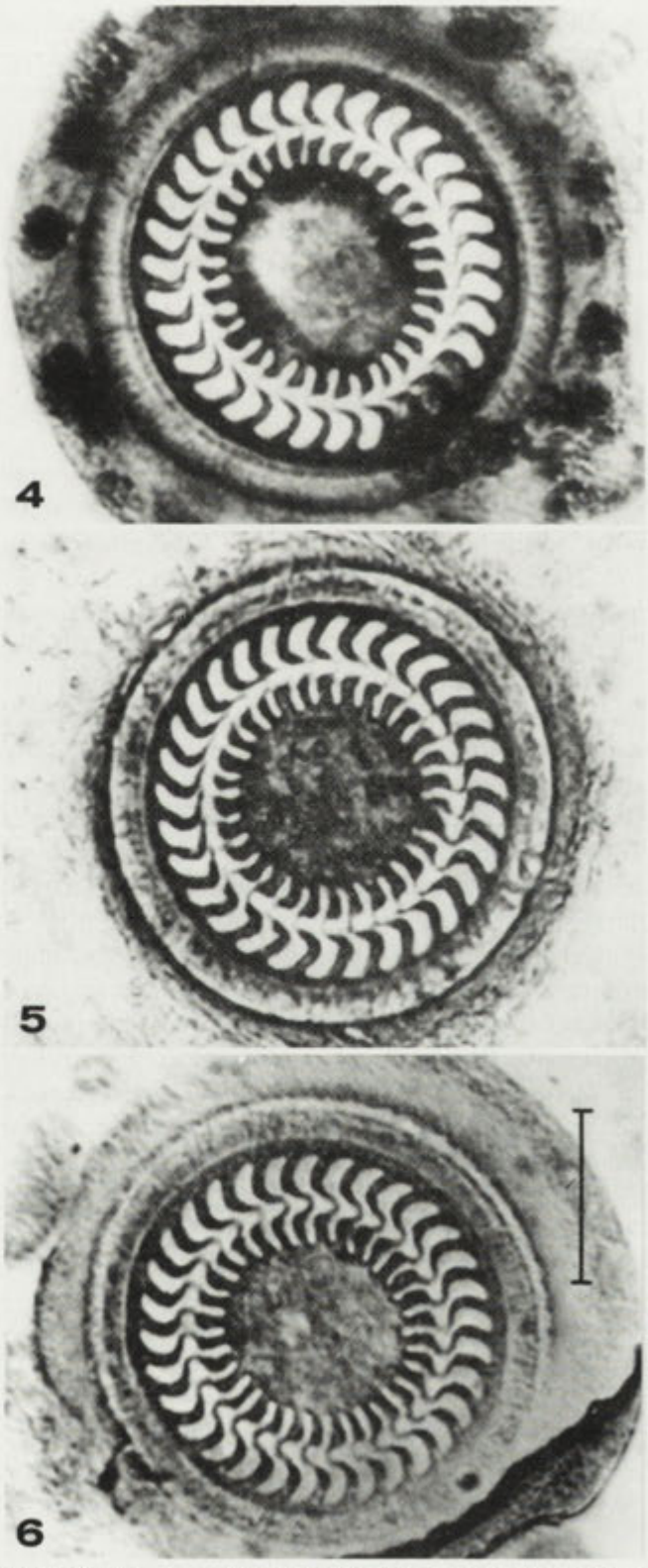

Figs. 4-6. Different specimens of *Trichodina trendafilovi* sp. n. Scale bar: 20 µm

from the skin of *Carassius auratus*, but is not identical to any of them differing in morphology of the denticles or body dimensions and adhesive disc and the structure of its central area. We propose therefore to establish this species as *Trichodina trendafilovi* after my husband K. Trendafilov.

The holetype slide (243-863) and syntype slides (243-864, 865) are in the Institute of Zoology of the Bulgarian Academy of Sciences, Sofia.

DISCUSSION

The representatives of the family Mugilidae, *Mugil cephalus, M. auratus* and *M. saliens*, are the hosts which provided the original description of *T. puytoraci* (Lom 1962). According to Stein (1975, 1984) *T. puytoraci* have been found also on other species from the family Clupeidae - *Alossa caspio tanica*, the family Gobiidae - *Gobius cobitis* and the family Labridae - *Symphodus tinca*. The location in all hosts are gills, the localities: the Black sea, the strait Kerchenski and lakes Tabacaria and Paleostomi. The finding of *T. puytoraci* in the Ovcharitza Dam is very interesting in several respects. The freshwater Ovcharitza Dam is without any direct contact with the sea water and is thermally affected through the year, so the conditions in it are very different from the previous localities. *A. alburnus* is also quite different from the hosts mentioned above - brackish or marine fishes and the location on it is the skin instead of gills (the finding of only one specimen *T. puytoraci* on *Perca fluviatilis* must be considered as accidental). The occurrence of *T. puytoraci* in the Ovcharitza Dam has explanation. Some specimens of *Mugil cephalus* have been introduced for breeding in the Ovcharitza Dam (Zivkov and Grupcheva 1987). As the conditions for reproduction of the species are absent only a few specimens of this fish are living there now. *T. puytoraci*, in our opinion, has been introduced with *M. cephalus* and with decreasing fish numbers had to change or to extend its hosts, so we find it now on a new host, *A. alburnus* and in a new location - skin in a very strong population.

REFERENCES

Arthur J. R., Lom J. (1984a) Some Trichodinid ciliates (Protozoa: Peritrichida) from Cuban fishes, with a description of *Trichodina cubanensis* n.sp. from the skin of *Cichlosoma tetracantha*. Trans. Am. Microsc. Soc. 103: 172-184.

Arthur J. R., Lom J. (1984b) Trichodinid protozoa (Ciliophora: Peritrichida) from freshwater fishes of Rybinsk Reservoir, USSR. J. Protozool. 31: 82-91.

Aschurova M., Stein G. A. (1972) Parasitic Ciliates (Peritricha, Urceolariidae) from fishes of the Alpine Pamirs (the Murgab basin). Parasitologya 6: 476-480 (in Russian).

Grupcheva G. (1987) Unicellular Parasites Found on Fish in some Bulgarian Reservoirs. IV. Ichthyoparasitofauna in the "Ovcharitza" Reservoir. Acta zool. bulg. 34: 68-78 (in Bulgarian).

Jirovec O. (1958) Zoologicka Technica. Statni pedagogicke nakladatelstvi, Praha (in Czech).

Kazubski S. L., Migała K. (1968) Urceolariidae from breeding carp - *Cyprinus carpio* L. in Żabieniec and remarks on the seasonal variability. Acta Protozool. 13: 137-160.

Lom J. (1958) A contribution to the systematics and morphology of endoparasitic trichodinids from amphibians, with a proposal of uniform specific characteristics. J. Protozool. 5: 251-263.

Lom J. (1962) Trichodinid ciliates from fishes of the Rumanian Black Sea coast. Parasitology 52: 49-61.

Lom J. (1970) Observation on trichodinid ciliates from freshwater fishes. Arch. Protistenk. 112: 153-170.

Stein G. A. (1975) Order Peritrichida F. Stein, 1859. In: Key to the Parasites of Vertebrates of the Black and Azov Seas, (Ed. V. N. Greze, S. L. Delyamure and V. M. Nikolaeva). Naukova Dumka, Kiev, 53-68 (in Russian).

Stein G. A. (1984) Fam. Trichodinidae Claus, 1874. In: Key to the Parasites of the Freshwater Fishes of the USSR, (Ed. O.N. Bauer), Nauka, Leningrad, 322-389 (in Russian).

Zivkov M., Grupcheva G. (1987) Specifities of the hydrochemical state, formation of the ichtyofauna and the fish-farming in the reservoir-cooler "Ovcharitza". Hydrobiology 30: 23-36 (in Bulgarian).

Received on 12th February, 1992; accepted on 18th October, 1992

Instruction to Authors

ACTA PROTOZOOLOGICA publishes original papers embodying the results of experimental or theoretical research in all fields of protistology with the exception of faunistic notices of local character and purely clinical reports. Short (rapid) communications are acceptable but also long review articles. The papers should be as concise as possible, be written in English, French or German, however the English language is preferred to keep printing costs lower. Submission of a manuscript to ACTA PROTOZOOLOGICA implies that it has not been submitted for publication elsewhere and that it contains unpublished, new information. There are no page charges. Authors should submit papers to:

Miss Malgorzata Woronowicz
Managing Editor of ACTA PROTOZOOLOGICA
Nencki Institute of Experimental Biology,
ul. Pasteura 3
02-093 Warszawa, Poland

Organization of Manuscripts

Submissions

Please enclose three copies of the text, one set of original illustrations and three sets of copy figures.

The ACTA PROTOZOOLOGICA can use the author's word-processor disks (5.25" and 3.5" format IBM or IBM compatible) of the manuscripts instead of rekeying articles. If available, please send a copy of the disk with your manuscript. Disks will be returned. Please observe the following instructions:

1. Label the disk with: your name: the word processor/computer used, e.g. IBM; the printer used, e.g. Laserwriter; the name of the program, e.g. Wordperfect 5.1; and any special characters used, and how you obtained them (i.e. dedicated key pressed or printer control codes used directly).
2. Send the manuscript as a single file; do not split it into smaller files.
3. Give the file a name which is no longer than 8 characters.
4. Create and/or edit your manuscript, using the document mode (or equivalent) in the word-processor program.
5. If necessary, use only italic, bold, underline, subscript and superscript. Multiple font, style or ruler changes, or graphics inserted the text, reduce the usefulness of the disc.
6. Do not right-justify text.
7. Avoid the use of footnotes.
8. Use paragraph indents.
9. Leave a blank line before and after all headings.
10. Distinguish the numerals 0 and 1 from the letters O and l.

Text

The text must be typewritten, doublespaced, with numbered pages. The manuscript should be organized into Summary, Introduction, Materials and Methods, Results, Discussion, Acknowledgments, References, Tables and Figure Legends. The Title Page should include the full title of the article, first name(s) in full and surname(s) of author(s), the address(es) where the work was carried out, page heading of up to 40 characters, and up to 6 Key Words. The present address for correspondence, the phone and FAX numbers should also be given.

The Titles, Summary and Key Words of the manuscripts submitted in French and German should be translated into English according to the demands of Current Contents. Each table must be on a separate page. Figure legends must be in a single series at the end of the manuscript. References must be listed alphabetically, abbreviated according to the World List of Scientific Periodicals, 4th ed. (1963). Nomenclature of genera and species names must agree with the International Code of Zoological Nomenclature, third edition, London (1985) or International Code of Botanical Nomenclature, adopted by XIV International Botanical Congress, Berlin, 1987. It is preferable to use SI units. References should be cited in the text by name and date in parentheses.

Examples for bibliographic arrangement of references:

Journals:

Ehret C. F., Powers E. L. (1959) The cell surface of Paramecium. Int. Rec. Cytol. 8: 97-133.

Books:

Wichterman R. (1986) The Biology of Paramecium. 2 ed. Plenum Press, New York.

Articles from books:

Allen R. D. (1988) Cytology. In: Paramecium, (Ed. H.-D. Görtz). Springer-Verlag, Berlin, Heidelberg, 4-40.

Illustrations

All line drawings and photographs should be labeled, with the first author's name written on the back. The figures should be numbered in the text as arabic numerals (e.g. Fig.1). Illustrations must fit within either one column (86 x 231 mm) or the full width and length of the page (177 x 231 mm). Figures and legends should fit on the same page.

Line drawings

Line drawings should be made suitable for reproduction in the form of well-defined line drawings and should have a white background. Computer printouts of laser printer quality may be accepted. Avoid fine stippling or shading. Line drawings must be no more than twice final size.

Photographs

Photographs at final size should be sharp, with a glossy finish, bromide prints, and mounted on firm board. Photographs grouped as plates must be trimmed at right angles very accurately mounted with edges touching. The engraver will then cut a fine line of separation between figures. Magnification should be indicated.

Proof sheets and offprints

Authors will receive one set of page proofs for correction and return to the Editor. Fifty reprints will be furnished free of charge.

ANNONCEMENT

The Coccidia of the World: A Central Clearing House. We are attempting to assemble a complete collection of the World's literature on the coccidia (Family Eimeriidae) of both invertebrate and vertebrate animals on a computer data base. Descriptive data on all oocyst and life cycle stages will be entered and cross-referenced by species, host(s), locality, author, and perhaps other parameters. The data will then be compiled by host group in whatever way seems most useful (e. g., invertebrate hosts by Phylum; vertebrate hosts by Family). Once established, the data base can be added to and archived in appropriate places (e.g., the U.S. National Parasite Collection, Beltsville MD) on a regular basis (e.g., each decade), and it can be made available to workers in the field for the cost of reproducing and mailing computer disks or hard copy. We would appreciate receiving a copy of any and all published papers in your reprint collection in which new species of coccidia are described or redescribed. Of most value are copies of old papers that have appeared in specialty journals or in non-English journals with limited circulations. Please mail reprints to: Dr.Donald W. Duszynski, at the address below. Also, please continue to send copies of new papers as they are forthcoming. Any constructive suggestions you may have in this regard are welcomed. We thank you in advance for your cooperation.

Dr Donald W Duszynski
Department of Biology
The University of New Mexico
Albuquerque, New Mexico 87131
U.S.A.

Dr. Steve J. Upton
Division of Biological Sciences
Ackert Hall
Kansas State University
Manhattan , Kansas 66506
U.S.A.

SUBSCRIPTION and BACK VOLUMES

ACTA PROTOZOOLOGICA may be ordered directly from the Nencki Institute of Experimental Biology, ul. Pasteura 3, 02-093 Warszawa, Poland (account No. 370044-3522 at Państwowy Bank Kredytowy, XIII Oddział, Warszawa) or from agents. Annual subscription rate for 1992 will be US $ 70.- for individual subscribers, US $ 80.- for Instituton and Library, and additionaly: surface mail US $ 10, or air mail for European and overseascountries US $ 40 and 60 respectively.

The Nencki Institute is in possesion of a limited number of back volumes of ACTA PROTOZOOLOGICA available at reduced rates. Please contact the Managing Editor for prices and conditions of delivery.

Subscription may be ordered also at ARS POLONA, 00-950 Warszawa, Krakowskie Przedmieście 7, Poland.

The Nencki Institute of Experimental Biology is publishing also quarterly journal ACTA NEUROBIOLOGIAE EXPERIMENTALIS.

Printed by "MARBIS" 60 Kombatantów St., 05-070 Sulejówek, Poland

ACTA PROTOZOOLOGICA